Investigation of Failure Theory in Structures Made

of Fiber-Reinforced Composites

عميد كلية الدراسات العليا

By

Iyad Mahmood Ali Muslih

Supervisor

Dr. Saad Mohammad Habali

Submitted in partial fulfillment of the requirements for the

degree of master of science in

mechanical engineering

Faculty of Graduate Studies
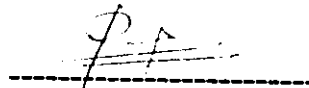
University of Jordan

August 1998

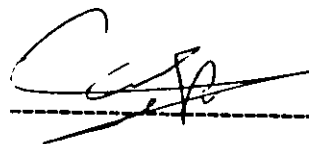This thesis was successfully defended and approved on: August, 4,1998.

Examination Committee   **Signature**

-----------------------------------   ------------------------

Dr. Saad Mohammad Habali , Chairman   -----------------------

Prof. Yasser Hunaiti, Member   -----------------------

Dr. Naser AL- Huniti, Member   _Naser Al-Huniti_

Dr. Samer Masoud, Member

DEDICATION

TO MY PARENTS

CONTENTS

XII

NOMENCLATURE

σ_i : Normal stress components .

τ_{ij} : Shear stress components .

ε_j : Normal strain components .

γ_{ij} : Shear strain components .

C_{ij} : Stiffness constants.

S_{ij} : Compliance constants.

S_{ij}^{-1} : Inverse of compliance matrix .

E_i : Young's modulus.

υ_{ij} : Poisson's ratio.

θ : Positive angle of fibers rotation.

G_{ij} : Shear modulus.

W : Strain energy function.

Q_{ij} : Reduced stiffnesses.

$\overline{Q}_{ij}$: Transformed reduced stiffnesses.

$\overline{S}_{ij}$: Transformed reduced compliances.

$\overline{C}_{ij}$: Stiffnesses of bilayered material .

$C_{ij}^{(i)}$: Stiffnesses of I-material.

V : Total volume .

V_1, V_2 : Volume fractions of materials 1 and 2 .

$\varepsilon_x^o, \varepsilon_y^o, \varepsilon_{xy}^o$: Laminate middle surface strains in x-y plane .

K_x, K_x, K_{xy} : Curvatures of the laminate middle surface .

u_o, v_o, w_o : Middle surface displacements in x,y and z directions .

[T] : Transformation matrix

[A] : Extensional-stiffness matrix

[B] : Coupling-stiffness matrix

[D] : Bending-stiffness

N_x, N_y, N_{xy} : Resultant forces in x-y plane.

M_x, M_y, M_{xy} : Resultant moments in x-y plane.

Q_x, Q_y : Shear resultants in the z – direction.

F_x, F_y, F_z : Body forces in x,y and z directions ,

X_t : Maximum tensile stress in the principal material direction "1"

X_c : Maximum compressive stress in the principal material direction "1"

Y_t : Maximum tensile stress in the principal material direction "2"

Y_c : Maximum compressive stress in the principal material direction "2"

S : Maximum shear stress 1-2 plane .

S_ε : Maximum shear strain in 1-2 plane .

Y_a : Maximum tensile strain in the material direction 2 .

Y_{ac} : Maximum compressive strain in the material direction 2

X_a : Maximum tensile strain in the material direction 1

$X_{\varepsilon c}$: Maximum compressive strain in the material direction 1 .

Z : Distance from the laminate middle plane .

Z_k, Z_{k-1} : Distances of the top and bottom of layer k, respectively.

K^{th} : The k-th lamina in the laminate.

K : Lamina number .

N : Number of laminae in the laminate.

M : Cross-ply ratio.

F : Stiffness ratio.

V_n : Effective shear resultant.

M_b : Bending moment .

F_t, F_{ij} : Quantities related to tensile and compressive yield strengths.

ε_{iu} : Principal ultimate strain components.

U_l : Equivalent linear elastic extensional strain .

U_{ij} : Equivalent linear elastic shear strain energy densities.

σ^* : Biaxial tensile failure stress .

$P(x,y)$: Applied load on the plate .

$P(x)$: Applied load on the beams .

$W(x,y)$: Deflection of a plate .

$W(x)$: Deflection of a beam .

P_o : A uniform lateral load .

P_1, P_2 : Normal surface tractions on the top and bottom surface of the structure , respectively.

$U_o(x)$: Displacement function in x- direction.

C_o, C_1, C_2, C_3, C_4 : Constants of integration .

$\bar{\sigma}_x, \bar{\sigma}_y, \bar{\sigma}_{xy}$: Normalized stresses .

q_o : Critical failure load .

t : Laminate thickness .

t_k : Laminate thickness .

a : Length of the plate or beam .

b : Width of the plate or beam .

ABSTRACT

Investigation of Failure Theory in Structures Made of Fiber –
Reinforced composite Materials

By

Iyad Mahmood Ali Muslih

Supervisor

Dr. Saad Habali

In this study, the micromechanical modeling of fiber-reinforced composites is considered by using the strain energy approach. Failure of structures made of fiber-reinforced composites is studied by using three different failure theories: Tsai-Wu theory , Tsai-Hill theory, and maximum stress theory .

Laminated composite structures made of composite materials such as; boron-epoxy, glass-epoxy, and E glass-epoxy are considered.

The laminates are symmetric with different stacking sequences of cross-ply and angle-ply.

Also, bending of plates and beams made of Eglass-epoxy under different loading and supporting conditions is studied.

Results of this study are compared with available results in literature, where the comparison shows that the predicted results are close to the experimental results for materials and laminates considered in this study .

Chapter One

INTRODUCTION

1.1 General

A composite material can be defined as a heterogeneous mixture of two or more homogeneous phases, which have been bonded together mechanically. The resulting mixture has many characteristics, which are different from more conventional engineering materials, so the advantage of composite material is that it usually exhibits the best qualities of its constituents and often some qualities that neither constituent possesses.

Composite materials can be commonly classified into three different types :

1. Fibrous Composites which consist of fibers in a matrix, so the result is a fibrous composite lamina where fibers are either unidirectional or woven as shown in Fig.1-1, and work as the main load-carrying agents with major characteristics of high aspect ratios and high strength and stiffness to density ratios while the matrix acts as a protecting agent and provides a mean to distribute the load (Jones,1975).

2. Laminated Composites which consist of layers of at least two different materials that are bonded together, without any possibility to slip, by means of a resin layer of zero thickness.

3. Particulate Composites which consist of particles of one material embedded into a matrix of another material.

Typical composite materials are shown in Fig. 1-2.

In this study, laminated fibrous composites will be considered, where these composites involve both fibrous composites and lamination techniques as shown in Fig. 1-3. A more common name for these composites is laminated fiber-reinforced composites where the fibers are infinitely long, parallel circular cylinders of identical properties, and the materials of the fiber and matrix are homogenous, isotropic and linearly elastic. In this type of materials, layers of fiber-reinforced material are built up with different fibers directions to give different strengths and stiffnesses in the various directions. Thus, the strengths and stiffnesses of the laminated fiber-reinforced composite can be tailored to the specific design requirements. Also, the properties of the structure that can be emphasized by this type of composites are, low weight, corrosion resistance, wear resistance, beauty or attractiveness, thermal insulation, etc. (Jones, 1975, Mal and chatterjee, 1977).

Therefore, in most engineering applications, composite materials are used in the from of laminates, where laminated beams and plates are finding an increasing use in the mechanical, aerospace, marine, and other branches of engineering. Many applications of laminated
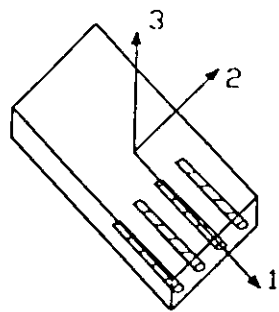
Lamina with Unidirectional Fibers   Lamina with Woven Fibers
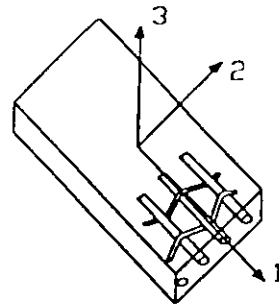
FIG. 1-1. Tow Principal Types of Lamina
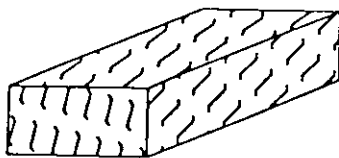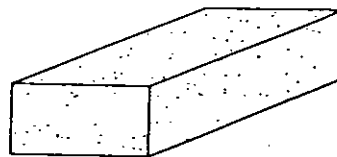
Fiber Composite   Particulate Composite   Laminar Composite
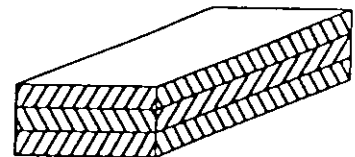
FIG. 1-2. Illustration of Various Types of Composite Materials.
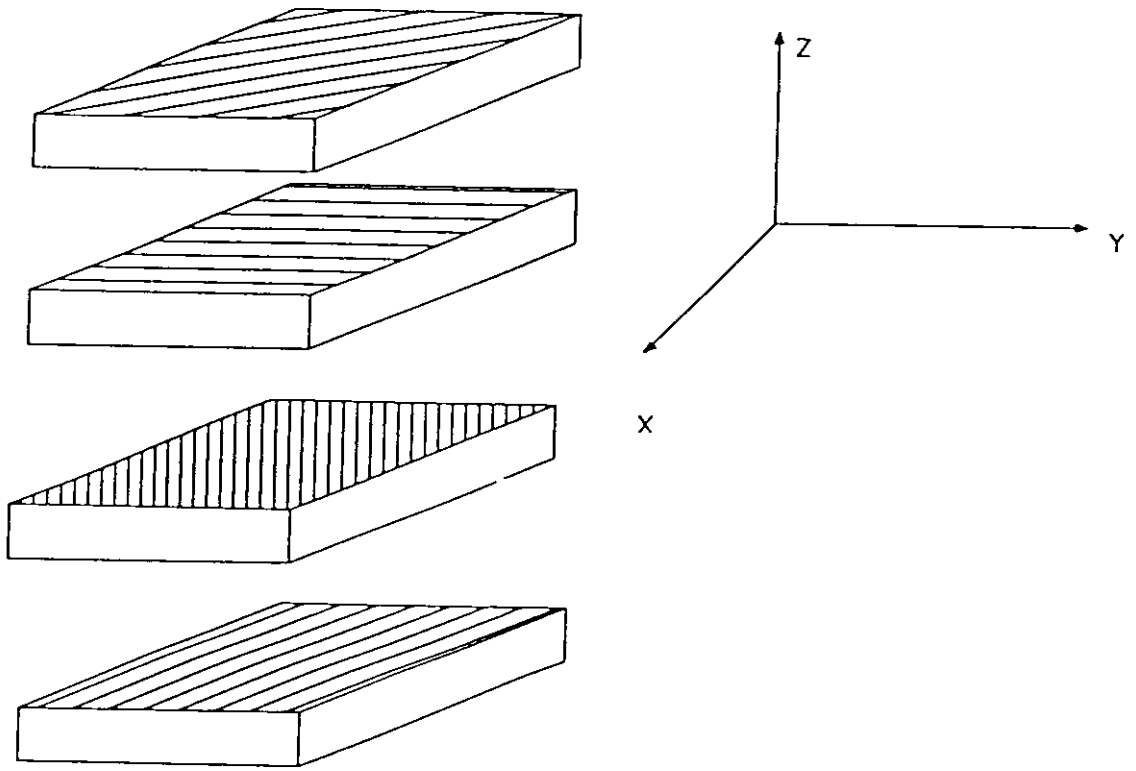
FIG. 1-3. Laminate construction.

are based on the macromechanical behavior of the composite to predict the failure surface under combined loading conditions. The macromechanical behavior is the study of composite material behavior wherein the material is presumed homogeneous and the effects of the constituent materials are detected only as averaged apparent properties of the composite (Jones, 1975).

1.2 Objectives

The objectives of this study can be summarized as follows:

1- To study the effects of fiber orientation and loading on the strength characteristics of fibrous composites.

2- To study the various failure criteria with application to fiber-reinforced composite plates with different loading conditions.

3- To compare the available results in literature with predicted ones.

1.3 Methodology

In order to achieve the previous objectives the following steps are followed :

1- A micromechanical modeling is investigated for unidirectional fibrous composites and the strain energy

1-A micromechanical modeling is investigated for unidirectional fibrous composites and the strain energy approach is used in programs.

2-Developing a strength analysis procedure for structures made of fiber-reinforced composites.

3-Computer programs for different failure theories are developed to study the first-ply failure for laminated composites.

4-Failure of special cases of laminated composites is investigated under different conditions.

5- As an application, bending of composite plates and beams is investigated.

6-Results of different failure criteria are compared together and with available results in literature.

Chapter Two

MECHANICAL BEHAVIOR OF
COMPOSITE MATERIALS

2.1 Introduction

A lamina is the basic building block in a laminated fiber-reinforced composite, so the knowledge of mechanical behavior of a lamina is very important to understanding the behavior of the fiber-reinforced structures.

Laminated composites have many characteristics that are different from more conventional engineering materials, for they are often both heterogeneous and nonisotropic (orthotropic, or more generally, anisotropic); a heterogeneous body has properties that are a function of position in the body, and anisotropic body has material properties that are different in all directions at a point in the body while an orthotropic body has material properties that are different in three mutually perpendicular directions at a point in the body, i. e the properties are a function of orientation at a point in the body (Jones, 1975).

The lamina constituents, the fibers and matrix, are homogenous and isotropic and their stress- strain behavior is typified as one of the classes depicted in Fig. 2-1.

For example, fiber-reinforced composites such as graphite-epoxy and boron-epoxy are often treated as linear elastic materials since fibers provide the majority of the strength and stiffness (Jones, 1975).

This variety of material properties will result in different stress-strain relations inside the body affected by similar stresses; when a normal stresses act on isotropic materials, the result will be extension in the direction of the normal stresses and contraction in the perpendicular direction, and the result of applying shear stresses will be only shearing deformation. However, for orthotropic materials, normal stresses in a principal material direction result in extension in the direction of the applied stresses and contraction perpendicular to the direction of applied stresses, but this contraction can be either more or less than the contraction of a similarly loaded isotropic material with the same elastic modulus in the direction of the load. For the case of shear stresses, shearing deformation will result with a magnitude independent of the Young's moduli and Poisson's ratios (Jones, 1975, Tsia and Hahn, 1980).

FIG. 2-1 Various Stress-Strain Behaviour.
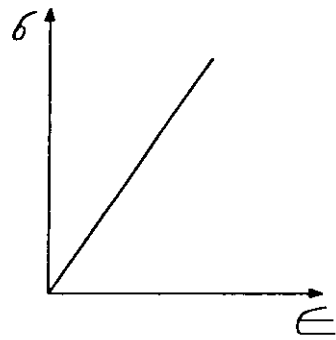
Linear Elastic
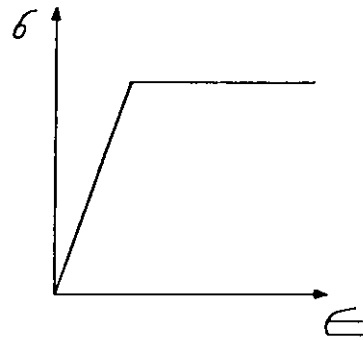
Elastic – Perfectly Plastic
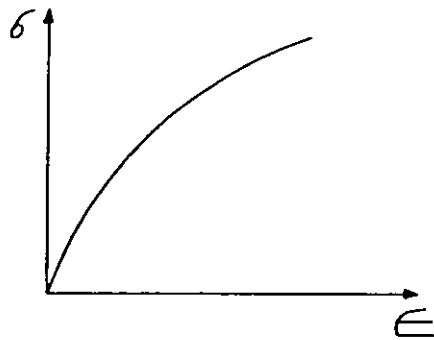
Elastic –Plastic

Viscoelastic $(\dot{\in}1,\dot{\in}2,\dot{\in}3)$

2.2 Stress-Strain Relations for Orthotropic Materials

From the knowledge of strength of materials (Marin, 1966), both stress, σ_{ij}, and strain , ε_{ij}, are second order tensor quantities, and they are equated by means of a fourth order tensor quantity, C_{ijkl}. Thus, the generalized Hooke's law relating stresses to strains can be written as;

$$\sigma_{ij} = C_{ijkl} \ \varepsilon_{kl}$$
(2.1)

where i,j,k and l assume values of 1,2 and 3 in commonly defined Cartesian Coordinated System.

Both the stress and strain are symmetric (Whitney, 1987, Jones, 1975), and therefore the following shorthand notation can be used (Whitney, 1987).

$$\sigma_{11} = \sigma_1 \qquad \sigma_{23} = \sigma_4 = \tau_{23} \qquad \varepsilon_{11} = \varepsilon_1 \qquad 2\varepsilon_{23} = \varepsilon_4 = \gamma_{23}$$

$$\sigma_{22} = \sigma_2 \qquad \sigma_{31} = \sigma_5 = \tau_{31} \qquad \varepsilon_{22} = \varepsilon_2 \qquad 2\varepsilon_{31} = \varepsilon_5 = \gamma_{31}$$

$$\sigma_{33} = \sigma_3 \qquad \sigma_{12} = \sigma_6 = \tau_{12} \qquad \varepsilon_{33} = \varepsilon_3 \qquad 2\varepsilon_{12} = \varepsilon_6 = \gamma_{12}$$

In addition, if a strain energy density function ,W, exists (Jones, 1975),i.e,

$$W = \frac{1}{2} \sigma_{ij} \varepsilon_{ij}$$

(2.2)

in such a way that

$$\frac{dw}{d\varepsilon_{ij}} = C_{ijkl} \varepsilon_{kl} = \sigma_{ij}$$

(2.3)

Then the independent components of C_{ijkl} reduced from 81 to 21, since $C_{ijkl} = C_{klij}$, or it can be written $C_{ij} = C_{ji}$ (i,j = 1,2, ... , 6).

Therefore, another form of the generalized Hooke's Law is ;

$$\sigma_{ij} = C_{ij} \varepsilon_j \qquad i,j = 1,.........,6$$

(2.4)

Now, for orthotropic elastic bodies , such as reinforced composite materials, there are nine elasticity independent constants, so the stiffness matrix for orthotropic materials is (Jones, 1975):

$$C_{ij} = \begin{bmatrix} C_{11} & C_{12} & C_{13} & 0 & 0 & 0 \\ C_{12} & C_{22} & C_{23} & 0 & 0 & 0 \\ C_{31} & C_{32} & C_{33} & 0 & 0 & 0 \\ 0 & 0 & 0 & C_{44} & 0 & 0 \\ 0 & 0 & 0 & 0 & C_{55} & 0 \\ 0 & 0 & 0 & 0 & 0 & C_{66} \end{bmatrix}$$

(2.5)

12

2.3 Micromechanical Modeling Of Unidirectional Fibrous Composites

2.3.1 Introduction

It is essential to study the micromechanical modeling of unidirectional fibrous composites to find the equivalent elastic properties of these materials. For micromechanical modeling, both the materials of the fibers and the matrix are homogeneous and their behavior is linearly elastic.

There are different methods to evaluate these properties. One of them is the strain energy method that will be considered in this study for its simplicity and accurate results (Al-Huniti, 1996). In the strain energy method, a square cross section is used to approximate the circular cross section of the fibers, also this method is based on the assumption that for any section of the composite body, straight lines remain straight after deformation. These two assumptions are valid since the results of this method are very close to the results of finite element methods and experimental works (Al-Huniti, 1996).

Strain energy method for a composite material states that total strain energy is the sum of the strain energies of each material in the composite.

wi

$$\overline{C}_{11} = C_{11}^{(1)}V_1 + C_{11}^{(2)}V_2 - V_1V_2 \; \frac{\left(C_{13}^{(1)} - C_{13}^{(2)}\right)^2}{C_{33}^{(1)}V_2 + C_{33}^{(2)}V_1}$$

$$\overline{C}_{12} = C_{12}^{(1)}V_1 + C_{12}^{(2)}V_2 - V_1V_2 \; \frac{\left(C_{13}^{(1)} - C_{13}^{(2)}\right)\left(C_{23}^{(1)} - C_{23}^{(2)}\right)}{C_{33}^{(1)}V_2 + C_{33}^{(2)}V_1}$$

$$\overline{C}_{13} = \frac{C_{13}^{(1)}C_{33}^{(2)}V_1 + C_{33}^{(1)}C_{13}^{(2)}V_2}{C_{33}^{(1)}V_2 + C_{33}^{(2)}V_1}$$

$$\overline{C}_{22} = C_{22}^{(1)}V_1 + C_{22}^{(2)}V_2 - V_1V_2 \; \frac{\left(C_{13}^{(1)} - C_{13}^{(2)}\right)^2}{C_{33}^{(1)}V_2 + C_{33}^{(2)}V_1}$$

$$\overline{C}_{23} = \frac{C_{23}^{(1)}C_{33}^{(2)}V_1 + C_{33}^{(1)}C_{23}^{(2)}V_2}{C_{33}^{(1)}V_2 + C_{33}^{(2)}V_1}$$

$$\overline{C}_{33} = \frac{C_{33}^{(1)}C_{33}^{(2)}}{C_{33}^{(1)}V_2 + C_{33}^{(2)}V_1}$$

$$\overline{C}_{44} = \frac{C_{44}^{(1)}C_{44}^{(2)}}{C_{44}^{(1)}V_2 + C_{44}^{(2)}V_1}$$

$$\overline{C}_{55} = \frac{C_{55}^{(1)}C_{55}^{(2)}}{C_{55}^{(1)}V_2 + C_{55}^{(2)}V_1}$$

$$\overline{C}_{66} = C_{66}^{(1)}V_1 + C_{66}^{(2)}V_2 \qquad\qquad (2.11)$$

where ;

$\overline{C}_{ij}$: Stiffnesses of bilayered material.

$C_{ij}^{(1)}$: Stiffnesses of material 1.

$C_{ij}^{(2)}$: Stiffnesses of material 2.

V_1, V_2 : Volume fractions of material 1 and material 2, respectively.
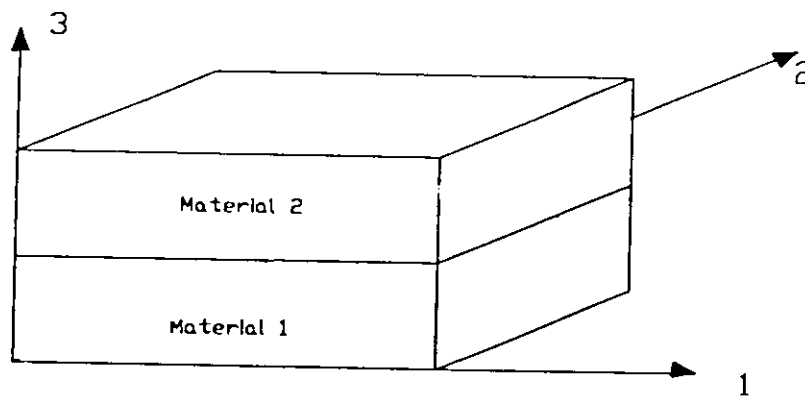
FIG. 2-2 A Layered Model Consisting of Two Different Materials.

2.3.2 Fibrous Case

Fibrous composites can be analyzed to find the stiffness matrix by using a unit cell as shown in Fig.2-3 to represent the whole composite body. The circular cross section of the fiber is approximated by a square cross section which has the same area of the circular cross section. The unit cell is devided to different regions as shown in Fig.2-4a; regions 1 and 3 consist of matrix material only whereas region 2 consists of two layers of material. For region 2, Eq.(2.11) can be applied to find the properties $\overline{C_{ij}}$. Then the method considers region 2 as a one homogenous material with properties $\overline{C_{ij}}$ in combination with regions 1 and 3 consisting of the matrix material . And for this case, as shown in Fig.2-4a, the equivalent properties are (Al-Huniti, 1996)

$$\overline{\overline{C}}_{11} = \overline{C}_{11}\ \overline{V}_1 + C_{11}^{(2)}\overline{V}_2 - \frac{\overline{V}_1\overline{V}_2\left(\overline{C}_{12} - C_{12}^{(2)}\right)^2}{\overline{C}_{22}\ V_2 + C_{22}^{(2)}\overline{V}_1}$$

$$\overline{\overline{C}}_{12} = \frac{\overline{C}_{12} + C_{22}^{(2)}\overline{V}_1 + \overline{C}_{22}\ \overline{C}_{12}^{(2)}\overline{V}_2}{\overline{C}_{22}V_2 + C_{22}^{(2)}\overline{V}_1}$$

$$\overline{\overline{C}}_{13} = \overline{C}_{13}\overline{V}_1 + C_{13}^{(2)}\overline{V}_2 - \overline{V}_1\overline{V}_2\frac{\left(\overline{C}_{12} - C_{12}^{(2)}\right)\left(\overline{C}_{23} - C_{23}^{(2)}\right)}{\overline{C}_{22}V_2 + C_{22}^{(2)}\overline{V}_1}$$

$$\overline{\overline{C}}_{22} = \frac{\overline{C}_{22}\ C_{22}^{(2)}}{\overline{C}_{22}V_2 + C_{22}^{(2)}\overline{V}_1}$$

$$\overline{\overline{C}}_{23} = \frac{\overline{C}_{23}C_{22}^{(2)}\overline{V}_1 + \overline{C}_{22}C_{23}^{(2)}\overline{V}_2}{\overline{C}_{22}V_2 + C_{22}^{(2)}\overline{V}_1}$$

18

$$\overline{\overline{C}}_{33} = \overline{C}_{33}\overline{V}_1 + C_{33}^{(2)}\overline{V}_2 - \overline{V}_1\overline{V}_2 \frac{\left(\overline{C}_{23} - C_{23}^{(2)}\right)^2}{\overline{C}_{22}\overline{V}_2 + C_{22}^{(2)}\overline{V}_1}$$

$$\overline{\overline{C}}_{44} = \frac{\overline{C}_{44}\,C_{44}^{(2)}}{\overline{C}_{44}\overline{V}_2 + C_{44}^{(2)}\overline{V}_1}$$

$$\overline{\overline{C}}_{55} = \overline{C}_{55}\overline{V}_1 + C_{55}^{(2)}\overline{V}_2$$

$$\overline{\overline{C}}_{66} = \frac{\overline{C}_{66}\,C_{66}^{(2)}}{\overline{C}_{66}\overline{V}_2 + C_{66}^{(2)}\overline{V}_1} \qquad (2.12)$$

where ;

$\overline{\overline{C}}_{ij}$: Properties of the model in Fig. 2-4a.

$\overline{C}_{ij}$: Properties of compound region 2.

$C_{ij}^{(2)}$: Properties of regions 1 and 3.

$\overline{V}_1, \overline{V}_2$: Volume fractions of region 2 and regions (1,3), respectively.

The same principle can be used for the case shown in Fig. 2-4b, and without going into details the final properties for unidirectional fibrous composites are the average of the two cases in Fig. 2-4a and Fig. 2-4b , and can be written as (Al-Huniti, 1996).

$$C_{11f} = C_{33f} = \frac{\overline{\overline{C}}_{11} + \overline{\overline{C}}_{33}}{2}$$

$$C_{22f} = \overline{\overline{C}}_{22}$$

$$C_{12f} = C_{23f} = \frac{\overline{\overline{C}}_{12} + \overline{\overline{C}}_{33}}{2}$$

$$C_{13f} = \overline{\overline{C}}_{13}$$

$$C_{44f} = C_{66f} = \frac{\overline{\overline{C}}_{44} + \overline{\overline{C}}_{66}}{2}$$

$$C_{55f} = \overline{\overline{C}}_{55} \qquad\qquad (2.13)$$

Where $\overline{\overline{C}}_{ij}$ are the equivalent properties of the case in Fig. 2-4a.

Material properties for the laminate can be evaluated from the components of the compliance matrix, S_{ij}, where

$$C_{ij} = S_{ij}^{-1} \qquad\qquad (2.14)$$

For an orthotropic material , the compliance matrix, S_{ij}, can be given in terms of engineering constants as in the following form (Jones, 1975):

$$
S_{ij} = \begin{bmatrix}
\dfrac{1}{E_1} & -\dfrac{\upsilon_{21}}{E_2} & -\dfrac{\upsilon_{31}}{E_3} & 0 & 0 & 0 \\[2mm]
-\dfrac{\upsilon_{12}}{E_1} & \dfrac{1}{E_2} & -\dfrac{\upsilon_{32}}{E_3} & 0 & 0 & 0 \\[2mm]
-\dfrac{\upsilon_{13}}{E_1} & -\dfrac{\upsilon_{23}}{E_2} & \dfrac{1}{E_3} & 0 & 0 & 0 \\[2mm]
0 & 0 & 0 & \dfrac{1}{G_{23}} & 0 & 0 \\[2mm]
0 & 0 & 0 & 0 & \dfrac{1}{G_{31}} & 0 \\[2mm]
0 & 0 & 0 & 0 & 0 & \dfrac{1}{G_{12}}
\end{bmatrix}
\qquad (2.15)
$$

where ;

E_1, E_2, E_3: Young's moduli in 1,2 and 3 directions, respectively.

υ_{ij} : Poison's ratio for transverse strain in the j-direction when stressed in the i-direction, that is

$$
\upsilon_{ij} = - \frac{\varepsilon_j}{\varepsilon_i} \qquad (2.16)
$$

for $\sigma_i = \sigma$ and all other stresses are zero.

G_{23}, G_{31}, G_{12}: Shear moduli in the 2-3, 3-1 and 1-2 planes, respectively.

2.4 Stress-Strain Relations For Plane Stress State In A Composite Lamina.

Most applications of laminated composites are in beams and plates where theory of thin-plates is often considered, so plane stress state will take place .

Generalized stress-strain relations for orthotropic material or a composite lamina can be written , as given before , in the following expanded form:

$$
\begin{bmatrix} \sigma_1 \\ \sigma_2 \\ \sigma_3 \\ \tau_{23} \\ \tau_{13} \\ \tau_{12} \end{bmatrix} = \begin{bmatrix} C_{11} & C_{12} & C_{13} & 0 & 0 & 0 \\ C_{12} & C_{22} & C_{23} & 0 & 0 & 0 \\ C_{31} & C_{32} & C_{33} & 0 & 0 & 0 \\ 0 & 0 & 0 & C_{44} & 0 & 0 \\ 0 & 0 & 0 & 0 & C_{55} & 0 \\ 0 & 0 & 0 & 0 & 0 & C_{66} \end{bmatrix} \begin{bmatrix} \varepsilon_1 \\ \varepsilon_2 \\ \varepsilon_3 \\ \gamma_{23} \\ \gamma_{13} \\ \gamma_{12} \end{bmatrix} \qquad (2.17)
$$

Where now, C_{ij} is the stiffness properties for the composite lamina in 1-2 plane as shown in Fig. 2-5.

For plane stress state, stresses in the direction perpendicular to the 1-2 plane are zero, i.e. $\sigma_3 = \tau_{23} = \tau_{13} = 0$, therefore , stress-train relations for plane stress state in a composite lamina are reduced to the following form. (Jones, 1975, Tsai and Hahn, 1980).

23
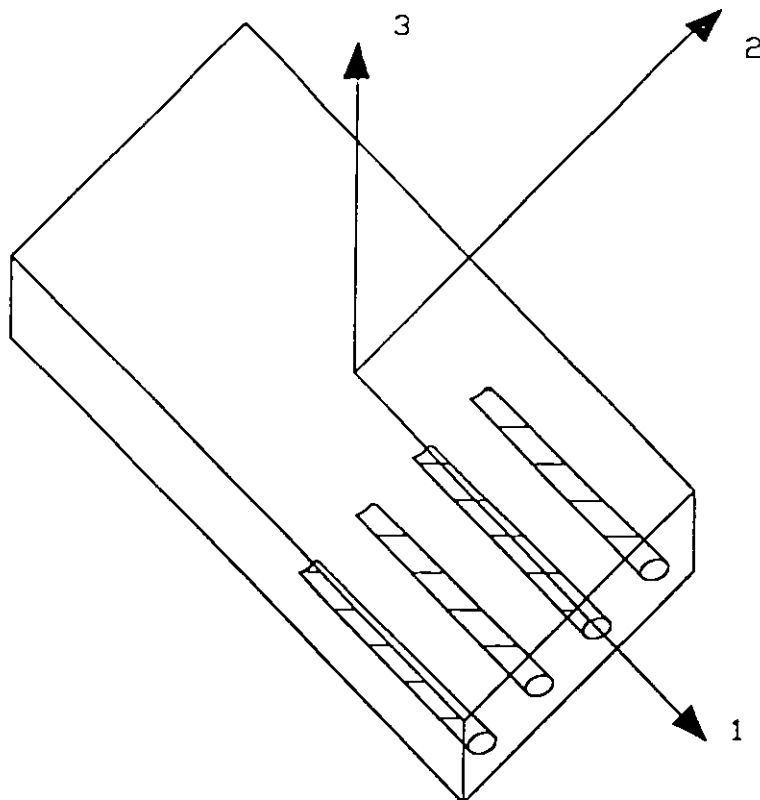
FIG. 2-5. Unidirectional Reinforced Lamina .

$$\begin{bmatrix} \sigma_1 \\ \sigma_2 \\ \tau_{12} \end{bmatrix}_k = \begin{bmatrix} Q_{11} & Q_{12} & 0 \\ Q_{21} & Q_{22} & 0 \\ 0 & 0 & Q_{66} \end{bmatrix}_K \begin{bmatrix} \varepsilon_1 \\ \varepsilon_2 \\ \gamma_{12} \end{bmatrix}_K \tag{2.18}$$

where directions 1 and 2 are the principal material directions, and k is the layer number in a multilayerd laminate, and Q_{ij} are the reduced stiffnesses given by (Jones, 1975, Tsai and Hahn, 1980).

$$Q_{11} = \frac{E_1}{1 - \upsilon_{12}\upsilon_{21}}$$

$$Q_{12} = \frac{\upsilon_{12}E_2}{1 - \upsilon_{12}\upsilon_{21}} = \frac{\upsilon_{21}E_1}{1 - \upsilon_{12}\upsilon_{21}}$$

$$Q_{22} = \frac{E_2}{1 - \upsilon_{12}\upsilon_{21}}$$

$$Q_{66} = G_{12} \tag{2.19}$$

For a lamina shown in Fig. 2-6, the plane stress-strain relations in the x - y plane can be written as (Jones, 1975);

$$\begin{bmatrix} \sigma_x \\ \sigma_y \\ \tau_{xy} \end{bmatrix} = \begin{bmatrix} \overline{Q}_{11} & \overline{Q}_{12} & \overline{Q}_{16} \\ \overline{Q}_{21} & \overline{Q}_{22} & \overline{Q}_{26} \\ \overline{Q}_{61} & \overline{Q}_{62} & \overline{Q}_{66} \end{bmatrix} \begin{bmatrix} \varepsilon_x \\ \varepsilon_y \\ \gamma_{xy} \end{bmatrix} \tag{2.20}$$
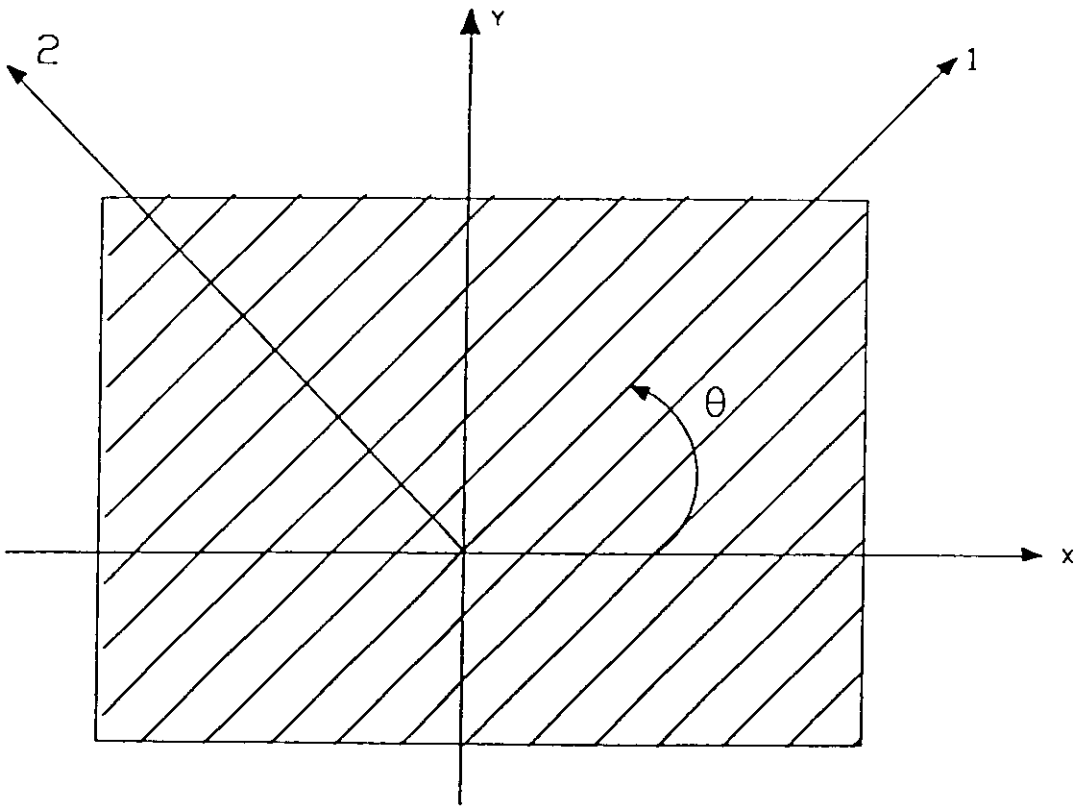
FIG.2-6. Positive Rotation of Principal Material
Axes from the geometry X and y Axes

where $\overline{Q}_{ij}$,called the transformed reduced stiffnesses, are given as (Jones, 1975);

$$\overline{Q}_{11} = Q_{11}\,\text{Cos}^4\,\theta + 2\,(Q_{12} + 2\,Q_{66})\sin^2\theta\theta\,\cos^2\theta + Q_{22}\sin^4\theta$$

$$\overline{Q}_{12} = (Q_{11} + Q_{22} - 4Q_{66})\sin^2\theta\,\cos^2\theta + Q_{12}(\sin^4\theta + \cos^4\theta)$$

$$\overline{Q}_{22} = Q_{11}\,\text{Sin}^4\,\theta + 2\,(Q_{12} + 2Q_{66})\sin^2\theta\,\cos^2\theta + Q_{22}\,\text{Cos}^4\,\theta$$

$$\overline{Q}_{16} = (Q_{11}-Q_{12}-2Q_{66})\sin\theta\,\cos^3\theta + (Q_{12}-Q_{22}+2Q_{66})\sin^3\theta\,\cos\theta$$

$$\overline{Q}_{26} = (Q_{11}-Q_{12}-2Q_{66})\sin^3\theta\,\cos\theta + (Q_{12}-Q_{22}+2Q_{66})\sin\theta\,\cos^3\theta$$

$$\overline{Q}_{66} = (Q_{11} + Q_{22} - 2Q_{12}-2Q_{66})\sin^2\theta\,\cos^2\theta + Q_{66}(\sin^4\theta + \cos^4\theta)$$

$$(\,2.21\,)$$

The positive angle θ is taken from the x-axis to the 1-axis counter clockwise, as shown in Fig. 2-6.

And ε_x, ε_y , and γ_{xy} are the strains at any point through the laminate thickness, and can be given as (Jones, 1975);

$$\varepsilon_x = \varepsilon_x^o + z\,k_x \qquad (2.22)$$

$$\varepsilon_y = \varepsilon_y^o + z\,k_y \qquad (2.23)$$

27

$$\gamma_{xy} = \gamma_{xy}^o + z \, k_{xy} \qquad (2.24)$$

Also, they can be written in the matrix form;

$$\begin{bmatrix} \varepsilon_X \\ \varepsilon_Y \\ \gamma_{XY} \end{bmatrix} = \begin{bmatrix} \varepsilon_x^o \\ \varepsilon_y^o \\ \gamma_{xy}^o \end{bmatrix} + Z \begin{bmatrix} K_x \\ K_y \\ K_{xy} \end{bmatrix} \qquad (2.25)$$

Where ε_x^o, ε_y^o and γ_{xy}^o are the laminate middle surface strains, and they are given as ;

$$\varepsilon_x^o = \frac{\partial u_o}{\partial x} \qquad (2.26)$$

$$\varepsilon_y^o = \frac{\partial v_o}{\partial y} \qquad (2.27)$$

$$\gamma_{xy}^o = \frac{\partial u_o}{\partial y} + \frac{\partial v_o}{\partial x} \qquad (2.28)$$

28

The curvatures K_x, K_y, and K_{xy} of the laminate middle surface are given as (Jones, 1975);

$$K_x = - \frac{\partial w_o^2}{\partial x^2} \tag{2.29}$$

$$K_y = - \frac{\partial w_o^2}{\partial y^2} \tag{2.30}$$

$$K_{xy} = - \frac{2 \partial w_o^2}{\partial x \partial y} \tag{2.31}$$

where ;

u_o, v_o and w_o : The middle surface displacements in x, y, and z directions of the laminate, respectively.

z : The distance from the middle surface of the laminate to any point through its thickness.

Thus, the stresses in the kth layer can be expressed in terms of the laminate middle surface strains and curvatures as;

$$\begin{bmatrix} \sigma_x \\ \sigma_y \\ \tau_{xy} \end{bmatrix}_K = \begin{bmatrix} \overline{Q}_{11} & \overline{Q}_{12} & \overline{Q}_{16} \\ \overline{Q}_{21} & \overline{Q}_{22} & \overline{Q}_{26} \\ \overline{Q}_{61} & \overline{Q}_{62} & \overline{Q}_{66} \end{bmatrix}_K \left\{ \begin{bmatrix} \varepsilon_x^o \\ \varepsilon_y^o \\ \varepsilon_{xy}^o \end{bmatrix} + Z \begin{bmatrix} K_x \\ K_y \\ K_{xy} \end{bmatrix} \right\} \tag{2.32}$$

Also, the stress-strain relation for a composite lamina can be given by using the compliance matrix, S_{ij}, (Jones, 1975).

$$\begin{bmatrix} \varepsilon_1 \\ \varepsilon_2 \\ \gamma_{12} \end{bmatrix} = \begin{bmatrix} S_{11} & S_{12} & 0 \\ S_{21} & S_{22} & 0 \\ 0 & 0 & S_{66} \end{bmatrix} \begin{bmatrix} \sigma_1 \\ \sigma_2 \\ \tau_{12} \end{bmatrix} \tag{2.32}$$

Where

$$S_{11} = \frac{1}{E_1}$$

$$S_{12} = \frac{-\upsilon_{12}}{E_1} = \frac{-\upsilon_{21}}{E_2}$$

$$S_{12} = \frac{1}{E_2}$$

$$S_{66} = \frac{1}{G_{12}} \tag{2.34}$$

and for a generally orthotropic lamina, the strain-stress relationships in the x-y plane are (Jones, 1975);

$$\begin{bmatrix} \varepsilon_x \\ \varepsilon_y \\ \gamma_{xy} \end{bmatrix} = \begin{bmatrix} \overline{S}_{11} & \overline{S}_{12} & \overline{S}_{16} \\ \overline{S}_{21} & \overline{S}_{22} & \overline{S}_{26} \\ \overline{S}_{61} & \overline{S}_{62} & \overline{S}_{66} \end{bmatrix} \begin{bmatrix} \sigma_x \\ \sigma_y \\ \tau_{xy} \end{bmatrix} \tag{2.35}$$

30

where

$$\bar{S}_{11} = S_{11} \cos^4\theta + 2(S_{12} + S_{66})\sin^2\theta \cos^2\theta + S_{22}\sin^4\theta$$

$$\bar{S}_{12} = S_{12}(\sin^4\theta + \cos^4\theta) + (S_{11} + S_{22} - S_{66})\sin^2\theta \cos^2\theta$$

$$\bar{S}_{22} = S_{11}\sin^4\theta + (2S_{12} + S_{66})\sin^2\theta \cos^2\theta + S_{22}\cos^4\theta$$

$$\bar{S}_{16} = (2S_{11} - 2S_{12} - S_{66})\sin\theta \cos^3\theta - (2S_{22} - 2S_{12} - S_{66})\sin^3\theta \cos^4\theta$$

$$\bar{S}_{26} = (2S_{11} - 2S_{12} - S_{66})\sin^3\theta \cos\theta - (2S_{22} - 2S_{12} - S_{66})\sin^3\theta \cos^4\theta$$

$$\bar{S}_{66}$$

$$\bar{S}_{66} = (2S_{11} + 2S_{22} - 4S_{12} - S_{66})\sin^2\theta \cos^2\theta - S_{66}(\sin^4 + \cos^4\theta)$$

(2.36)

For arbitrary orientation of a lamina, the stresses in x and y directions can be transferred to 1 and 2 directions (i.e, principal material directions) by using the transformation matrix [T] as follows   (Jones, 1975, Vinson and Sierakowski, 1986).

$$\begin{bmatrix} \sigma_1 \\ \sigma_2 \\ \tau_{12} \end{bmatrix} = [T] \begin{bmatrix} \sigma_x \\ \sigma_y \\ \tau_{xy} \end{bmatrix}$$

(2.37)

where [T] , the transformation matrix, is given as (Jones, 1975);

2.5 Forces and Moments

By integrating the stresses in each lamina through the laminate thickness, the result will be forces per unit length and moments per unit length acting on the lamina as shown in Fig. 2-7.

$$
\begin{bmatrix} N_x \\ N_y \\ N_{xy} \end{bmatrix} = \int_{-t/2}^{t/2} \begin{bmatrix} \sigma_x \\ \sigma_y \\ \tau_{xy} \end{bmatrix} dz = \sum_{K=1}^{N} \int_{z_{k-1}}^{z_k} \begin{bmatrix} \sigma_x \\ \sigma_y \\ \tau_{xy} \end{bmatrix} dz
\tag{2.40}
$$

and

$$
\begin{bmatrix} M_x \\ M_y \\ M_{xy} \end{bmatrix} = \int_{-t/2}^{t/2} \begin{bmatrix} \sigma_x \\ \sigma_y \\ \tau_{xy} \end{bmatrix} Z\, dz = \sum_{K=1}^{N} \int_{z_{k-1}}^{z_k} \begin{bmatrix} \sigma_x \\ \sigma_y \\ \tau_{xy} \end{bmatrix}_K Z\, dz
\tag{2.41}
$$

where

N_x, N_y, and N_{xy} : Forces per unit length.

M_x, M_y and M_{xy} : Moments per unit length.

t : laminate thickness.

Z_k and Z_{k-1} : Distances of the top and the bottom of a layer, respectively, from the middle axis , and defined in Fig. 2-8.

Note that Zo = -t/2

N : Number of layers in the laminate.
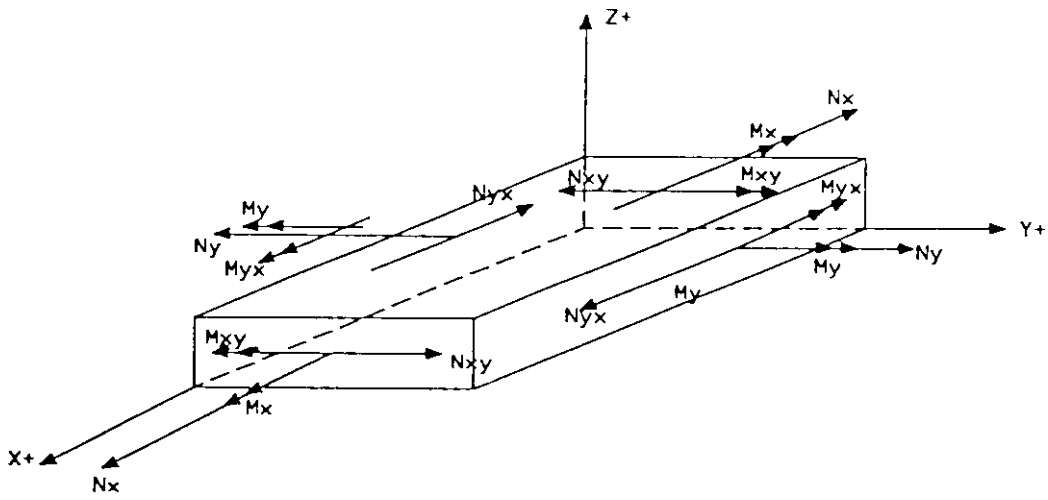
FIG. 2-7. Positive Directions for Stress Resultant and Stress Couples for A Plate .
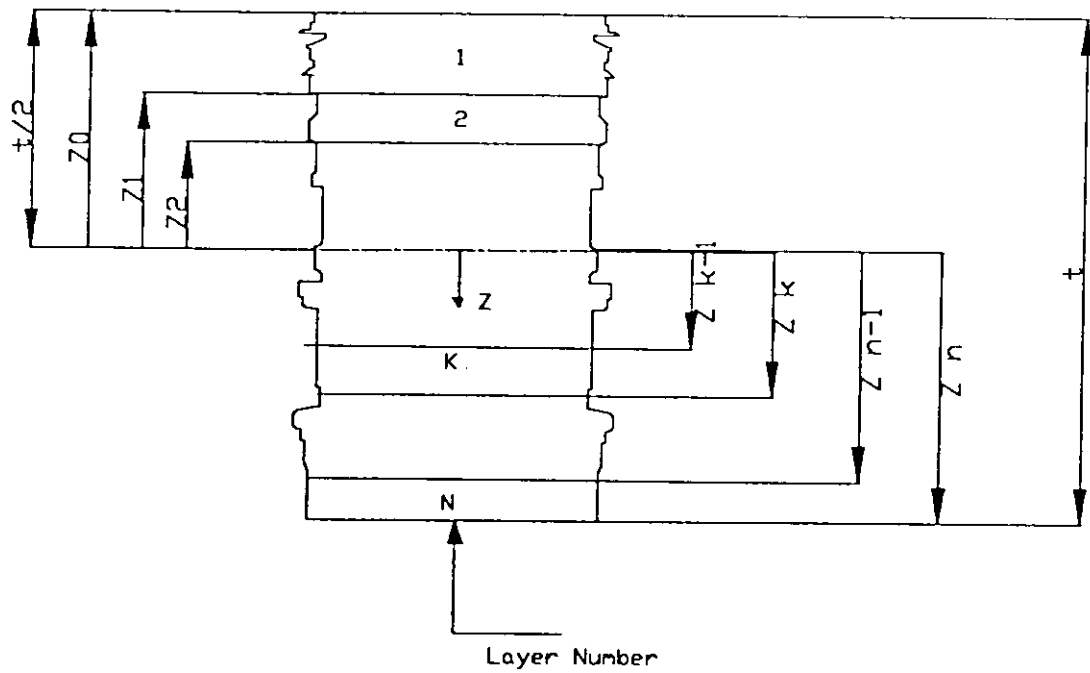
FIG. 2-8. Geometry of an N-Layered Laminate.

The integration indicated in Eqs.(2.40) and (2.41) can be rearranged by replacing the stress vector in these equations with the form in Eq.(2.32) to take the advantage of the fact that the stiffness matrix for a lamina is constant within the lamina.

$$
\begin{bmatrix} N_x \\ N_y \\ N_{xy} \end{bmatrix} = \sum_{K=1}^{N} \begin{bmatrix} \overline{Q}_{11} & \overline{Q}_{12} & \overline{Q}_{16} \\ \overline{Q}_{21} & \overline{Q}_{22} & \overline{Q}_{26} \\ \overline{Q}_{61} & \overline{Q}_{26} & \overline{Q}_{66} \end{bmatrix}_K \left(\int_{z_{k-1}}^{z_k} \begin{bmatrix} \varepsilon_x^o \\ \varepsilon_y^o \\ \gamma_{xy} \end{bmatrix} dz + \int_{z_{k-1}}^{z_k} \begin{bmatrix} k_x \\ k_y \\ K_{xy} \end{bmatrix} Z \, dz \right)
$$

$$(2.42)$$

and

$$
\begin{bmatrix} M_x \\ M_y \\ M_{xy} \end{bmatrix} = \sum_{K=1}^{N} \begin{bmatrix} \overline{Q}_{11} & \overline{Q}_{12} & \overline{Q}_{16} \\ \overline{Q}_{21} & \overline{Q}_{22} & \overline{Q}_{26} \\ \overline{Q}_{61} & \overline{Q}_{62} & \overline{Q}_{66} \end{bmatrix}_K \left(\int_{z_{k-1}}^{z_k} \begin{bmatrix} \varepsilon_x \\ \varepsilon_y \\ \gamma_{xy}^o \end{bmatrix} Z dz + \int_{z_{k-1}}^{z_k} \begin{bmatrix} K_x \\ k_y \\ K_{xy} \end{bmatrix} Z^2 dz \right)
$$

$$(2.43)$$

Since the middle surface strain ($\varepsilon_x^o, \varepsilon_y^o$ and γ_{xy}^o) and middle surface curvatures (k_x, k_y and k_{xy}) are independent of Z, these values can be removed out of the integration sings. Therefore, Eqs. (2.42) and (2.43) can be rearranged as (Jones, 1975, Vinson and Sierakowski, 1986).

$$\begin{bmatrix} N_x \\ N_y \\ N_{xy} \end{bmatrix} = \begin{bmatrix} A_{11} & A_{12} & A_{16} \\ A_{21} & A_{22} & A_{26} \\ A_{61} & A_{62} & A_{66} \end{bmatrix} \begin{bmatrix} \varepsilon_x^o \\ \varepsilon_y^o \\ \gamma_{xy}^o \end{bmatrix} + \begin{bmatrix} B_{11} & B_{12} & B_{16} \\ B_{21} & B_{22} & B_{26} \\ B_{61} & B_{62} & B_{66} \end{bmatrix} \begin{bmatrix} K_x \\ K_y \\ K_{xy} \end{bmatrix}$$

$$(2.44)$$

and ,

$$\begin{bmatrix} M_x \\ M_y \\ M_{xy} \end{bmatrix} = \begin{bmatrix} B_{11} & B_{12} & B_{16} \\ B_{21} & B_{22} & B_{26} \\ B_{61} & B_{62} & B_{66} \end{bmatrix} \begin{bmatrix} \varepsilon_x^o \\ \varepsilon_y^o \\ \gamma_{xy}^o \end{bmatrix} + \begin{bmatrix} D_{11} & D_{12} & D_{16} \\ D_{21} & D_{22} & D_{26} \\ D_{61} & D_{62} & D_{66} \end{bmatrix} \begin{bmatrix} K_x \\ K_y \\ K_{xy} \end{bmatrix}$$

$$(2.45)$$

where

A_{ij} is   the extensional stiffnesses and

$$A_{ij} = \sum_{k=1}^{N} (\overline{Q}ij)_k (Z_k - Z_{k-1}) \qquad (2.46)$$

B_{ij} is   the coupling stiffnesses and

$$B_{ij} = \frac{1}{2} \sum_{k=1}^{N} (\overline{Q}ij)_k (Z_k^2 - Z_{k-1}^2) \qquad (2.47)$$

D_{ij} is   the bending siffnesses and

$$D_{ij} = \frac{1}{3} \sum_{k=1}^{N} (\overline{Q}ij)_k (Z_k^3 - Z_{k-1}^3) \qquad (2.48)$$

Also, A_{ij}, B_{ij} and D_{ij} matrices can be written in terms of the layer thickness (t_k) and the distance to the centroid of the kth layer (Jones, 1975).

$$A_{ij} = \sum_{k=1}^{N} (\overline{Q}ij)_k (t_k) \qquad (2.49)$$

$$B_{ij} = \sum_{k=1}^{N} (\overline{Q}ij)_k (t_k) (\overline{Z}_K) \qquad (2.50)$$

$$D_{ij} = \sum_{k=1}^{N} (\overline{Q}ij)_k (t_k \overline{Z}_k^2 + \frac{t_k^3}{12}) \qquad (2.51)$$

It is seen that the [A] matrix is the extensional stiffnesses matrix relating the in-plane stress resultants (N's) to the mid - surface strains (ε^o's), and the [D] matrix is the flexural stiffness matrix relating the stress couples (M's) to the curvatures (K's). Since the [B] matrix relates (M's) to (ε^o's) and (N's) to (K's), it is called the bending-stretching coupling matrix (Vinson and Sierakowski, 1986).

2.6 Middle Surface Strains And Curvatures

The resultant forces and moments given in Eqs. (2.44) and (2.45) can be written in the compact form (Jones, 1975).

$$\begin{bmatrix} N \\ M \end{bmatrix} = \begin{bmatrix} A & B \\ B & D \end{bmatrix} \begin{bmatrix} \varepsilon^o \\ K \end{bmatrix} \qquad (2.52)$$

or

$$N = A \, \varepsilon^o + Bk \qquad (2.53)$$

$$M = B \varepsilon^o + DK \qquad (2.54)$$

Solving Eq. (2.53) for ε^o :

$$\varepsilon^o = A^{-1} \, N - A^{-1} \, B \, K \qquad (2.55)$$

Whereupon Eq. (2.54) becomes ;

$$M = B \, A^{-1} \, N + (-BA^{-1} \, B + D) K \qquad (2.56)$$

Eqs. (2.55) and (2.56) can be written in matrix form;

$$\begin{bmatrix} \varepsilon^o \\ M \end{bmatrix} = \begin{bmatrix} A^{-1} & -A^{-1}B \\ BA^{-1} & D - BA^{-1}B \end{bmatrix} \begin{bmatrix} N \\ K \end{bmatrix} \qquad (2.57)$$

or

$$\varepsilon^o = A^* N + B^* K \qquad (2.58)$$

$$M = H^* N + D^* K \qquad (2.59)$$

Solving Eq.(2.59) for (k) and substitute in Eq.(2.58) to get :

$$K = D^{*-1} M - D^{*-1} H^* N \tag{2.60}$$

$$\varepsilon^o = B^* D^{*-1} M + (A^* - B^* D^{*-1} H^*) N \tag{2.61}$$

Thus,

$$\begin{bmatrix} \varepsilon^o \\ K \end{bmatrix} = \begin{bmatrix} A^* - B^* D^{*-1} H^* & B^* D^{*-1} \\ -D^{*-1} H^* & D^{*-1} \end{bmatrix} \begin{bmatrix} N \\ M \end{bmatrix} \tag{2.62}$$

or rewrite Eq. (2.62) as (Jones, 1975).

$$\begin{bmatrix} \varepsilon^o \\ K \end{bmatrix} = \begin{bmatrix} a_1 & b_1 \\ h_1 & d_1 \end{bmatrix} \begin{bmatrix} N \\ M \end{bmatrix} \tag{2.63}$$

wherein (h_1) can be shown to be equal to (b_1) by virtue of the symmetry of A,B and D matrices and the definitions of the a_1, b_1, d_1, A*, B* and D* matrices, and the matrix coefficients in Eq. (2.63) are symmetric (Jones, 1975).

2.7 Symmetric Laminates

2.7.1 Introduction

When the structure is exactly symmetric about its middle surface, this requires symmetry in laminate properties, oreintation, and location from the middle surface , all of the Bij components are

equal to zero, for the symmetry of the $(\overline{Q_{ij}})_k$ and the thickness (t_k). such laminates are usually much easier to analyze than laminates with coupling, unless some applications require structures with an unsymmetric laminates (Jones, 1975, Whitney, 1987).

Therefore, Eqs.(2.44) and (2.45) for symmetric laminates are simplified to :

$$
\begin{bmatrix} N_x \\ N_y \\ N_{xy} \end{bmatrix} = \begin{bmatrix} A_{11} & A_{12} & A_{16} \\ A_{21} & A_{22} & A_{26} \\ A_{61} & A_{62} & A_{66} \end{bmatrix} \begin{bmatrix} \varepsilon_x^o \\ \varepsilon_y^o \\ \gamma_{xy}^o \end{bmatrix} \tag{2.64}
$$

and

$$
\begin{bmatrix} M_x \\ M_y \\ M_{xy} \end{bmatrix} = \begin{bmatrix} D_{11} & D_{12} & D_{16} \\ D_{21} & D_{22} & D_{26} \\ D_{61} & D_{62} & D_{66} \end{bmatrix} \begin{bmatrix} Kx \\ Ky \\ Kxy \end{bmatrix} \tag{2.61}
$$

Special cases of symmetric Laminates will be described in the following subsections.

2.7.2 Cross - Ply Laminates

A special case of symmetric laminates, regular cross-ply laminates, occurs when the laminae are all of the same thicknesses and material properties, but have their major principal material

directions alternating at 0^0 and 90^0 to the laminate axes. The laminate must have an odd number of layers to be considered as a symmetric laminates, for example $90^{\circ}/0^{\circ}/90^{\circ}$, where fibrous direction of even -numbered layers are in the 1- direction of the laminate, and the odd-numbered layers are in the 2- direction of the laminate as shown in Fig. 2-9.

A more general example of symmetric cross- ply laminate is shown in Table 2-1.

TABLE 2-1 Symmetric cross-ply Laminate with five layers

Layer	Material properties				Orientation	Thickness
k	Q_{11}	Q_{12}	Q_{22}	Q_{66}	θ	t_k
1	H_1	H_2	H_3	H_4	0°	$2h^\circ$
2	G_1	G_2	G_3	G_4	90°	$4h^\circ$
3	H_1	H_2	H_3	H_4	0°	$2h^\circ$
4	G_1	G_2	G_3	G_4	90°	$4h^\circ$
5	H_1	H_2	H_3	H_4	0°	$2h^\circ$

For symmetric cross-ply laminates, resultant forces and moments, in which there is no bending -extension coupling can be given as (Jones, 1975).

FIG. 2-9. View of Unbonded Three Layered Regular Symmetric Cross-Ply Laminate.

$$
\begin{bmatrix} N_x \\ N_y \\ N_{xy} \end{bmatrix} = \begin{bmatrix} A_{11} & A_{12} & 0 \\ A_{12} & A_{22} & 0 \\ 0 & 0 & A_{66} \end{bmatrix} \begin{bmatrix} \varepsilon_x^o \\ \varepsilon_y^o \\ \gamma_{xy}^o \end{bmatrix} \qquad (2.66)
$$

and

$$
\begin{bmatrix} M_x \\ M_y \\ M_{xy} \end{bmatrix} = \begin{bmatrix} D_{11} & D_{12} & 0 \\ D_{21} & D_{22} & 0 \\ 0 & 0 & D_{66} \end{bmatrix} \begin{bmatrix} K_x \\ K_y \\ K_{xy} \end{bmatrix} \qquad (6.67)
$$

As shown above, values of A_{16}, A_{26}, D_{16} and D_{26} are equal to zero, for the zero values of $(\overline{Q}_{16})_k$ and $(\overline{Q}_{26})_k$. Where $(\overline{Q}_{16})_k$ and $(\overline{Q}_{26})_k$ are zero for lamina principal material property orientations of $0°$ and $90°$ to the laminate coordinate axes.

If one consider the special, but practical, case of odd-numbered layers with equal thicknesses and even- numbered layers with equal thicknesses, but not necessarily the same as that of the odd-numbered layers. Then, two geometrical parameters are important : N, the total number of layers, and M, the ratio of the total thickness of odd-numbered layers to the total thickness of even-numbered layers (called the cross-ply ratio) (Jones, 1975). Thus,

$$
M = \frac{\sum_{k=odd} t_k}{\sum_{k=even} t_k} \qquad (2.68)
$$

44

For example, the cross-ply ratio, M, for the liminate given in Table 2-1 is calculated as ;

$$M = \frac{2h^o + 2h^o + 2h^o}{4h^o + 4h^o} = \frac{3}{4}$$

where h^o has a constant value.

Also, for such laminates, the ratio of principal lamina siffnesses , F, can be defined as (Jones, 1975) ;

$$F = \frac{Q_{22}}{Q_{11}} = \frac{E_2}{E_1} \qquad (2.69)$$

Therefore, the laminate siffnesses, A_{ij}, B_{ij} and D_{ij}, can be given in terms of N,M and F (Jones, 1975) ;

.

$$A_{11} = \frac{1}{(1+M)} \ (M+F) \, tQ_{11}$$

$$A_{12} = tQ_{12}$$

$$A_{22} = \frac{1+MF}{M+F} \ A_{11}$$

$$A_{16} = A_{26} = 0$$

$$A_{66} = t Q_{66} \qquad (2.70)$$

$$B_{ij} = O \qquad (2.71)$$

$$D_{11} = \frac{[(F-1)P+1]Q_{11}t^3}{12}$$

$$D_{12} = \frac{Q_{12}t^3}{12}$$

$$D_{22} = \frac{[(1-F)P+1]Q_{11}t^3}{12}$$

$$D_{16} = D_{26} = O$$

$$D_{66} = \frac{Q_{66}t^3}{12} \qquad (2.72)$$

Where

$$P = \frac{1}{(1+M)^3} + \frac{M(N-3)[M(N-1)+2(N+1)]}{(N^2-1)(1+M)^3} \qquad (2.73)$$

2.7. 3 Angle -Ply Laminates

Regular symmetric angle-ply laminate has orthortropic laminae of equal thicknesses and opposite signs of the angle of orientation of the principal material properties with respect to the

laminate axes, and to satisfy the symmetry requirement there must be an odd number of layers. For example an angle-ply laminate with 3-layers arranged in the following sequence $+\theta$ / $-\theta$ / $+\theta$, as shown in Fig. 2-10.

A more general example of symmetric angle-ply laminate is shown in Table 2-2.

TABLE 2-2 Symmetric angle-ply Laminate with five layers

Layer	Material Properties				Orientation	Thickness
k	Q_{11}	Q_{12}	Q_{22}	Q_{66}	θ	t_k
1	N_1	N_2	N_3	N_4	$+60°$	$2h°$
2	R_1	R_2	R_3	R_4	$-30°$	$4h°$
3	L_1	L_2	L_3	L_4	$+15°$	$2h°$
4	R_1	R_2	R_3	R_4	$-30°$	$4h°$
5	N_1	N_2	N_3	N_4	$+60°$	$2h°$

The force and moment resultants for symmetric angle-ply laminate can be written as (Jones, 1975).

$$\begin{bmatrix} N_x \\ N_y \\ N_{xy} \end{bmatrix} = \begin{bmatrix} A_{11} & A_{12} & A_{16} \\ A_{21} & A_{22} & A_{26} \\ A_{61} & A_{62} & A_{66} \end{bmatrix} \begin{bmatrix} \varepsilon_x^o \\ \varepsilon_y^o \\ \gamma_{xy}^o \end{bmatrix}$$
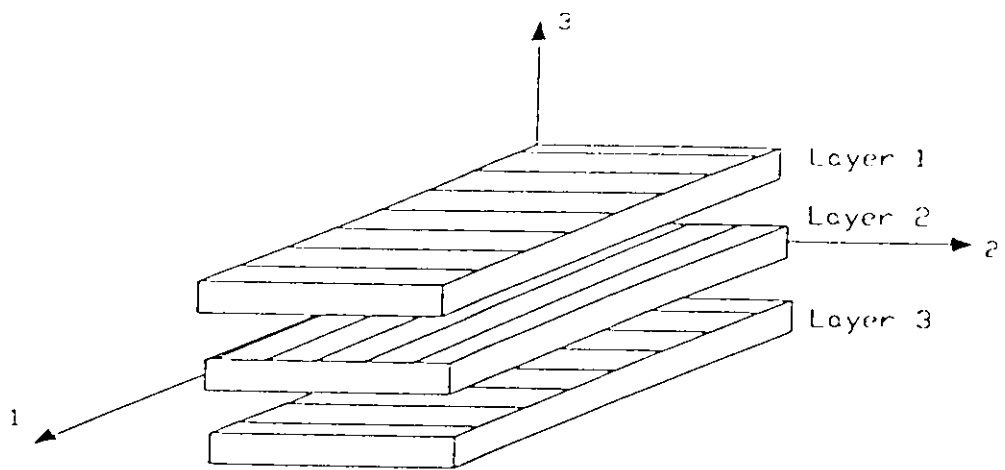
(2.74)

and
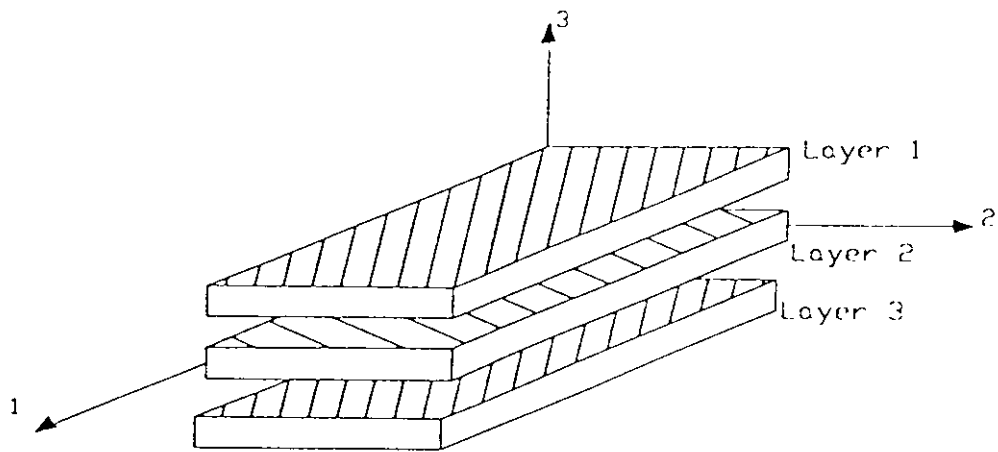
FIG. 2-10. View of Unbonded Three Layered Regular Symmetric Angle-Ply Laminate.

$$\begin{bmatrix} M_x \\ M_y \\ M_{xy} \end{bmatrix} = \begin{bmatrix} D_{11} & D_{12} & D_{16} \\ D_{21} & D_{22} & D_{26} \\ D_{61} & D_{62} & D_{66} \end{bmatrix} \begin{bmatrix} K_x \\ K_y \\ K_{xy} \end{bmatrix}$$

(2.75)

The laminate stiffnesses for a symmetric angle-ply laminate can be given as (Jones, 1975);

$$A_{11}, A_{12}, A_{22}, A_{66}, = t\,(\bar{Q}_{11}, \bar{Q}_{12}, \bar{Q}_{22}, \bar{Q}_{66})$$

$$A_{16}, A_{26}, = \frac{t}{N}\,(\bar{Q}_{16}, \bar{Q}_{26})$$

(2.76)

$$B_{ij} = 0$$

(2.77)

$$D_{11}, D_{12}, D_{22}, D_{66} = \frac{t^3}{12}\,(\bar{Q}_{11}, \bar{Q}_{12}, \bar{Q}_{22}, \bar{Q}_{66})$$

$$D_{16}, D_{26}, = \frac{t^3}{12}\left(\frac{3N^2 - 2}{N^3}\right)(\bar{Q}_{16}, \bar{Q}_{26})$$

(2.78)

All the A_{ij} and D_{ij} are required because of coupling between forces and shearing strain, shearing force and normal strain, a normal moment and twist, and twisting moment and normal strains. But values of A_{16}, A_{26}, D_{16} and D_{26} decrease in proportion to $(1/N)$ as N increases, where N is the number of layers in the symmetric angle-ply laminate (Jones, 1975). Also, small values of A_{16}, A_{26}, D_{16} and D_{26} can be quite small when compared to the other elements in A_{ij} and D_{ij}, respectively.

FAILURE THEORIES

3.1 Introduction

Failure of a structure can be defined by the occurrence of yielding or fracture of the material of that structure, where yielding will occur when a slip between two planes of atoms takes place, while fracture is the separation of a material under stresses into two or more parts (Jones, 1975); Therefore, many theories and models were developed to study the failure behavior of a structural material.

The failure behavior of fibrous composites differs considerably from that of homogeneous isotropic solids due to the large number of possible failure mechanisms in a loaded composite materials (Herrmann and Ferber, 1992), and because of various characteristics of composite materials, it is difficult to determine a strength theory in which all failure modes and their interactions are properly accounted for.

Failure modes can be either fiber dominated, matrix dominated or interface dominated, for example; fiber breaks, matrix and interface cracks, fiber pull out as well as the plastification of the matrix material (Herrmann and Ferber, 1992, Harris et al., 1988). But these basic micromechanics would appear as more important features to material scientists or material designers, for structural designers the important

element to consider is the lamina made of a chosen fiber-matrix system.

Strength theories of fibrous composites are based mainly on macromechanical behavior of composites, which predict the failure of a composite subjected to combined loading . These failure theories are necessarily anisotropic and generally form various extensions of the isotropic yield criteria. However, the prediction of yield surfaces in unidirectional metal matrix composites necessitates a micromechanics analysis because the yielding of the matrix is a localized phenomenon which requires a sufficiently accurate stress analysis of the representative volume element.(Aboudi, 1988), for example;

Pindera and Aboudi (1988) prepared a micromechanics model to generate initial yield surfaces of unidirectional and laminated metal matrix composites under a variety of loading conditions.

In this study, the lamina is assumed to be macroscopically homogeneous, linearly elastic and orthotropic, and the fibers and matrix are homogeneous, linearly elastic and isotropic.

Also, the fibers are assumed to be perfectly aligned and regularly spaced and the bond between the fibers and the matrix is considered to be perfect.

If the laminate stresses are known, then the stresses in each lamina (in the principal material directions) can be compared with the
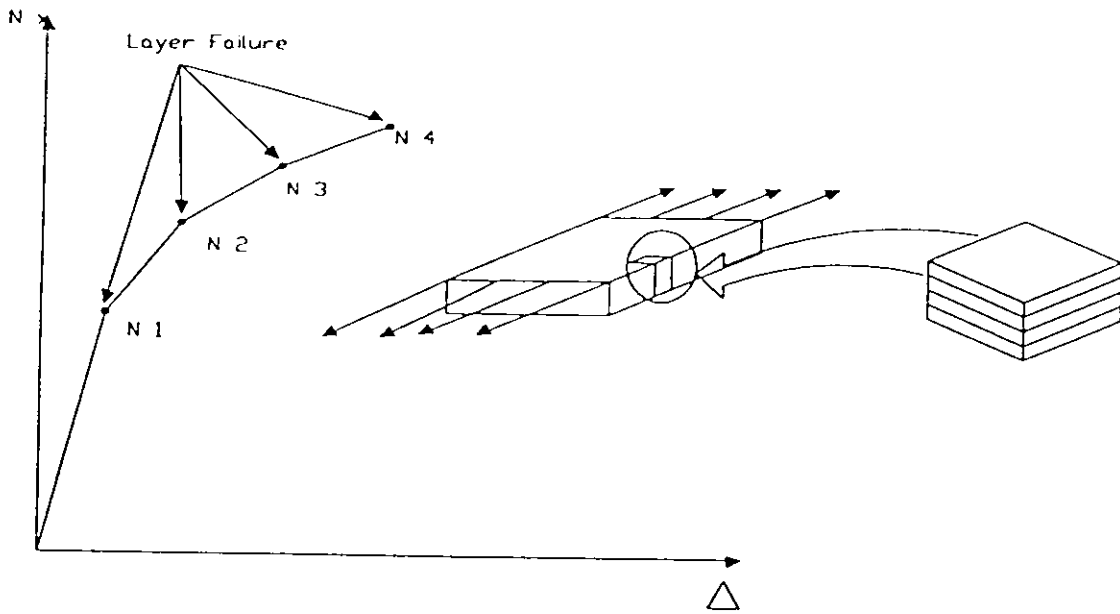
FIG. 3-1 Laminate Load-Deformation Behavior.

3.2 Literature Review of Failure Theories

Prediction of the failure strength of a material under effective stresses is very important to determine either the laminate characteristics necessary to withstand a given load or the maximum load a given laminate can withstand. To solve this problem, many theories and models were developed, and in this section some of these failure theories are presented.

The Maximum Principal Stress Theory was one of the earliest failure theories proposed by Rankine (1858) for the yielding of homogeneous isotropic material. This theory assumes failure to take place when the stress in a structural element exceeds the yield strength of the material in a simple tension or Compression test (Vinson and Sierakowski, 1986).

The Maximum Strain Theory proposed by Saint Venant (1797) for homgeneous isotropic material. This theory states that failure occurs when at any point in a structural element the maximum strain at that point reaches the yield value equal to that occurring in a simple uniaxial tension or compression test (Jones, 1975, Popov, 1968).

Two other failure criteria for homogeneous isotropic materials are the Maximum Shear Theory often referred to as Tresca's Theory and the Distortion Energy Criteria often referred to as Von Mises Criterion (Vinson and Sierakowski, 1986).

Maximum Shear Stress Theory suggests that yielding will occur in a material when the maximum shear stress in the material equals the maximum shear stress at yielding due to simple tension test.

Distortion Energy Criteria was attributed to Von Mises (1913). This theory assumes that yielding will take place when the distortional energy at any point in the body becomes equal to corresponding energy due to yielding in the simple tension test (Vinson and Sierakowski, 1986).

But fibrous composites are both heterogeneous and orthotropic, so the previous mentioned criteria and new other theories were extended for such composite materials.

Jenkins (1920) extended the Maximum Stress Theory to orthotropic materials. He stated that failure will occur when one or all of the orthotropic stress values exceed their maximum limits as obtained in uniaxial tension, Compression, or pure shear stress tests (Vinson and Sierakowski, 1986).

The Maximum Strain Theory extended by Waddoups (1967) assumes that failure will occur when the resulting strains along the principal material directions exceed their limiting values.

Hill (1948) initiated one of the earliest interactive failure criterion for anisotropic materials. This theory is a generalization of the isotropic yield behavior of ductile metals for the case of large strains (Vinson and Sierakowski, 1986).

An extension to Hill's criterion to account for unequal tension and compression for anisotropic materials was introduced by Marin (1956). Another extension was carried out by introducing nine stress components to define failure; three tensile, three compressive and three shear strength components.

The plane stress results by Hill were simplified for the case of fiber reinforced composites by Azzi and Tsai (1965) by assuming the composite material to be transversely isotropic. Hoffamn (1967) generalized this theory by considering the effect of brittle materials (Vinson and Sierakowski, 1986).

A generalization of Hoffman result was proposed by Tsai and Wu (1971) to incorporate a more comprehensive definition for failure (Vinson and Sierakowski, 1986).

Tennyson et al. have shown that the failure surface in three-dimensional (3-D) stress space is not closed in the compression-compression quadrant. Thus, infinite strengths are predicted . An analytical model was developed by Jaing and Tennyson (1989) to ensure the closure of the cubic tensor polynomial failure surface.

Feng (1991) introduced a failure criterion based on the strain invariants of finite elasticity. This criterion assumes the failure to occur at the position of maximum strain energy density. Another criterion developed by sandhu (1976) , was based on the concept that the lamina fails when the sum of the ratios of current energy levels to the corresponding maximum energies equals unity.

A new failure criteria based on the total strain energy density of an equivalent linear elastic system was developed by Abu-Farsakh and Abdel-Jawad (1994). In this criterion the multi-nonlinear responses of the material were taken into account. This criterion will be called AF - AJ Criterion.

3.3 Description of Failure Criteria

In this section , some of failure criteria mentioned previously will be described under plane stress conditions.

3.3.1 Maximum Stress Theory

Maximum Stress Theory assumes that failure occurs when the stress in any of the principal material directions $(\sigma_1, \sigma_2, \tau_{12})$ exceeds the maximum strength of the material in that direction, that is (Jones, 1975);

$$\sigma_1 > X_k$$

$$\sigma_2 > Y_k$$

$$|\tau_{12}| > S \qquad\qquad (3.1)$$

where

X_k, Y_k, and S are maximum strength of material (lamina) in principal material directions, k = t for tension and k = c for compression, and 1,2 are principal material directions.

X_k, Y_k, and S are maximum strength of material (lamina) in principal material directions, k = t for tension and k = c for compression, and 1,2 are principal material directions.

Note that shear strength is independent on the sign of τ_{12}.

3.3.2 Maximum Strain Theory

Maximum Strain Theory assumes that failure occurs when the strain in any of the principal material directions ($\varepsilon_1, \varepsilon_2, \gamma_{12}$) exceeds its limiting values, so failure will take place when one of the following inequalities is violated (Jones, 1975);

$$\varepsilon_1 < X_{\varepsilon_k}$$

$$\varepsilon_2 < Y_{\varepsilon_k}$$

$$|\gamma_{12}| < S_\varepsilon \qquad (3.2)$$

where

(X_ε, Y_ε and S_ε) are the maximum strains in the principal material directions, k = t for tension and k = c for compression and 1,2 are material principal directions.

3.3.3 Tsai - Hill Criterion

Hill developed a yield criterion for anisotropic materials which can be written in terms of the stress components as (Vinson and Sierakowki, 1986) ;

$$(G + H) \, \sigma_1^2 + (F + H) \, \sigma_2^2 + (F + G) \, \sigma_3^2 - 2H \, \sigma_1 \sigma_2 - 2G\sigma_1 \sigma_3 - 2F\sigma_2 \sigma_3 + 2L \, \tau_{23}^2 + 2M \, \tau_{13}^2 + 2N\tau_{12}^2 = 1 \qquad (3.3)$$

where the quantities F, G, H, L, M, and N reflect the current state of material anisotropy.

For unidirectional reinforced composites M = N, G = H. Therefore,

$$F(\sigma_2 - \sigma_3)^2 + G(\sigma_3 - \sigma_1)^2 + G(\sigma_1 - \sigma_2)2 + 2L\tau_{23}^2 + 2M(\tau_{31}^2 + \tau_{12}^2) = 1 \qquad (3.4)$$

For a composite lamina or laminates in a plane stress, Eq. (3.4) becomes (Vinson and Sierakowki, 1986) ;

$$F\sigma_2^2 + G\sigma_1^2 + H(\sigma_1 - \sigma_2)^2 + 2N \, \tau_{12}^2 = 1 \qquad (3.5)$$

Now to find values of F, G, H and N in terms of the lamina strengths in principal material directions (X, Y, and S). We can assume that only σ_1 acts on the body with its maximum value X. Then by returning to Eq. (3.3), this case will result in ;

$$G + H = \frac{1}{X^2} \qquad (3.6)$$

Similarly, if only σ_2 acts on the body, then

$$F + H = \frac{1}{Y^2} \tag{3.7}$$

And if only τ_{12} acts on the body, then

$$2N = \frac{1}{S^2} \tag{3.8}$$

Now if the strength in the 3- direction is denoted by Z and just σ_3 acts on the body, then

$$F + G = \frac{1}{Z^2} \tag{3.9}$$

By using Eqs. (3.7), (3.8) and (3.9) the following relations between F, G and H and X, Y, and Z can be written as ;

$$2H = \frac{1}{X^2} + \frac{1}{Y^2} - \frac{1}{Z^2} \tag{3.10}$$

$$2G = \frac{1}{X^2} - \frac{1}{Y^2} + \frac{1}{Z^2} \tag{3.11}$$

$$2F = \frac{1}{Y^2} + \frac{1}{Z^2} - \frac{1}{X^2} \tag{3.12}$$

Now by using the relations in Eq. (3.10) and by considering plane stress state, Eq. (3.5) can be rewritten in the following form;

$$\frac{\sigma_1^2}{X^2} + \frac{\sigma_2^2}{Y^2} - \frac{\sigma_1 \sigma_2}{X^2} + \frac{\tau_{12}^2}{S^2} = 1 \tag{3.13}$$

3.3.4 Tsai - Wu Criterion

This theory incorporates unequal tensile and compressive failure strengths as an inherent part of development . In this criterion failure is assumed to occur when the following equation is satisfied (Vinson and Sierakowki, 1986) ;

$$F_i \, \sigma_i \; = F_{ij} \, \sigma_i \, \sigma_i \; = 1 \qquad (i,j = 1,2 \; ...., 6) \qquad (3.14)$$

where the quantities F_i and F_{ij} are related to tensile and compressive yield strengths of the material.

For the case of plane stress state , Eq. (3.12) can be written in the following expanded form;

$$F_1 \, \sigma_1 + F_2 \, \sigma_2 + F_6 \, \tau_{12} + F_{11} \, \sigma_1^2 + F_{22} \, \sigma_2^2 + F_{66} \, \tau_{12}^2 + 2F_{12} \, \sigma_1 \sigma_2 = 1$$

$$(3.15)$$

where F_1, F_2, F_6, F_{11}, F_{22}, F_{66}, and F_{12} can be given as (Vinson and Sierakowki, 1986) ;

$$F_1 \; = \; \frac{1}{Xt} + \frac{1}{Xc}$$

$$F_{11} \; = \; \frac{-1}{Xt \, Xc}$$

$$F_2 = \frac{1}{Yt} + \frac{1}{Yc}$$

$$F_{22} = \frac{-1}{Yt\,Yc}$$

$$F_6 = \frac{1}{S+} - \frac{1}{S-}$$

$$F_{66} = \frac{1}{S^+S^-} \qquad (3.16)$$

By noting that shear strength in material principal directions is independent of the sign of the shear stress then;

$$F_6 = 0$$

$$F_{66} = \frac{1}{S^2} \qquad (3.17)$$

The remaining stress (F_{12}) is determined from a biaxial tension test where $\sigma_1 = \sigma_2 = \sigma^*$ and all other stresses are zero. After the biaxial tensile failure stress, σ^*, is determined and substituted in Eq. (3.13), the following result is obtained ;

$$F_1 \sigma^* + F_2 \sigma^* + F_{11} \sigma^{*2} + F_{22} \sigma^{*2} + 2F_{12} \sigma^{*2} = 1 \qquad (3.18)$$

Then , F_{12} can be obtained by using Eqs. (3.14) and (3.16) F_{12} can be given as;

$$F_{12} = \frac{1}{2}\sqrt{F_{11}F_{22}} \qquad (3.19)$$

3.3.5 Sandhu Criterion

This failure criterion assumes failure to occur in the lamina when the following equation is satisfied (Sandhu, 1976).

$$k_1 \left(\int_{\varepsilon_1} \sigma_1 d\varepsilon_1 \right)^{m1} + K_2 \left(\int_{\varepsilon_2} \sigma_2 d\varepsilon_2 \right)^{m2} + k_6 \left(\int_{\varepsilon_6} d\varepsilon_6 \right)^{m6} = 1 \tag{3.20}$$

where

$$Ki = \left(\int_{\varepsilon_{iu}} \sigma_i d\varepsilon_i \right)^{mi} \tag{3.21}$$

For i = 1,2 , and 6. where (ε_{iu}) are the principal ultimate strain components obtained from simple loading test and (m_i) are called the shape factors, parameters define the shape of the failure surface in the strain-energy space, and these factors are determined by using experimental data (Vinson and Sierakowki, 1986) ;

3-4 Analysis Procedure

In this section, a procedure for prediction of the failure load and its location is given in step by step as shown in the flow chart in Fig. 3-2. The methodology is to obtain the strength of the lamina by increasing the applied load gradually until the first-ply failure of the laminate occurs.

During each increment of the load, stresses and strains of each lamina are computed and transformed from x-y plane to the orthotropy plane. These transformed values can be used in one of the previous criteria, so failure can be predicted and located for the laminate . The analysis procedure can be summarized in the following steps:

1- Calculate lamina stiffnesses in the orthotropy plane by using either the lamina properties or the stiffnesses of the fibers and the matrix.

2- Calculate transformed stiffnesses for each lamina corresponding to the positive angle (θ) from the x - axis.

3- Calculate laminate stiffnesses [A] , [B] and [D] .

4- Calculate middle surface strains and curvatures of the laminate.

5- For each lamina, calculate its strains in the x-y plane.

6- From strains in step (5) , calculate lamina strains in 1-2 plane by using the transformation matrix, [T].

7- Calculate stresses for each lamina in principal material directions.

8- Stresses in step (7) can be used in a selected failure criterion to predict failure.

9- If no lamina fails, the load is increased and steps 4, 5, 6, 7, and 8 are repeated, successively.

10- If a lamina fails, the load and location of the failure are recorded.

```
┌─────────────────────────────────────────┐
│                 START                     │
└─────────────────────────────────────────┘

        ┌─────────────────────────────┐
        │     PROPERTIES OF THE        │
        │     FIBERS AND MATRIX        │
        └─────────────────────────────┘

   ┌──────────────────────────────────────┐
   │  LAMINA STIFFNESSES IN   1-2  PLANE    │
   └──────────────────────────────────────┘

   ┌──────────────────────────────────────┐
   │  TRANSFORMED LAMINA STIFFNESSES        │
   │         IN  X-Y PLANE                  │
   └──────────────────────────────────────┘

      ◇ UNSYMMETRY ◇        ◇ SYMMETRY ◇

   ┌──────────────┐      ┌──────────────┐
   │ STIFFNESSES  │      │ STIFFNESSES  │
   │  MATRICES    │      │  MATRICES    │
   │ [A],[B],[D]  │      │  [A],[D]     │
   └──────────────┘      └──────────────┘

   ┌──────────────────────────────────────┐
   │   CALCULATE COMPLIANCE MATRICES        │
   └──────────────────────────────────────┘

   ┌──────────────────────────────────────┐
   │ CALCULATE MID-SURFACE DEFORMATIONS     │
   │    DUE  TO  THE APPLIED LOAD           │
   │       [ε]_{xy} , [K]_{xy}              │
   └──────────────────────────────────────┘
```

2   1
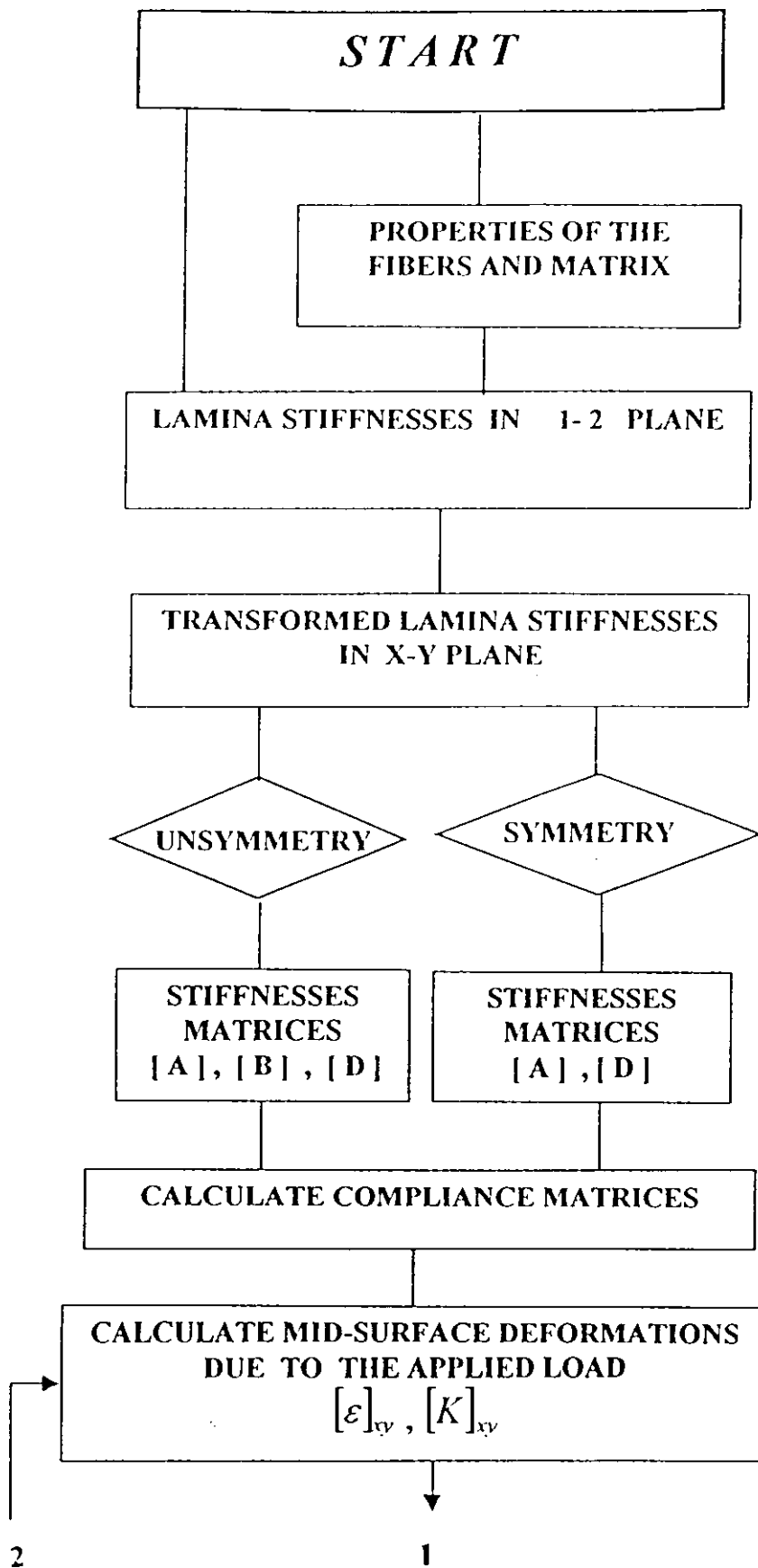
CHAPTER FOUR

Bending Of Composite Plates And Beams

4.1 Introduction

In Chapter 2, the governing constitutive equations were developed in detail describing the relationships between resultant forces (N_x, N_y, N_{xy}), resultant moments (M_x, M_y, M_{xy}), in-plane midsurface strains ($\varepsilon_x^o, \varepsilon_y^o, \varepsilon_{xy}^o$), and the curvatures ($K_x$, K_y, K_{xy}) as seen in Eqs. (2.44) and (2.45). These will be utilized with the strain–displacement relations and equilibrium equations, which will be given later in section (4.2) to develop structural theories for thin walled bodies, the structural from in which fibrous composite materials are most generally employed.

Also, in this chapter, plates and beams under different loading and supporting conditions will be studied to develop the governing differential equations for these structures. Then, these equations can be solved by using a direct method approach to find maximum stresses and deflections, so maximum stresses in each ply of the laminated composite can be compared with a selected failure criterion.

The laminated composite is considered to be symmetric (i.e, $B_{ij} = 0$), has no other coupling terms, $(\ )_{16} = (\ )_{26} = 0$, no surface shear stresses and no hygrothermal effects , Also , as in classical plate theory, transverse shear deformation is excluded, that is $\varepsilon_{xz} = \varepsilon_{yz} = 0.$ (Vinson and Sierakowski, 1986).

Special cases of loading and supporting conditions will be taken into consideration to show the analysis procedure.

4.2 Equilibrium Equations

In mathematically modeling solid materials, including the laminates, a continuum theory is generally employed where a representative material point within the elastic solid is selected as being typical of all materials points in the body or lamina. The material point is given a convenient shape; in this study the convenient shape is a small cube of dimensions dx, dy and dz as shown in Fig. 4-1.

In addition to the surface stresses acting on the control element shown in Fig 4-1, body force components F_x, F_y and F_z can also act on the body proportional to the control element volume (i.e, its mass) such as gravitational , magnetic or centrifugal forces (Vinson and Sierakowski, 1986).

A force balance can be made in the x, y and z directions resulting in three equations of equilibrium, respectively;
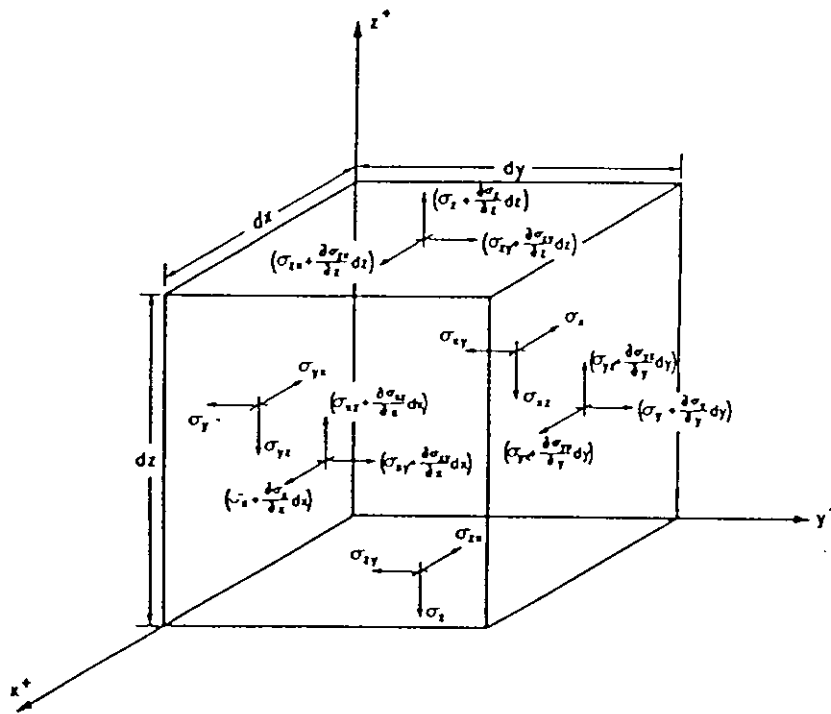
Fig.4-1. Coordinate system , geometry , and nomenclature .

$$\frac{\partial \sigma_x}{\partial x} + \frac{\partial \sigma_{yx}}{\partial y} + \frac{\partial \sigma_{zx}}{\partial z} + F_x = o \qquad (4.1)$$

$$\frac{\partial \sigma_{xy}}{\partial x} + \frac{\partial \sigma_y}{\partial y} + \frac{\partial \sigma_{zy}}{\partial z} + F_y = o \qquad (4.2)$$

$$\frac{\partial \sigma_{xz}}{\partial x} + \frac{\partial \sigma_{yz}}{\partial y} + \frac{\partial \sigma_z}{\partial z} + F_z = o \qquad (4.3)$$

For beam and plate theory, whether involving composite materials or not, one must integrate the stresses across the thickness of the thin walled structures to obtain solutions (Vinson and Sierakowski, 1986).

4.3 Bending Of Composite Plates

4.3.1 The Governing Differential Equation

A rectangular thin plate is defined as a body of length (a) in the x-direction, width (b) in the y-direction, and thickness (h) in the z-direction, where h << b, and h < a as shown in Fig. 4-2.

Consider a plate made of a laminated composite material that is symmetric and no body forces act on it.

The equilibrium equations for bending of such plates due to lateral loads are given as (Vinson and Sierakowski, 1986).

$$\frac{\partial M_x}{\partial x} + \frac{\partial M_{xy}}{\partial y} - Qx = o \qquad (4.4)$$
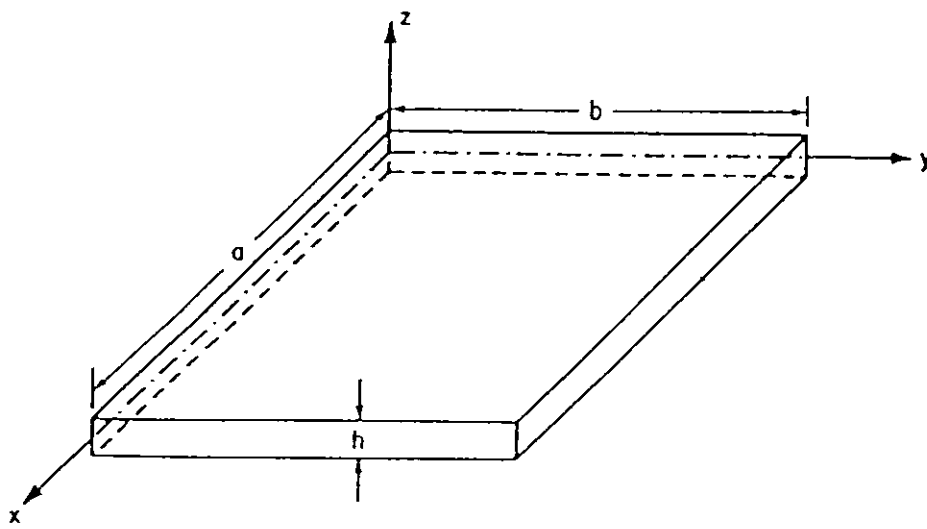
Fig.4-2. A rectangular thin plate .

$$\frac{\partial M_{xy}}{\partial x} + \frac{\partial M_y}{\partial y} - Qy = o \qquad (4.5)$$

$$\frac{\partial Q_x}{\partial x} + \frac{\partial Q_y}{\partial y} - P(x,y) = o \qquad (4.6)$$

Where

Q_x and Q_y are shear resultants in the z- direction defined by (Jones, 1975).

$$\begin{bmatrix} Q_x \\ Q_y \end{bmatrix} = \sum_{k=1}^{N} \int_{Z_{k-1}}^{Z_k} \begin{bmatrix} \sigma_{xz} \\ \sigma_{yz} \end{bmatrix} dZ_k \qquad (4.7)$$

Where

Z_k and Z_{k-1} are defined in Fig. 2-8.

$$p(x.y) = P_1(x,y) - P_2(x,y) \qquad (4.9)$$

Where

$$P_1(x,y) = \sigma_z(Z_n)$$

$$P_2(x,y) = \sigma_z(Z_o)$$

Without going into details and by following the derivation given by Vinson and Sierakowski (1986), the governing differential equation for bending of a plate composed of a composite material, excluding transverse shear deformation, no coupling terms ($B_{ij} = (\ )_{16} = (\ )_{26} = 0$), no hygrothermal terms and subjected to a lateral distributed load p (x,y) is given as ;

$$D_1 \frac{\partial^4 w}{\partial x^4} + 2D_3 \frac{\partial^4 w}{\partial x^2 \partial y^2} + D_2 \frac{\partial^4 w}{\partial y^4} = P(x,y)$$

(4.10)

Where

$$D_1 = D_{11}$$

$$D_2 = D_{22}$$

$$D_3 = (D_{12} + 2 D_{66})$$

(4.11)

Where D_{11}, D_{22}, D_{12} and D_{66} are elements in the [D] matrix and defined by Eq. (2.48).

Solution of Eq. (4.10) can be obtained by using direct methods, which fall into three categories: Navier Solutions, Levy Solutions and Perturbation Solutions. Each of them has its advantages and disadvantages (Vinson and Sierakowski, 1986).

4.3.2   Plate Boundary Conditions

In classical plate theory, only two boundary conditions are needed at each edge of the plate and they are identical to those of classical beam theory.

For Simply supported edge, the boundary conditions are ;

$$w = o$$

$$M_n = \frac{\partial^2 w}{\partial n^2} = o$$

(4.12)

For clamped edge, the boundary conditions are ;

$$w = o$$

$$\frac{\partial w}{\partial n} = o$$

(4.13)

For free edge , Kirchoff formulated an approximate solution with the boundary condition (Vinson and Sierakowski, 1986, Vinson and Chou, 1975);

$$M_n = o$$

$$V_n = Q_n + \frac{\partial M_{nt}}{\partial t} = o \qquad (4.14)$$

Where (n) is the direction normal to the plate edge, (t) is the direction parallel or tangent to the edge, V_n is the effective shear resultant, Q_n is given by equation (4.1) or (4.5) , M_n and M_{nt} is given by (2.45).

4.3.3 Navier Solutions For Plates Of Composite Materials

As mentioned before, three methods can be used to solve the governing differential equations for bending of plates, the method that will be considered is the Navier solutions. In the Navier approach for the case of the plate being simply supported on all four edges, one simply expands the lateral deflection, w (x, y) and the applied lateral load p (x, y) into a doubly infinite half range sine series because that series satisfies all of the boundary conditions (4.12) exactly . (Vinson and Sierakowski, 1986).

$$w(x,y) = \sum_{m=1}^{\infty} \sum_{n=1}^{\infty} A_{mn} \; Sin\frac{m\pi x}{a} \; Sin\frac{n\pi y}{b} \qquad (4.15)$$

$$P(x,y) = \sum_{m=1}^{\infty} \sum_{n=1}^{\infty} B_{mn} \; Sin\frac{m\pi x}{a} \; Sin\frac{n\pi y}{b} \qquad (4.16)$$

4.3.4 Uniformly Loaded Simply Supported Plate

A case study is taken so that the laminated plate is subjected to a uniformly lateral load, $P(x,y) = \bar{P}_o$, and simply supported on all four edges. The governing differential equations for such plates are solved by using Navier Direct Method for its excellent results for plates with all four edges simply supported as mentioned in (Vinson and Sierakowski, 1986).

Using the Navier Method discussed previously it is found that the stresses in each lamina for the case of $p(x,y) = \bar{P}_o$ are given by (Vinson and Sierakowski, 1986).

$$
\begin{bmatrix} \sigma_x \\ \sigma_y \\ \tau_{xy} \end{bmatrix}_k = \frac{16\, P_o\, z}{\pi^3} \sum_{m=1,3,5}^{\infty} \sum_{n=1,3,5}^{\infty} \frac{1}{mnD}
$$

$$
* \begin{bmatrix} \left[-Q_{11}^k \left(\frac{m}{a}\right)^2 - Q_{12}^k \left(\frac{n}{b}\right)^2 \right] & \sin\frac{m\pi x}{a}\cdot\sin\frac{n\pi y}{b} \\ \left[-Q_{12}^k \left(\frac{m}{a}\right)^2 - Q_{22}^k \left(\frac{n}{b}\right)^2 \right] & \sin\frac{m\pi x}{a}\cdot\sin\frac{n\pi y}{b} \\ \left[2Q_{66}^k \left(\frac{m}{a}\right)\left(\frac{n}{b}\right)\cos\frac{m\pi x}{a}\cos\frac{n\pi y}{b} \right] & \end{bmatrix}
$$

where (4.17)

$$
D = D_{11}\left(\frac{m}{a}\right)^4 + 2(D_{12} + 2D_{66})\left(\frac{mn}{ab}\right)^2 + D_{22}\left(\frac{n}{b}\right)^4
\tag{4.18}
$$

4.4 Beams And Rods Of Composite Materials
4.4.1 Simple Beam Theory

When the structure of Fig. 4-3 is subjected to a lateral load in the x-z plane, in the z- direction, the term beam is used to describe this structure, while when the same structure is loaded in the x- direction by tensile or compressive forces, the term rod or column is used, respectively.

Because the beam is so narrow (b <<L), strains are ignored in the y-direction, implying that all Poisson's ratio effects can be ignored (that is a classical beam assumption), and for simplicity, the beam has a mid-plane symmetry and has no hygrothermal effects. Lastly, there is no y- direction dependence on any quantity involved in the set of governing equations. The beam will only react to the difference between P_1 and P_2, the normal surface tractions on the top and bottom surfaces, hence (Vinson and Sierakowski, 1986).

$$P(x) = P_1 - P_2 \qquad (4.18)$$

The remaining constitutive equations for this beam are (Vinson and Sierakowski, 1986).

$$\begin{bmatrix} N_x \\ M_x \end{bmatrix} = \begin{bmatrix} A_{11} & 0 \\ 0 & D_{11} \end{bmatrix} \begin{bmatrix} \varepsilon_x^o \\ K_x \end{bmatrix} \qquad (4.19)$$
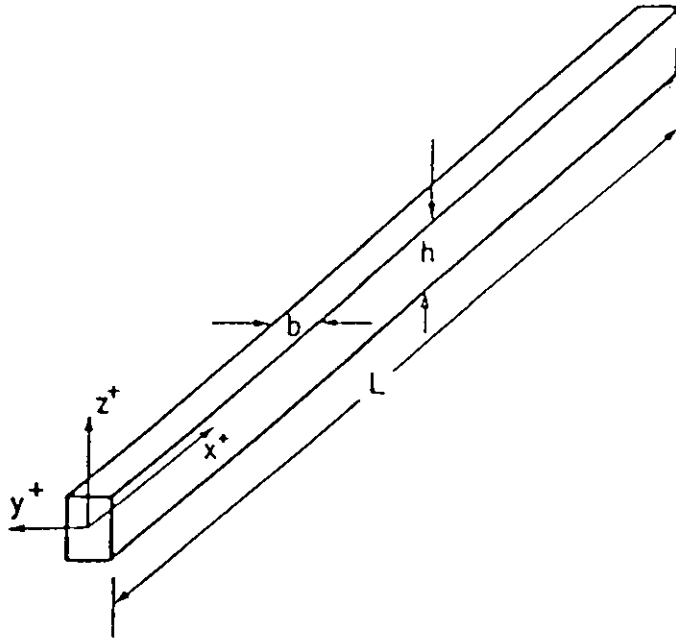
78

Fig.4-3. Nomenclature for a beam , column or rod .

Returning to the plate equilibrium equations in section 4.2, and from the beam assumptions made, the remaining equilibrium equations become (Vinson and Sierakowski, 1986).

$$\frac{dN_x}{dx} = o \tag{4.20}$$

$$\frac{dQ_x}{dx} + P(x) = o \tag{4.21}$$

$$\frac{dM_x}{dx} - Q_x = o \tag{4.22}$$

Since nothing varies in the y-direction for the beam, it is both traditional and easy to multiply all of the above equations by the beam width, b, hence:

$P = N_x\, b$

$V = Q_x\, b$

$M_b = M_x\, b$

$$q(x) = P(x)\, b \tag{4.23}$$

Therefore, the governing equations for a beam of composite materials subjected to lateral and in-plane loads and by ignoring hygrothermal effects and transverse shear deformation are (Vinson and Sierakowski, 1986).

$$P = b\, A_{11}\, \frac{du_o}{dx} \tag{4.24}$$

$$M_x = -b\, D_{11}\, \frac{d^2 w}{dx^2} \tag{4.25}$$

$$\frac{dp}{dx} = o \qquad\qquad (4.26)$$

$$\frac{dV}{dx} + q(x) = o \qquad\qquad (4.27)$$

$$\frac{dM_b}{dx} - V = o \qquad\qquad (4.28)$$

Integration of Eq. (4.24) gives the relation for the mid-surface in-plane displacement, u_0 :

$$u_0\,(x) = \left(\frac{P}{bA_{11}}\right)X + C_o \qquad\qquad (4.29)$$

Where

C_0 is constant of integration and can be determined by where $u_0\,(x)$ is specified. Note that P is constant as given in Eq. (4.26).

If a rod is loaded by a tensile axial load P only, Eq. (4.29) provides the displacement, from which all stresses in every ply can be determined by (Vinson and Sierakowski, 1986).

$$[\sigma_x]_k = [\overline{Q_{11}}]_k \ [\varepsilon_x^o] = [\overline{Q_{11}}]_k \ \left(\frac{du_o}{dx}\right) \qquad\qquad (4.30)$$

For the case where P is a compressive load, the same applies, except if the load P that would cause buckling is sought , a more refined theory is needed (Vinson and Sierakowski, 1986).

Substituting Eq. (4.25) into Eq. (4.28) and the result into Eq. (4.27) results in the following governing differential equation for bending of the beam :

$$bD_{11} \frac{d^4w}{dx^4} = q(x) \tag{4.31}$$

Once the solution of w (x) is found from (4.31) the stresses in each ply can be calculated by :

$$[\sigma_x]_k = z \left[\overline{Q_{11}}\right]_k [K_x] = -\left[\overline{Q_{11}}\right]_k z \frac{d^2w}{dx^2} \tag{4.32}$$

Now, if both in-plane and lateral loads occur simultaneously, then the stresses in each ply are found by the sum of Eqs. (4.30) and (4.32);

$$[\sigma_x]_k = \left[\overline{Q_{11}}\right]_k \frac{du_o}{dx} - \left[\overline{Q_{11}}\right]_k z \frac{d^2w}{dx^2} \tag{4.33}$$

4.4.1 Simplified Cases Of Composite Beam Solutions

For the bending of a beam, the solution of the governing differential Eq. (4.31) will result in four constants of integration which are used to solve boundary conditions at each end of the beam.

There are three boundary conditions: simple- support, clamped and free.

For simply supported edge:

$$w = o \qquad M_b = o \tag{4.34}$$

For clamped edge:

$$w = o \qquad \frac{dw}{dx} = o \tag{4.35}$$

For free edge :

$$M_b = o \qquad V_b = o \tag{4.36}$$

4.4.2.1 Clamped - Clamped Beam With A Uniform Lateral Load

If a beam is clamped at each end and subjected to a uniform lateral load, $q(x) = q_o$, where q_o is constant as shown in Fig 4-4 , then the solution of the governing differential equation results in the following form :

$$w(x) = \frac{-q_o}{bD_{11}} \frac{x^4}{24} + \frac{C_1 x^3}{6} + \frac{C_2 x^2}{2} + C_3 x + C_4 \qquad (4.37)$$

Where constants C_1 through C_2 can be determined by using the boundary conditions, Therefore,

$$C_1 = \frac{q_o L}{2bD_{11}} \qquad\qquad C_2 = \frac{-q_o L^2}{12bD_{11}} \qquad C_3 = C_4 = o \qquad (4.38)$$

Finally,

$$w(x) = \frac{-q_o}{24bD_{11}} \left[x^4 - 2Lx^3 + L^2 x^2 \right] \qquad (4.39)$$

Where the maximum deflection is :

$$W_{(max)} = w(L/2) = \frac{-q_o L^4}{384bD_{11}} \qquad (4.40)$$

To find maximum stresses in each ply, it is essential to evaluate the maximum bending moment, $M_{b(max)}$, and maximum curvature , $k_{x(max)}$. From Eqs. (4.25) and (4.39)

$$M_b = -bD_{11} \frac{d^2 w}{dx^2} = \frac{q_o}{12} \left[6xL - 6Lx + L^2 \right] \qquad (4.41)$$

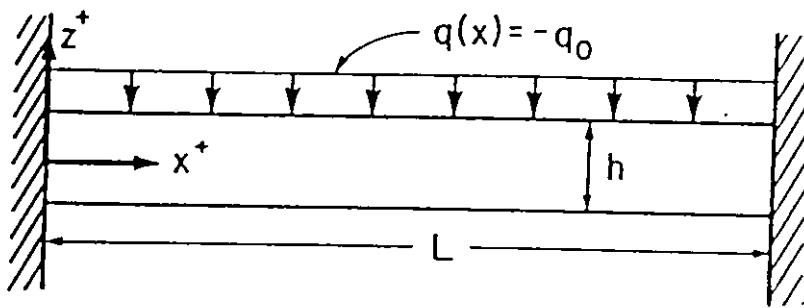Where the maximum bending moment occurs at $x = o$ and L , and is

Fig.4-4.Clamped-Clamped beam with a uniform lateral load .

$$M_{b(max)} = M_b(o, L) = \frac{q_o L^2}{12} \tag{4.42}$$

And the maximum Curvature is given by

$$K_{x(max)} = \frac{M_{b(max)}}{bD_{11}} = +\frac{q_o L^2}{12 \, bD_{11}} = \frac{-d^2 w}{dx^2} \tag{4.43}$$

Then, the maximum stress can be calculated for each ply through (4.32) ;

$$[\sigma_x]_{k \, (max)} = [\overline{Q_{11}}] [K_{x(max)}] Z = -[\overline{Q_{11}}] \left(\frac{d^2 w}{dx^2}\right)_{max} z \tag{4.44}$$

Then, this $[\sigma_x]_{k \, (max)}$ can be compared with the allowable strength values for each lamina with its specific orientation and composite material system (Vinson and Sierakowski, 1986).

4.4.2.2 Clamped – Free Beam Subjected To A Uniform Lateral Load.

Consider a beam cantilevered from the end x= o as shown in Fig. 4-5. The deflection can be determined by using Eqs. (4.37), (4.35) and (4.36) as ;

$$w(x) = \frac{-q_o}{24bD_{11}}\left[x^4 - 4Lx^3 + 6L^2 x^2\right] \tag{4.45}$$
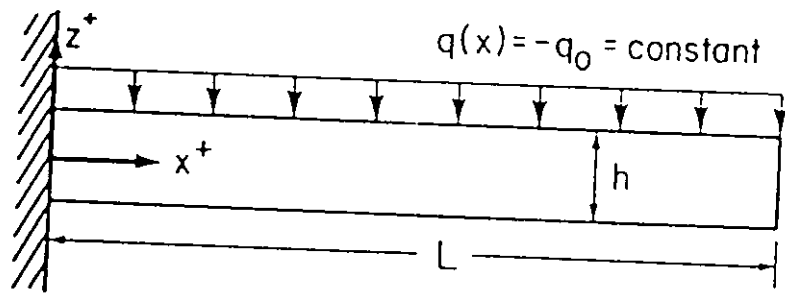
Fig.4-5.Clamped free beam with a uniform lateral load .

And therefore, maximum deflection and bending moment are given as;

$$w_{(max)} = w(L) = \frac{-q_o L^4}{8bD_{11}}$$

(4.46)

$$M_{b(max)} = M_b(0) = \frac{q_o L^3}{2}$$

(4.47)

Then, maximum stresses in such laminated composite beam are given by

$$\sigma_{x(max)} = \left[\overline{Q_{11}}\right]_k Z \quad K_{x(max)}$$

(4.48)

Where

$$K_{x(max)} = K_x(o) = \frac{M_b}{bD_{11}} = \frac{q_o L^2}{2bD_{11}}$$

(4.49)

CHAPTER FIVE
RESULTS AND DISCUSSION

5.1 Introduction

In the previous chapters, theory and applications of fiber-reinforced composites are studied for special cases of laminated composites; regular cross-ply laminates and regular angle-ply laminates. Also, bending in composite plates and beams is investigated under different uniformly lateral loads with simply-supported boundary conditions for the plate and with clamped-clamped and clamped-free boundary conditions for the beam.

In this study, three composite materials are considered. These materials are selected for their wide usage in industry, and they are:

- Glass-epoxy 3M XP251S.

- E glass-epoxy.

- Boron-epoxy Narmco 5505.

Mechanical properties of these materials are given in Table 5-1,where the mechanical properties of many other composite materials are given in Appendix A. Typical stress-strain curves for born-epoxy and glass-epoxy are adapted from (Jones, 1975) and given in Appendix B.

Variations in lamina stiffnesses, $\bar{Q}_{ij}$, with angle of orientation, θ, are studied and presented in Fig.5-1 through Fig. 5-6 . Also , variations in the elements of the compliance matrix, $\bar{S}_{ij}$, are studied and presented in Fig. 5-7 through Fig. 5-12. Also , for a symmetric cross-ply laminate , the relation between the extensional stiffnesses, A_{11} and A_{22} , and the cross-ply ratio, M, and stiffness ratio, F, are presented in charts.

Failure of a single lamina made of boron-epoxy is determined for different angle of rotation from the x-axis.

TABLE 5-1. Typical mechanical properties of composites used in the study (Jones, 1975, Vinson and Sierakowski, 1986)

Property	Glass-epoxy 3M XP251S	E glass-epoxy	Boron-epoxy Narmco 5505
E_1 $(10^6 psi)$	7.80	8.80	30.100
E_2 $(10^6 psi)$	2.00	3.68	2.870
υ_{12}	0.25	0.23	0.225
G_{12} $(10^6 psi)$	1.30	1.74	0.800
X_t $(10^3 psi)$	150.00	187.00	197.500
Y_t $(10^3 psi)$	4.00	119.00	7.800
S $(10^3 psi)$	6.00	6.67	9.300
X_c $(10^3 psi)$	150.00	25.30	417.658
Y_c $(10^3 psi)$	20.00	6.50	37.885

Numerical results of two different failure theories, Tsai-Hill theory and Tsai-Wu theory, are determined and studied for the two

special cases of laminated composites; regular cross-ply laminate and regular angle-ply laminate, so these results can be compared together and with other available results in literature. The applied loads are per unit area.

Stresses and deflections in plates and beams subjected to a uniformly lateral load are studied and presented in charts for two cases; the first one is studying bending in plates and beams made of three unidirectional layers $\theta_k = o$, where k is the layer number. The other case is studying bending in plates and beams made of three cross-ply layers with $0°/90°/0°$ stacking sequence.

A Computer program using FORTRAN 77 is developed by Abu-Ayada (1998) to study the mechanical behavior of Fibrous composites is extended to the applications in this work, and other computer programs are developed to study the failure due to bending stresses in composite structures.

All numerical results are presented and discussed in the following subsections.

5.2 Variations In Lamina Properties With Angle Of Orientation

5.2.1 Variations In Lamina Stiffness

Equations (2.21) show how the lamina stiffness vary with angle of rotation, θ, Fig. 5-1 through Fig. 5-6 show the variation of stiffness, $\overline{Q}_{ij}$, with angle of rotation for the E glass-epoxy composite material. One can note that the variation of $\overline{Q}_{11}$ is similar to that of $\overline{Q}_{22}$ but out of phase, where maximum value of $\overline{Q}_{11}$ occurs at 0° and 180° while for these two angles the value of $\overline{Q}_{22}$ is minimum. $\overline{Q}_{12}$

and $\overline{Q}_{66}$ vary in a similar manner and they are in phase. Also, there is some similarity in the variations of $\overline{Q}_{16}$ and $\overline{Q}_{26}$.

The dependence of $\overline{Q}_{ij}$ on angle θ holds true regardless of the material properties.

5.2.2 Variations In Lamina Compliances.

Equations (2.36) show how the lamina compliances vary with angle of rotation, θ. Fig.5-7 through Fig.5-12 show the variation of compliance , $\overline{S}_{ij}$, with angle of rotation for the E glass-epoxy composite material.

Variation in $\overline{S}_{11}$ with angle θ is similar to that of $\overline{S}_{22}$ but out of phase; the maximum values of $\overline{S}_{11}$ occurs at $\theta = 90°$ and minimum at $\theta = 0°$ and $180°$, where the maximum value of $\overline{S}_{22}$ occurs at $\theta = 0°$ and $180°$ and minimum at $\theta = 90°$. $\overline{S}_{12}$ has negative values of all θ, and $\overline{S}_{16}$ and $\overline{S}_{26}$ are negative for $\theta \langle 90°$, and with zero values at $\theta = 0°$, $90°$ and $180°$. Finally $\overline{S}_{66}$ has its maximum value at $\theta = 0°$, $90°$ and $180°$ and its minimum at $\theta = 45°$ and $135°$.

It is obvious to mention that the designer can make the lamina in the laminated composite with different rotation angles to get the best properties, $\overline{Q}_{ij}$ and $\overline{S}_{ij}$ of the lamina to control on stresses and strains in different axes.
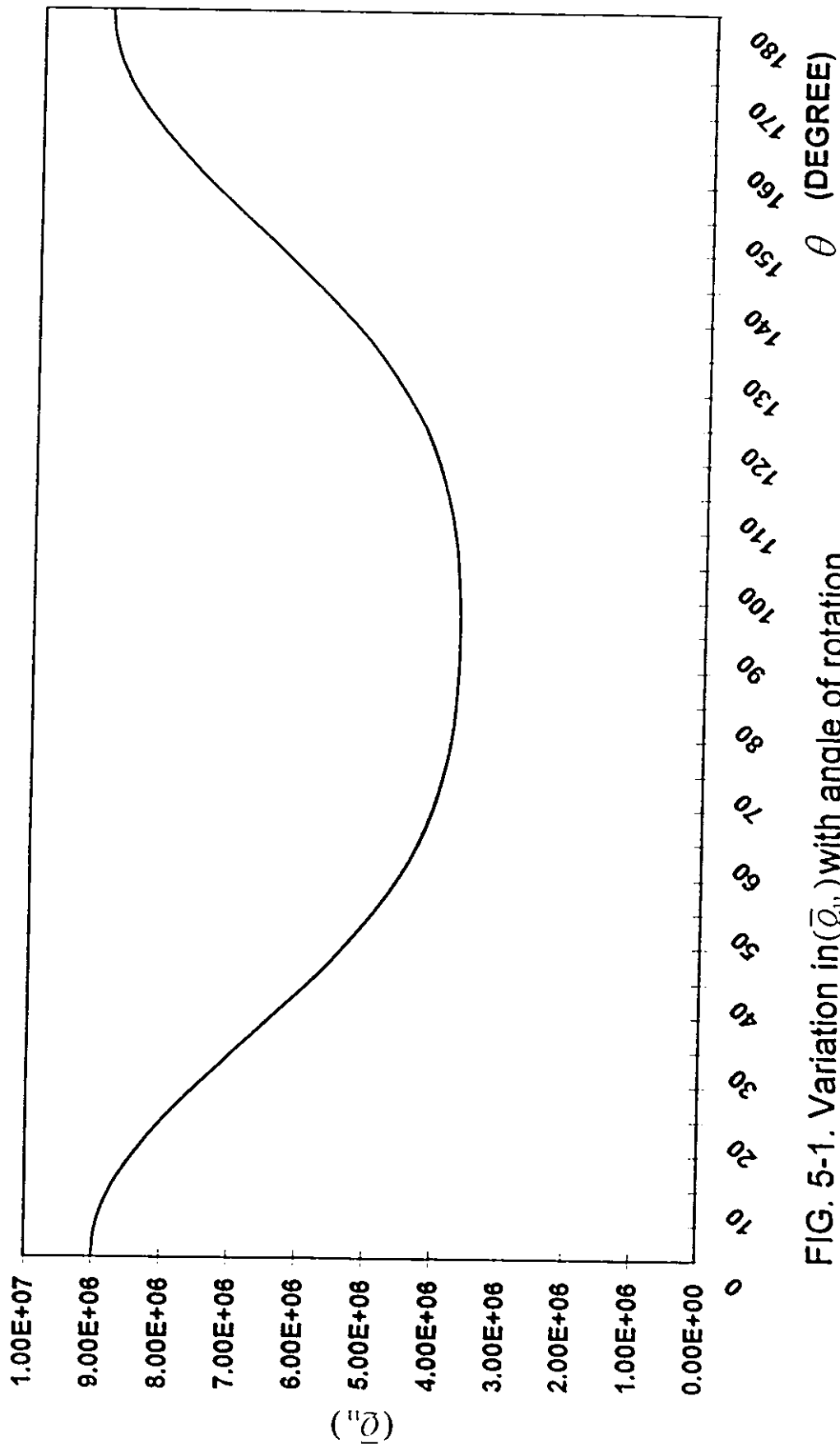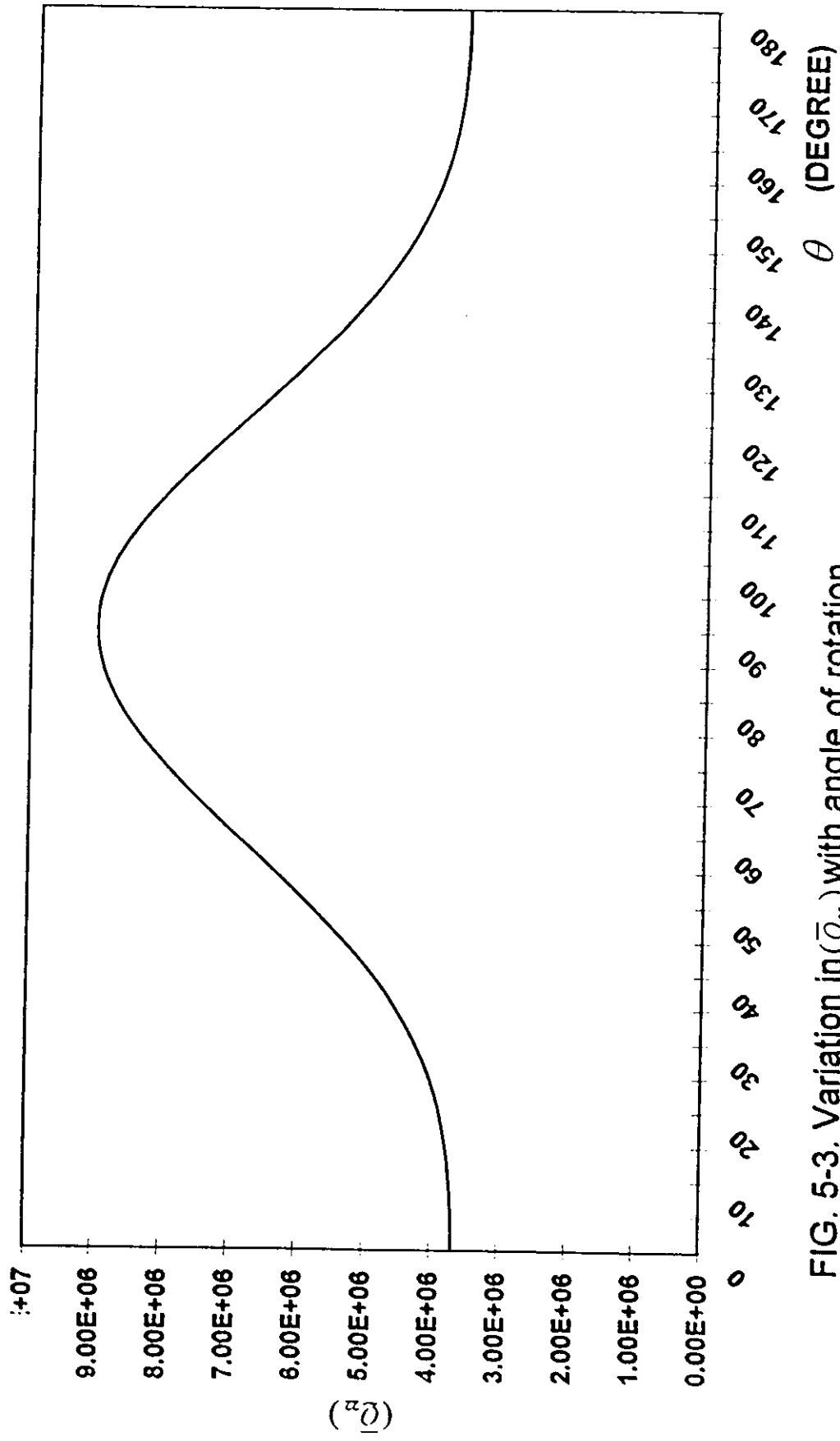
FIG. 5-1. Variation in $(\bar{Q}_{11})$ with angle of rotation.
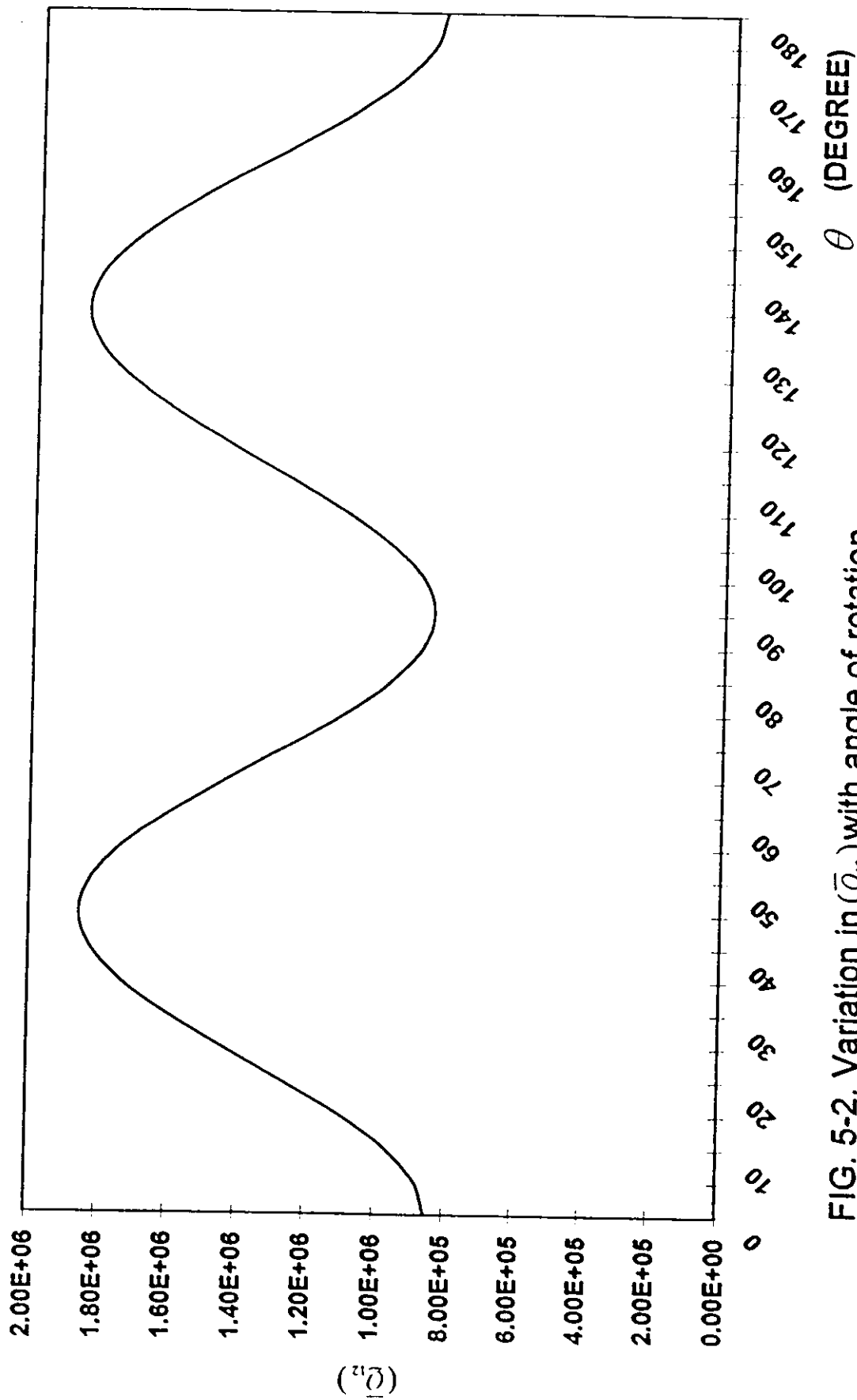
FIG. 5-2. Variation in $(\bar{Q}_{12})$ with angle of rotation.

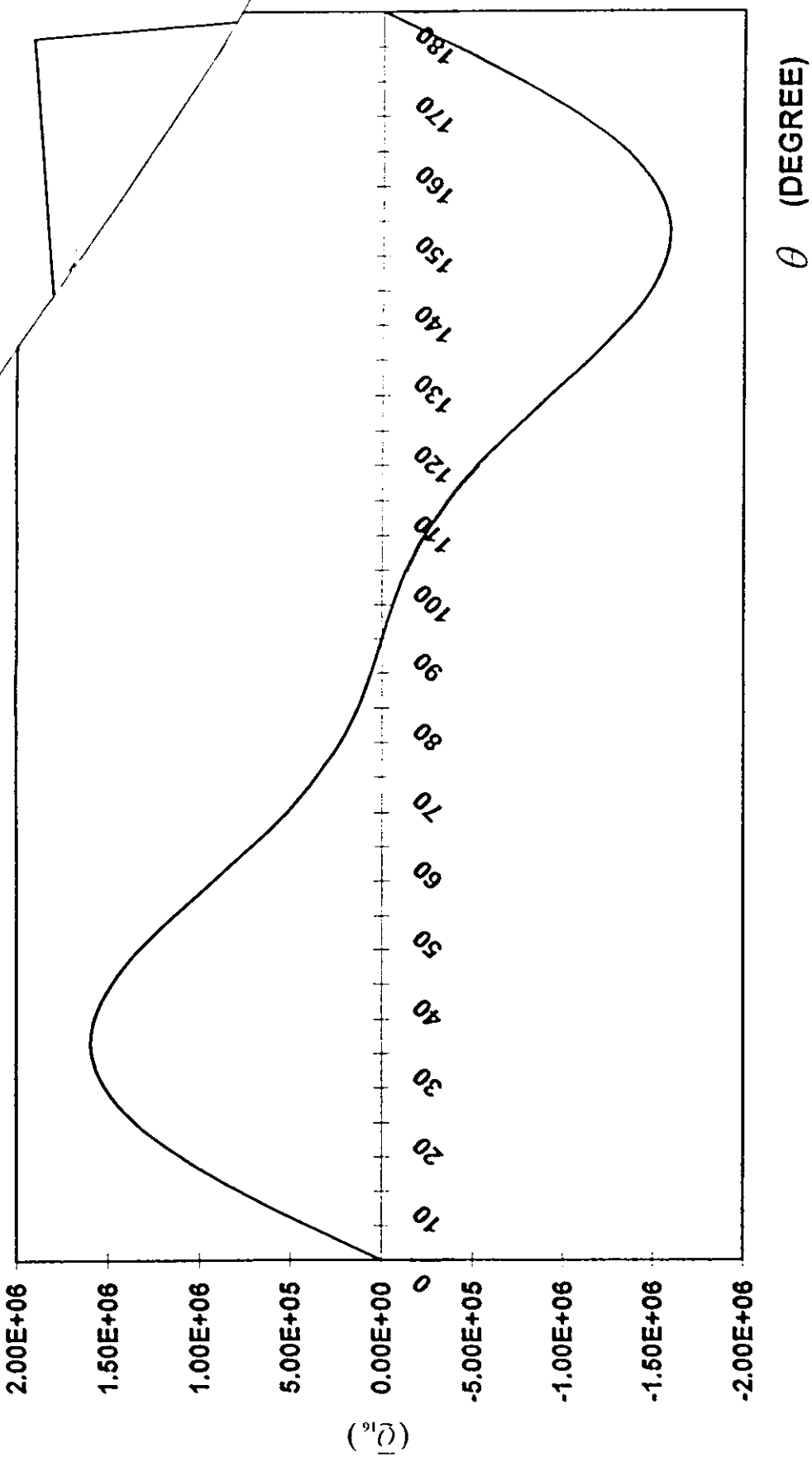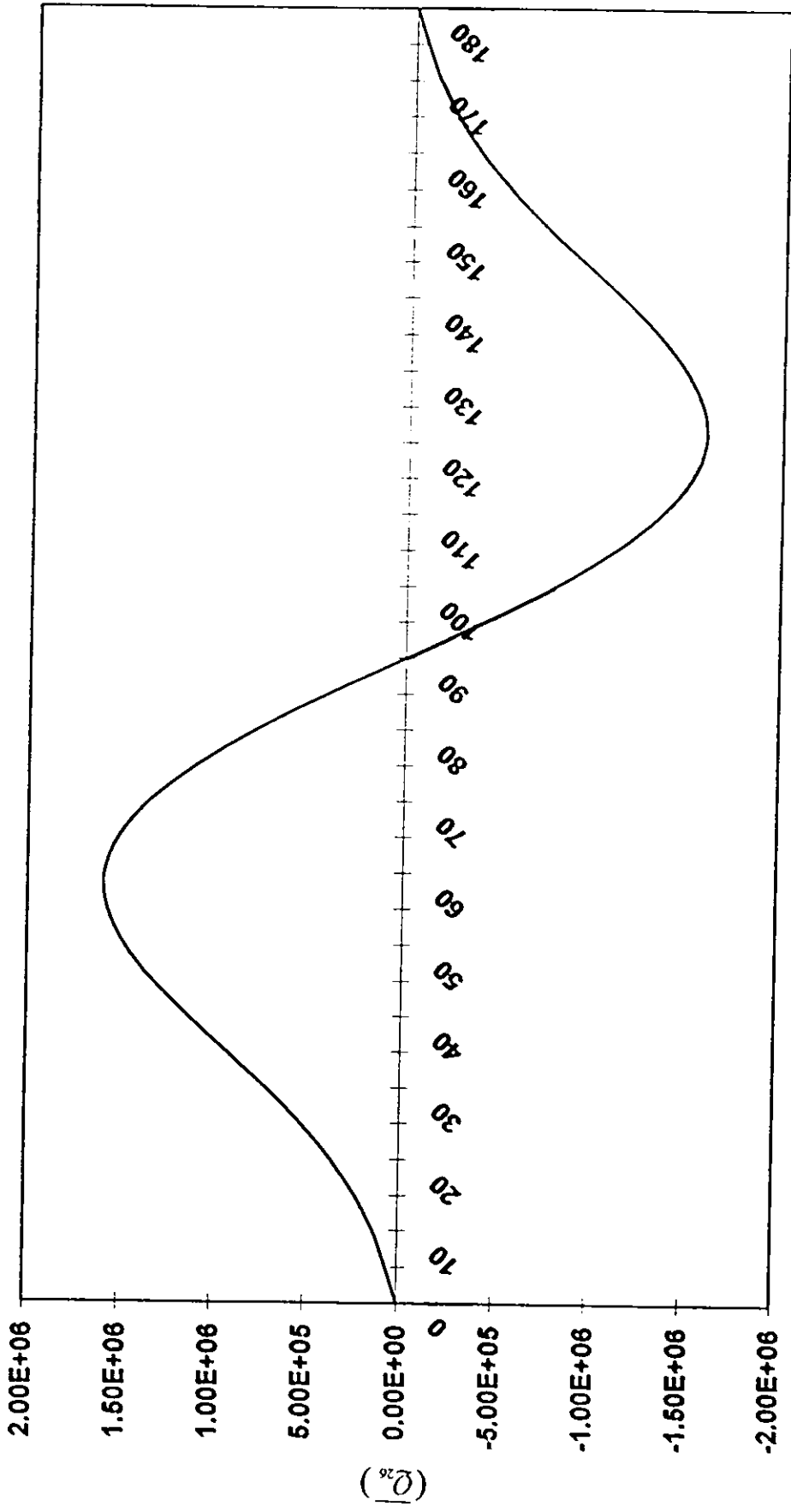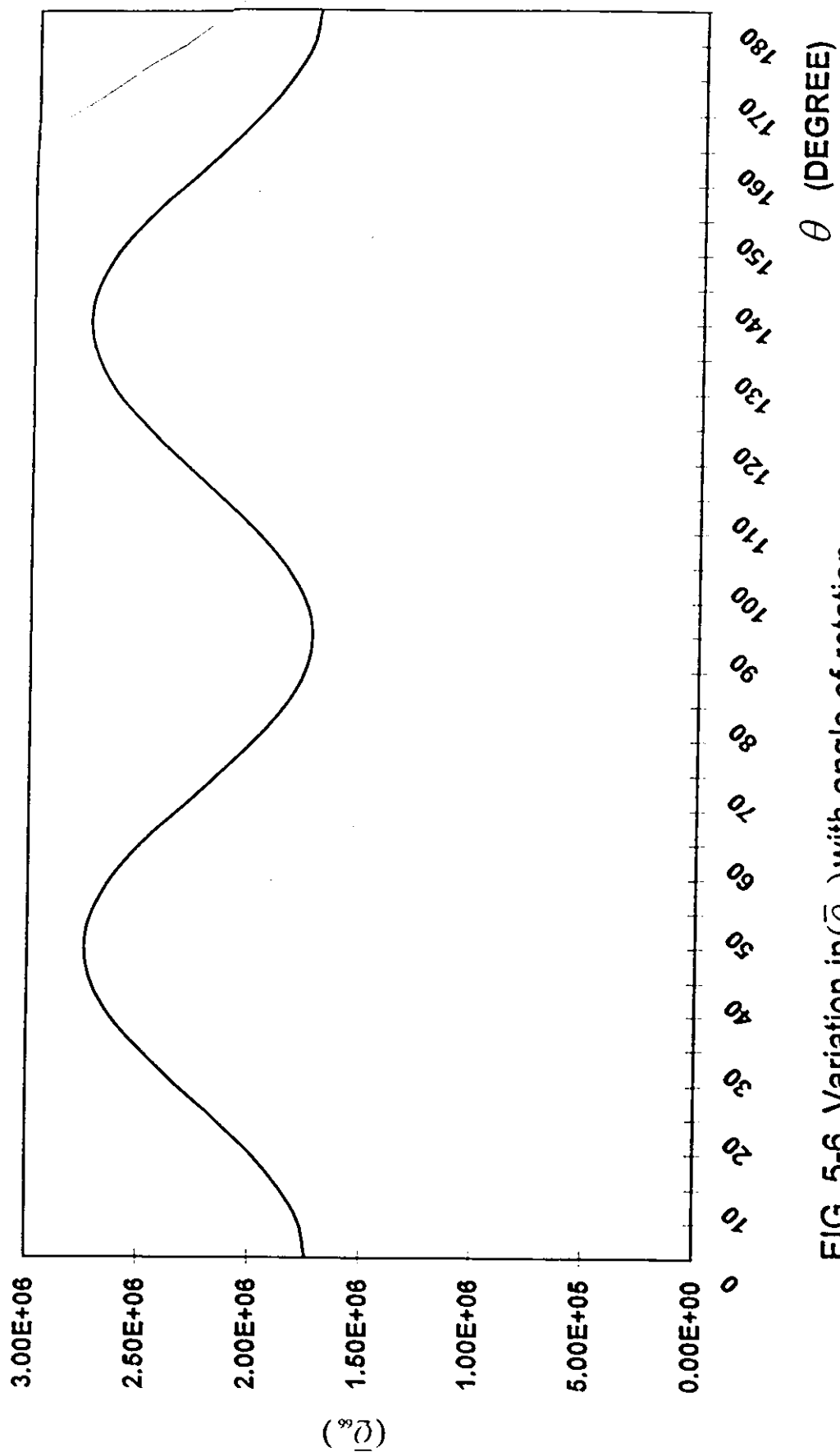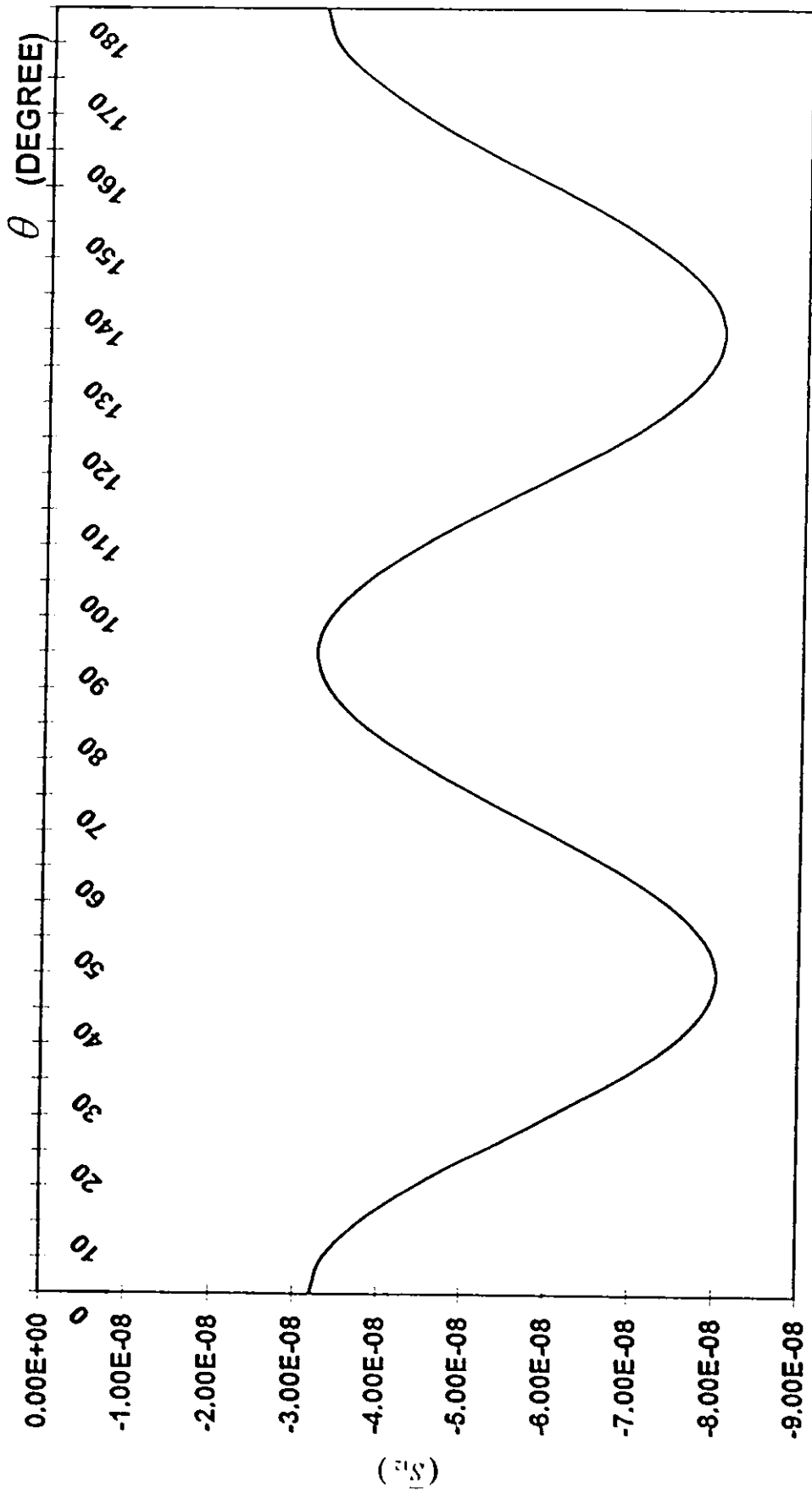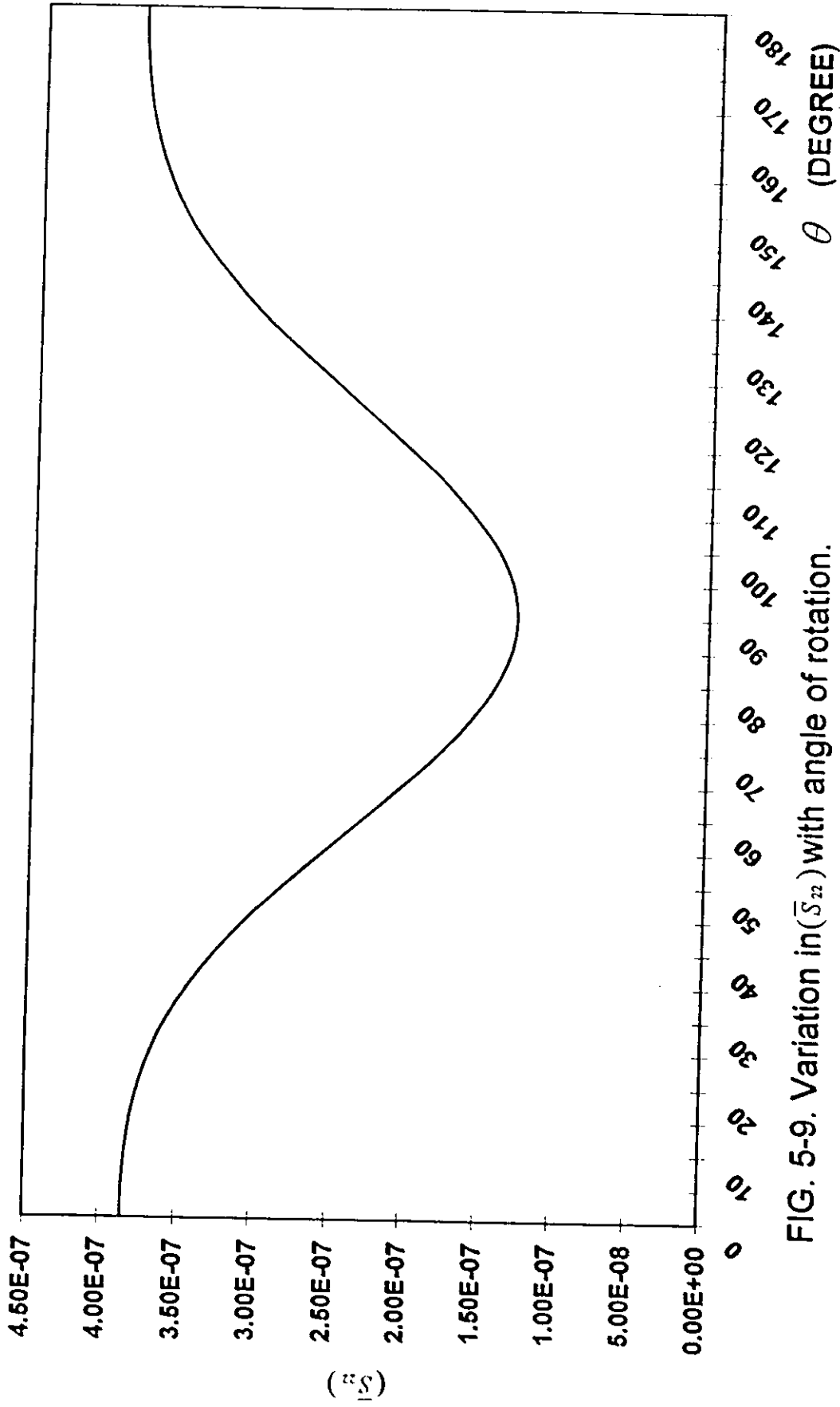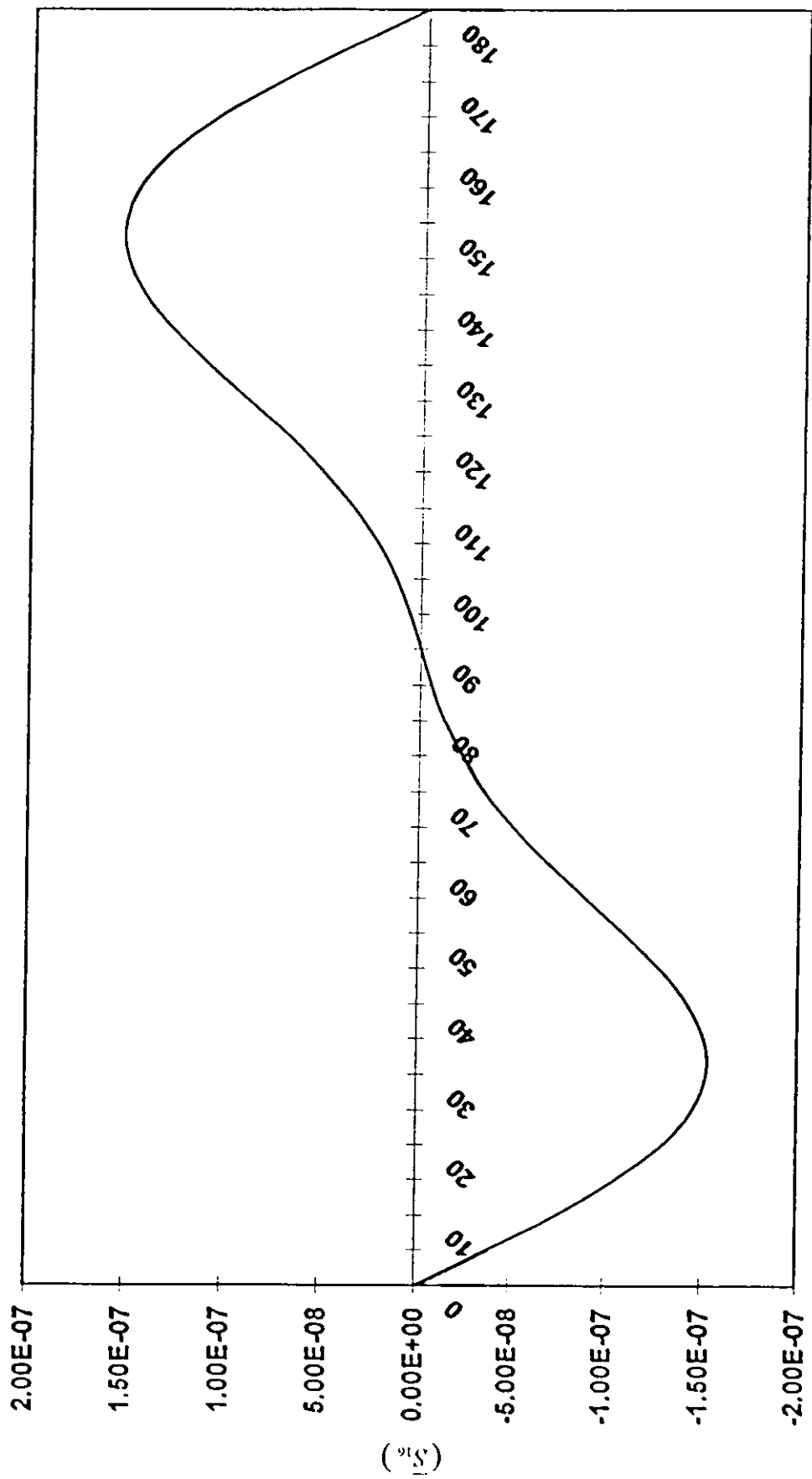FIG. 5-3. Variation in $(\overline{Q}_{22})$ with angle of rotation, .

FIG. 5-4. Variation in $(\overline{Q}_{16})$ with angle of rotation.

FIG. 5-5. Variation in $(\overline{Q_{26}})$ with angle of rotation.

FIG. 5-6. Variation in $(\bar{Q}_{66})$ with angle of rotation.

θ (DEGREE)

$(\bar{Q}_{66})$

97

FIG. 5-8. Variation in $(\bar{S}_{12})$ with angle of rotation.

$(\bar{S}_{12})$

θ (DEGREE)

FIG. 5-9. Variation in $(\bar{S}_{22})$ with angle of rotation.

FIG. 5-10. Variation in $(\overline{S}_{16})$ with angle of rotation.
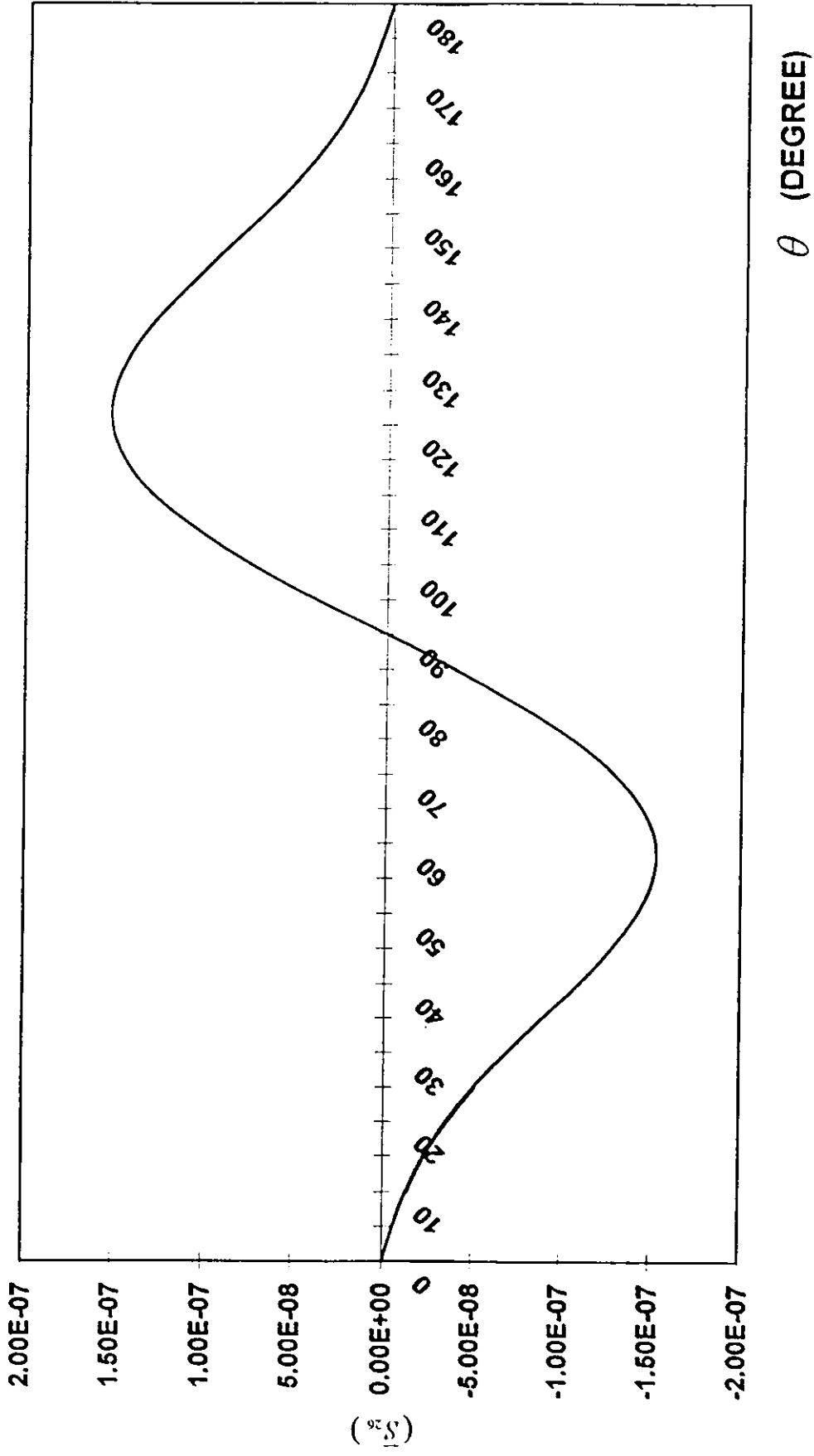
FIG. 5-11. Variation in $(\overline{S}_{26})$ with angle of rotation.

5.3 Failure Of A Generally Orthotropic Single Layer

A single lamina is considered to study the relation between failure stresses and angle of rotation, so a computer program is developed to determine failure stresses of a generally orthotropic single layer using two failure theories; Tsai-Hill and Tsai-Wu.

Results predicted by these theories are presented and discussed for a lamina made of boron-epoxy Narmco 5505. Failure stresses of this lamina with different angles of rotation are compared with experimental failure stresses (Cole and Pipes, 1973), and failure stresses predicted by AF-AJ failure theory (Abu-Farsakh and Abdel-Jawad, 1994)as given in Table 5-2 Data in Table 5-2 is represented in Fig 5-13 to make easy comparison.

TABLE 5-2. Failure stresses (ksi) for boron-epoxy Narmco 5505 under tension loads.

θ	Tsai-Hill	Tsai-Wu	AF-AJ	Exp.
15°	34.97	35.21	36.46	36.0
30°	17.65	17.82	19.74	18.2
45°	11.95	12.22	13.65	12.9
60°	9.36	9.42	10.07	9.45
75°	8.17	8.03	8.31	7.25
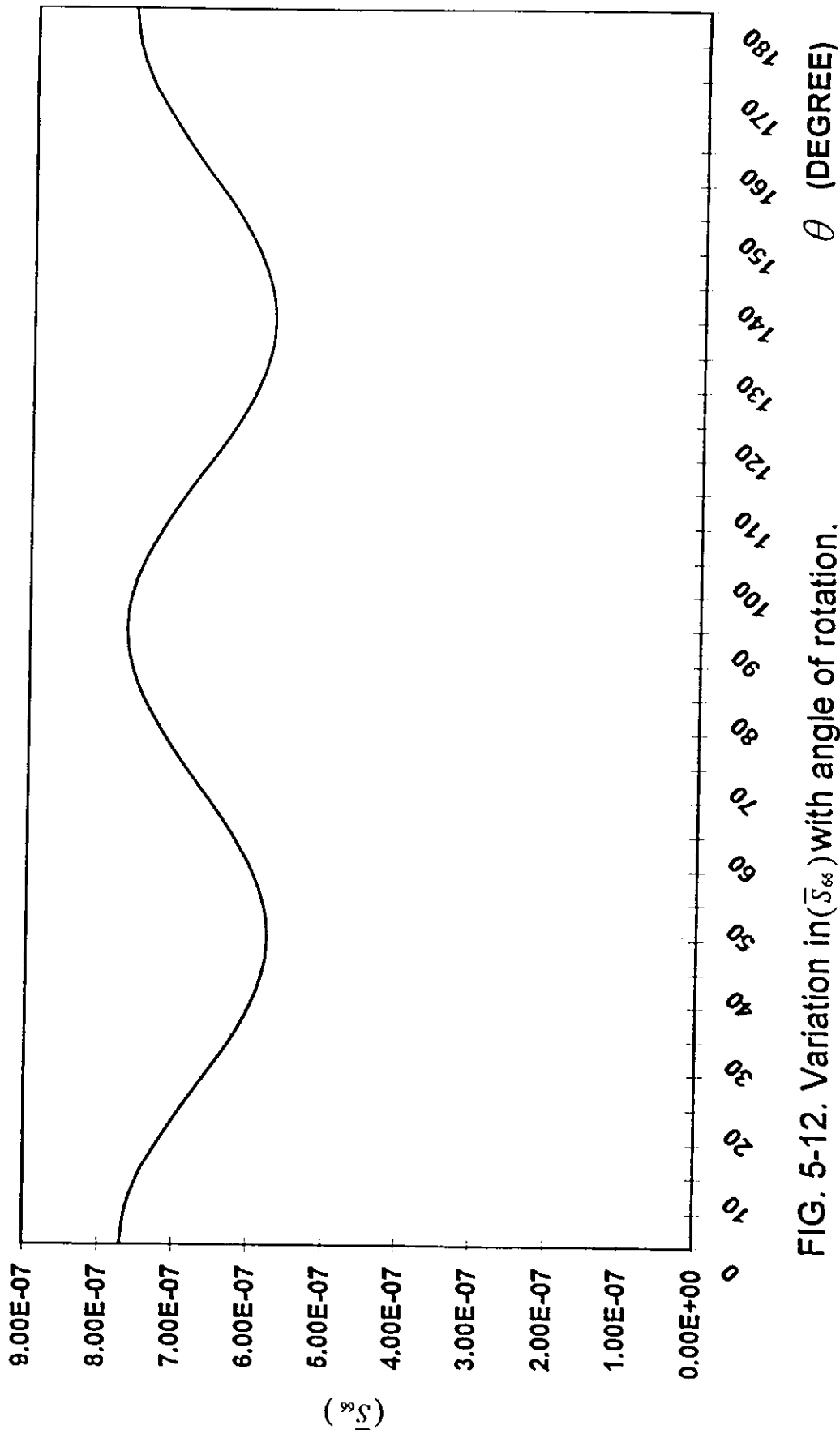
FIG. 5-12. Variation in $(\bar{S}_{66})$ with angle of rotation.

$(\bar{S}_{66})$

θ (DEGREE)

As shown in Fig 5-13, the stresses predicted by using Tsai-Hill, Tsai-Wu and AF-AJ criteria are in good agreement with the corresponding experimental results but the Tsai-Wu failure theory appears to be much more applicable to failure prediction for this boron-epoxy Narmco 5505 composite than the Tsai-Hill criterion .

In Tsai-Wu failure theory, number of terms in the prediction equation is more than that in Tsai-Hill theory, Eq.(3.14.), and for an orthotropic lamina under plane stress state, terms in Eq.(3.15.) that are linear in the stresses are useful in representing different strengths in tension and compression and the terms that are quadratic in the stresses are used to represent an ellipsoid in stress space. However, the term involving F_{12} is used to represent the interaction between normal stresses in the 1-and 2-direction in a manner quite unlike the shear strength (Jones, 1975). Thus, Tsai-Wu tensor failure theory is obviously of more accurate.
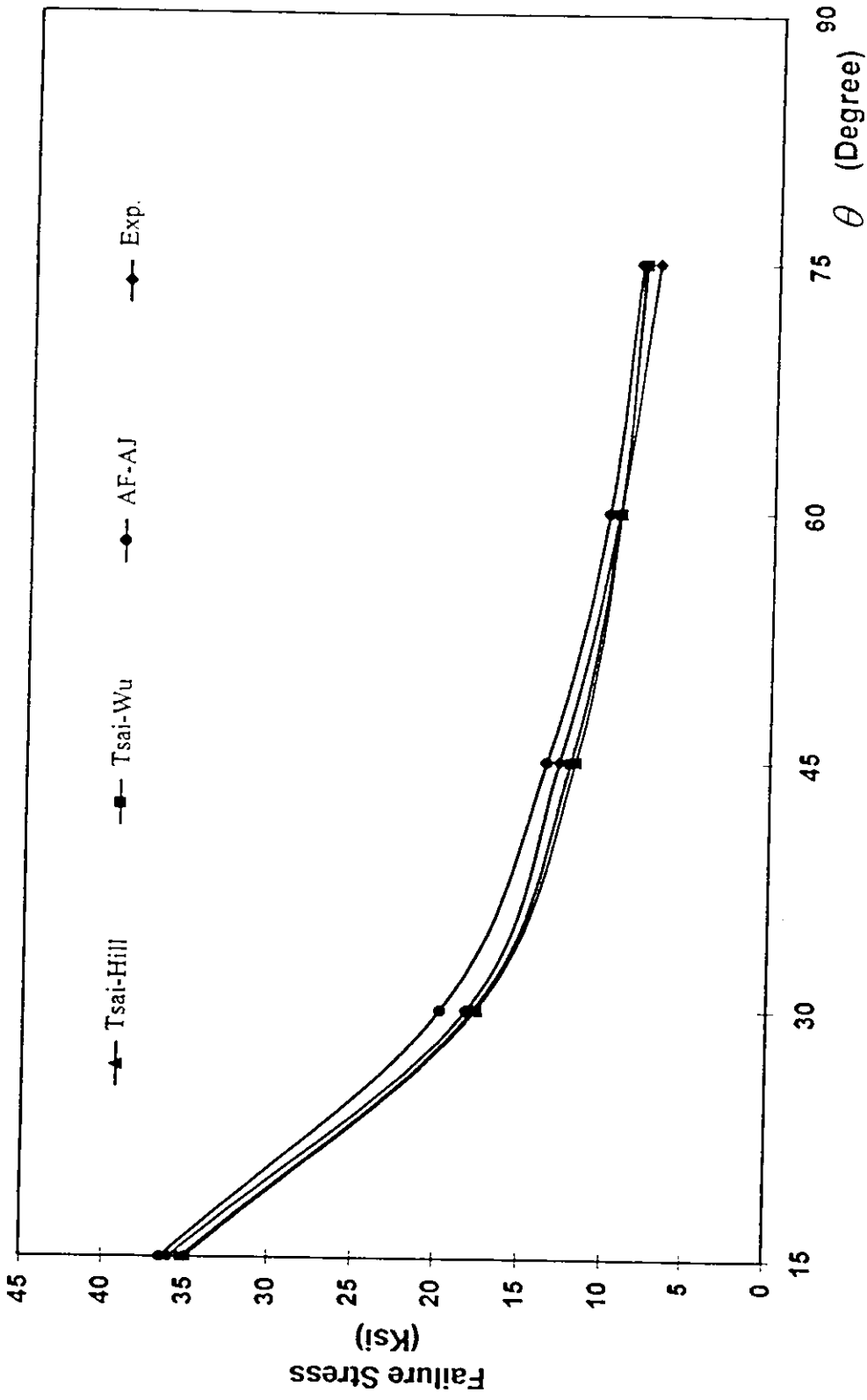
FIG.5-13. Failure stresses of a single lamina made of boron-epoxy Narmco 5505 .

5.4 First-Ply Failure Of Symmetric Laminated Composite

In this section, two cases of symmetric laminated composites are considered: Regular symmetric cross-ply laminate, and regular symmetric angle-ply laminate. Through the following subsections, failure stresses predicted by different failure theories are presented in tables and charts to ease the comparison between experimental and theoretical results.

5.4.1 Regular Symmetric Cross-Ply Laminate

Before going to study the failure in the cross-ply laminate, it is very important to study the effect of the cross-ply ratio, M, and stiffness ratio, F, on the extensional stiffnesses A_{ij} of the cross-ply laminate, where any change in the extensional stiffnessees, A_{ij}, will affect the failure stress of the laminate.

5.4.1.1 The Effect Of Cross-Ply Ratio And Stiffness Ratio On The Laminate Properties.

As defined in section (2.7.2), the cross-ply ratio is the ratio of the total thickness of odd-numbered layers to the total thickness of even-numbered layers.

As given in Eq.(2.70), extensional stiffnesses, A_{ij}, are independent of number of layers in the laminate, N. However, A_{11} and A_{22} depend on M, the cross-ply ratio, and on F, the stiffness ratio, as shown in Fig. 5-14 and Fig 5-15. For a composite material with F =0.4, A_{11} varies from $(0.7\ Q_{11}t)$ to $(0.94\ Q_{11}t)$ as M changes from (1) to (10). Similarly, A_{22} varies from (A_{11}) to $(0.44\ A_{11})$ over the same range of M. The stiffnesses A_{12} and A_{66} are independent on M and F. The remaining stiffness A_{16} and A_{26} are zero for all cross-ply laminates.

5.4.1.2 Failure Of Regular Symmetric Cross-Ply Laminate

In this subsection, failure stresses are predicted for a regular symmetric cross-ply laminate made of glass-epoxy 3M XP251S composite material. This laminate has three layers of the composite material with (0°/90°/0°) stacking sequence and equal thicknesses.

Now, to study the effect of cross-ply ratio on the strength of the laminate, predicted failure stresses under tension load for a cross-ply laminate with a stacking sequence of (0°/90°/0°) and different cross-ply ratio are given in Table 5-3 with other available results from (Tsai et al., 1966). Also, these results are shown in Fig. 5-16 to get easy comparison.

TABLE 5-3. Failure stresses, (ksi) for three layerd cross-ply glass-epoxy 3M XP2515 laminate under tension loads.

Cross-ply Ratio	Tsai-Hill	Tsai-Wu	Exp.
1	9.98	9.15	8.47
2.5	12.59	11.93	11.29
4	13.7	14.31	15.53

As shown in Fig.5-16, for the cross-ply laminae with $0°/90°/0°$ stacking sequence, failure stresses increase with increasing the cross-ply ratio, M, and this increment is due to the increment in the extensional stiffness A_{11} of the laminate and the reduction in extensional stiffness A_{22}.
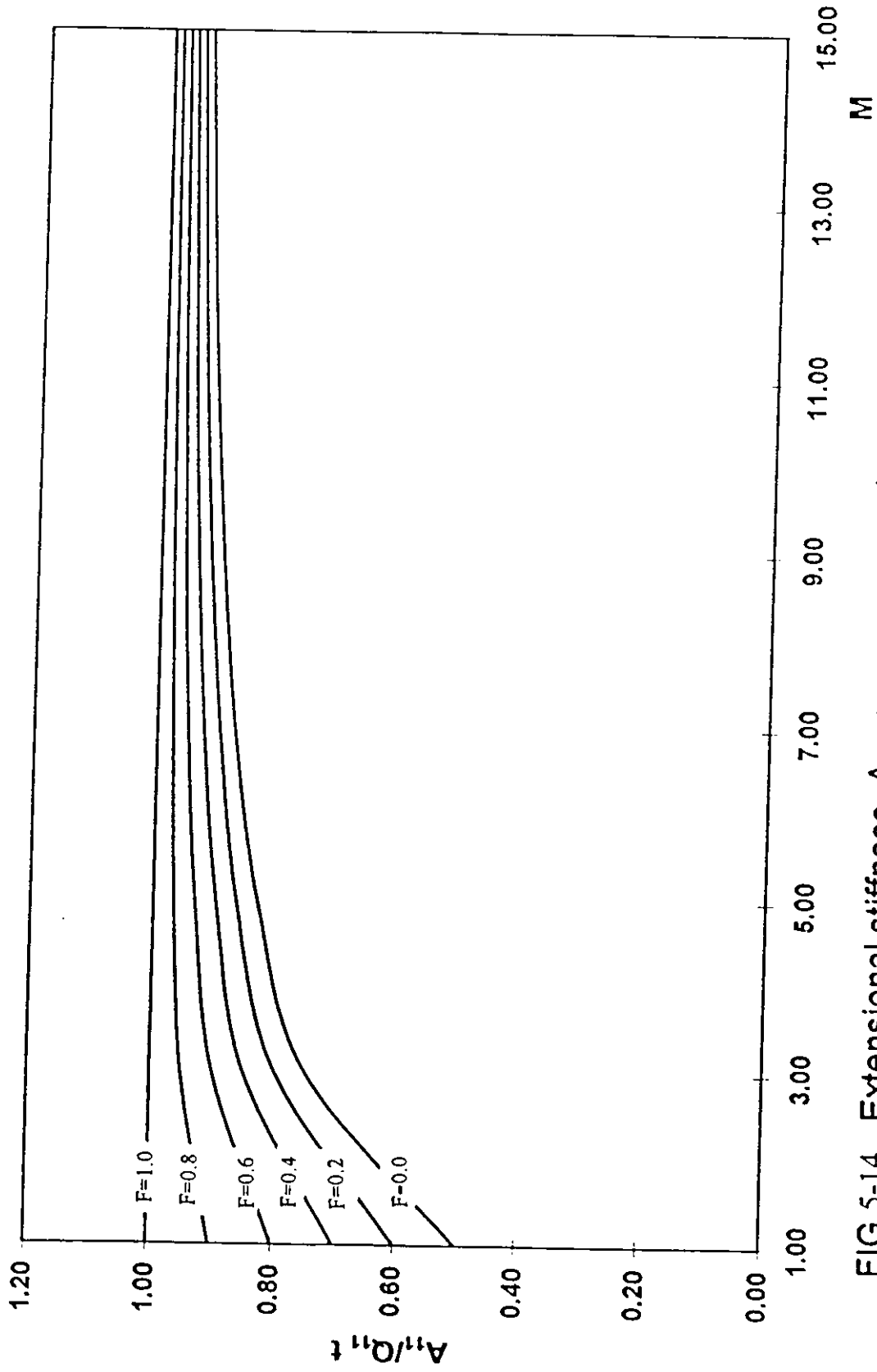
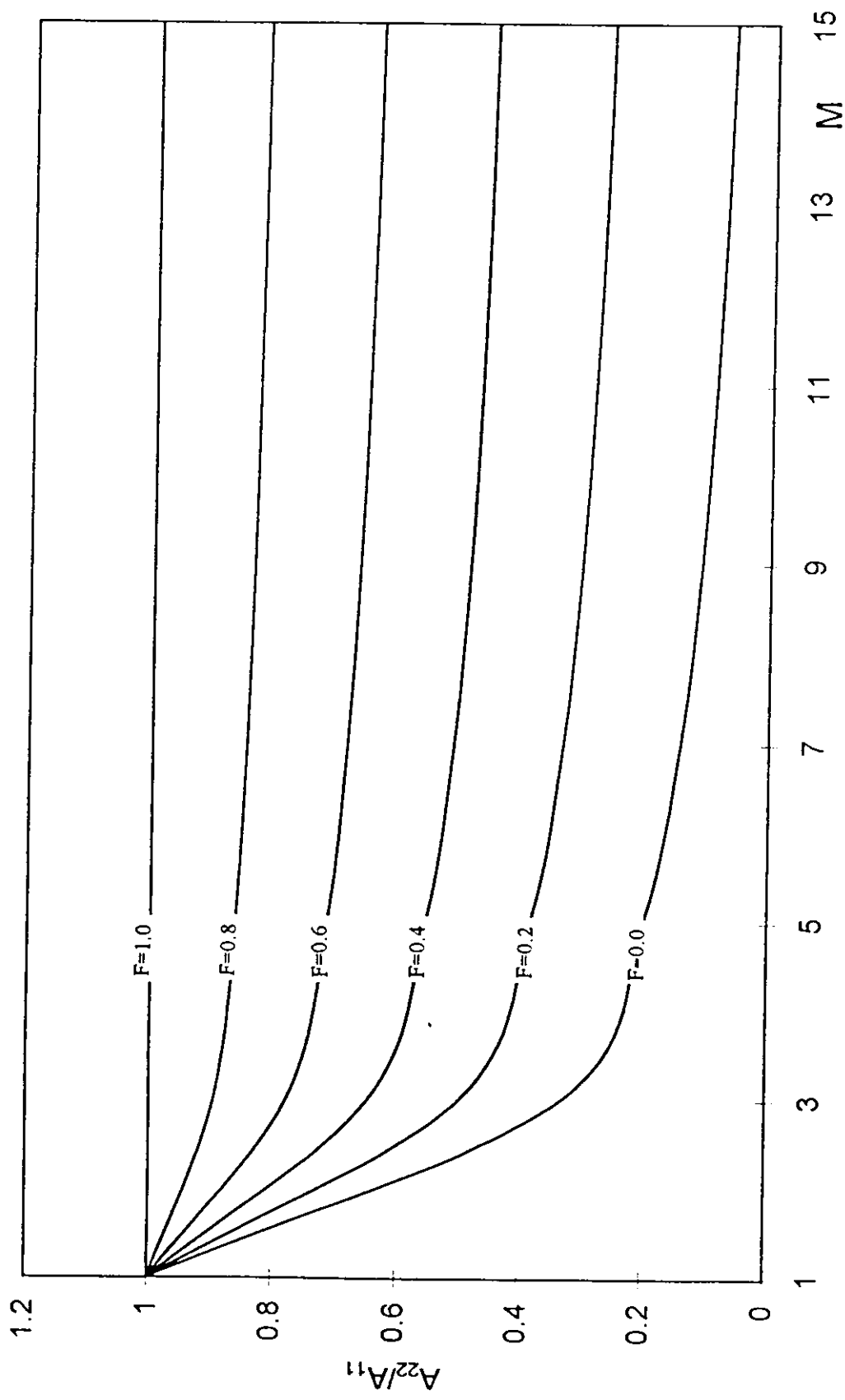FIG.5-14. Extensional stiffness, A_{11}, versus cross-ply ratio, M.

Curves labeled: F=1.0, F=0.8, F=0.6, F=0.4, F=0.2, F=0.0

Vertical axis: $A_{11}/Q_{11}\,t$

Horizontal axis: M

FIG.5-15. Extensional stiffness, A_{22}, versus cross-ply ratio, M.

The vertical axis is labeled A_{22}/A_{11} with values 0, 0.2, 0.4, 0.6, 0.8, 1, 1.2. The horizontal axis is labeled M with values 1, 3, 5, 7, 9, 11, 13, 15. Curves are labeled F=1.0, F=0.8, F=0.6, F=0.4, F=0.2, F=0.0.
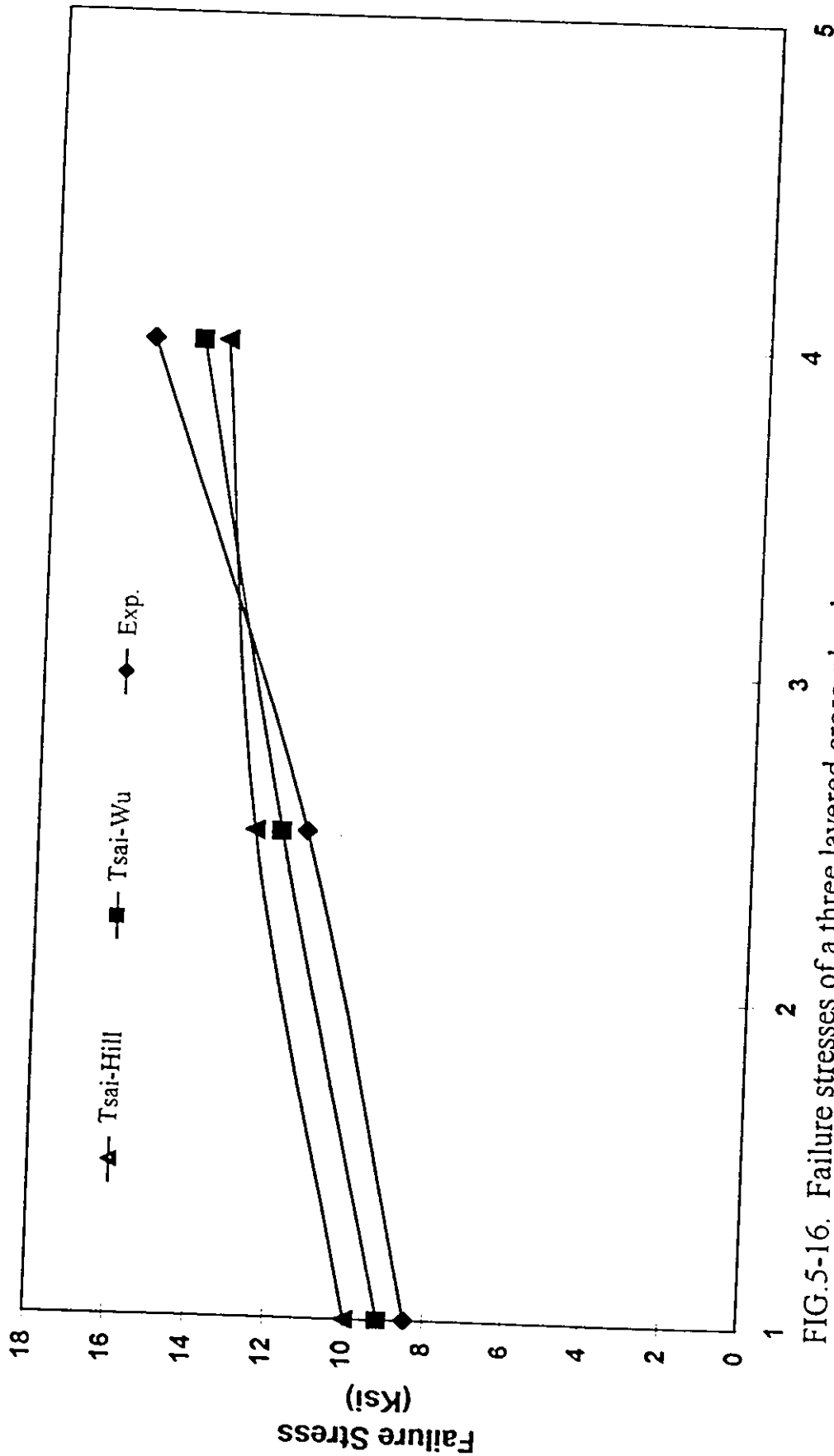
FIG.5-16. Failure stresses of a three layered cross-ply glass-epoxy 3M XP251S laminate with different cross-play ratios under tension loads .

5.4.2 Failure Of A Regular Angle-Ply Laminate

Angle-ply laminates are used in mechanical applications more than cross-ply laminates, for its ability to be in different stacking sequences with different angles or rotation, which give the designer many choices to satisfy the design requirements. Therefore, more discussion of the behavior of this laminate is done than that of the brevious case, cross-ply laminate.

Two composite materials are used, boron-epoxy Narmco 5505 and glass-epoxy 3M XP251S, with different orientation angles, θ, in the stacking sequence $+\theta/-\theta/+\theta$.

The angle-ply laminate made of boron-epoxy Narmco 5505 is studied under tension test with the following sequences:
- +30 /-30 /+30
- +45/-45 /+45
- + 60/-60 /+60

These stacking sequences are selected in this way for boron-epoxy Narmco 5505, because the main aim is to compare the predicted results in this study with the available results (Cole and Pipes, 1966) as given in Table 5-4.

TABLE 5-4. Failure stresses (ksi) for three layered angle-ply boron-epoxy Narmco 5505 under tension loads.

Stacking sequence	Tsai-Hill	Tsai-Wu	Exp.
30/-30/30	38.50	40.71	65.23
45/-45/45	16.27	17.25	19.20
60/-60/60	8.66	8.81	9.18

Where the angle-ply laminate made of glass-epoxy 3M XP251S is studied under tension and compression tests with different angles. Predicted values for tension and compression tests are compared with available results adapted from Tsai (1968). The comparison is given in Table 5-5 and Table 5-6.

TABLE 5-5. Failure stresses (ksi) for three layered angle-ply glass-epoxy 3M XP2512 laminate under tension loads.

Stacking sequence	Tsai-Hill	Tsai-Wu	Exp.
30/-30/30	14.54	13.87	12.83
45/-45/45	8.98	8.31	6.33
60/-60/60	4.25	4.35	4.60

TABLE 5-6. Failure stresses (ksi) for three layered angle-ply glass-epoxy 3M XP2512 laminate under compressive loads.

Stacking sequence	Tsai-Hill	Tsai-Wu	Exp.
45/-45/45	11.77	12.21	14.90
60/-60/60	11.41	11.98	13.72
75/-75/75	15.38	15.87	16.47

For angle-ply laminates made of boron-epoxy Narmaco 5505, the stress-strain curves for this material show that the behavior in fiber directions is linear in tension, the behavior in the direction transverse to fibers is nearly linear in tension and the behavior is highly nonlinear in shear, Appendix B. Therefore, this laminate made of boron-epoxy Narmco 5505, is affected by the nonlinearity of shear behavior which explains the difference between the predicated and measured values as shown in Fig. 5-17. One can note that the (+60°/-60°/+60°) laminate has a very close predicted failure stresses to the experimental values, where other laminates are highly affected by the nonlinearity.

For angle-ply laminate made of glass-epoxy 3M XP251S, the stress-strain curves for this composite material show that the behavior in fiber directions is linear in both tension and compression, the behavior in the direction transverse to the fiber directions is linear in tension and very nonlinear in compression, and the behavior is nonlinear in shear, Appendix B.

Therefore, and as shown in Fig 5-18, predicted failure stresses for angle-ply laminates under tension load are in good agreement with the measured values, but for the laminate with the stacking sequence (+ 45° / - 45°/ +45°) the predicted failure stresses are very high and far from the experimental values, for the high nonlinearly of shear stress-strain curve, so shear failure takes place at this angle.

Now, for the other case, the predicted failure stresses for angle-ply laminates under compression load are very far from the experimental values as given in Fig 5-19. This is due to the nonlinear behavior in the direction transverse to fiber directions under compression and the failure theories that don't take into consideration the nonlinearity behavior of the composite material will give misleading result. In this study, criteria used to predict failure stresses consider the material to behave linearly.
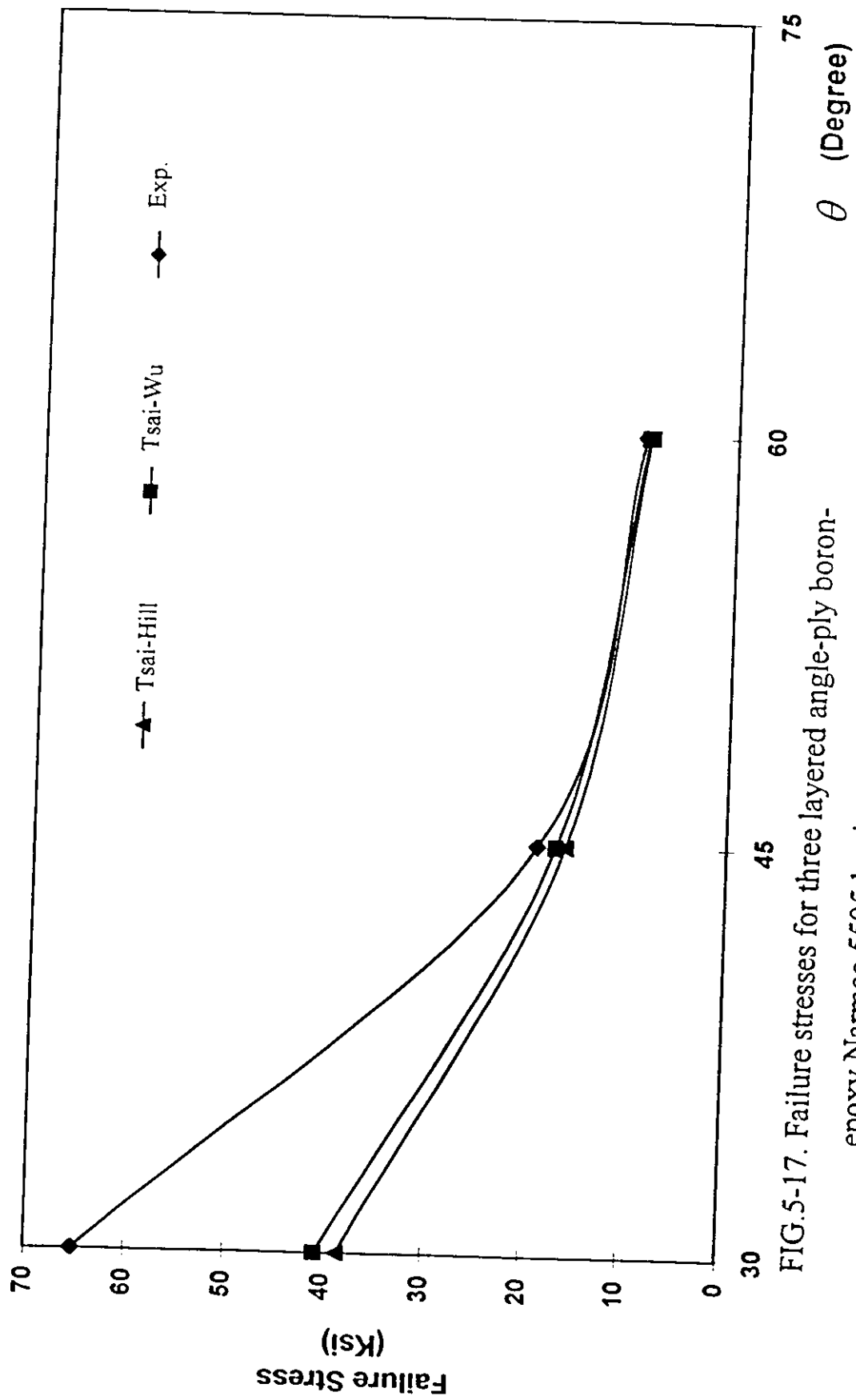
FIG.5-17. Failure stresses for three layered angle-ply boron-
epoxy Narmco 5505 laminate with different stacking
sequences under tension loads .

117
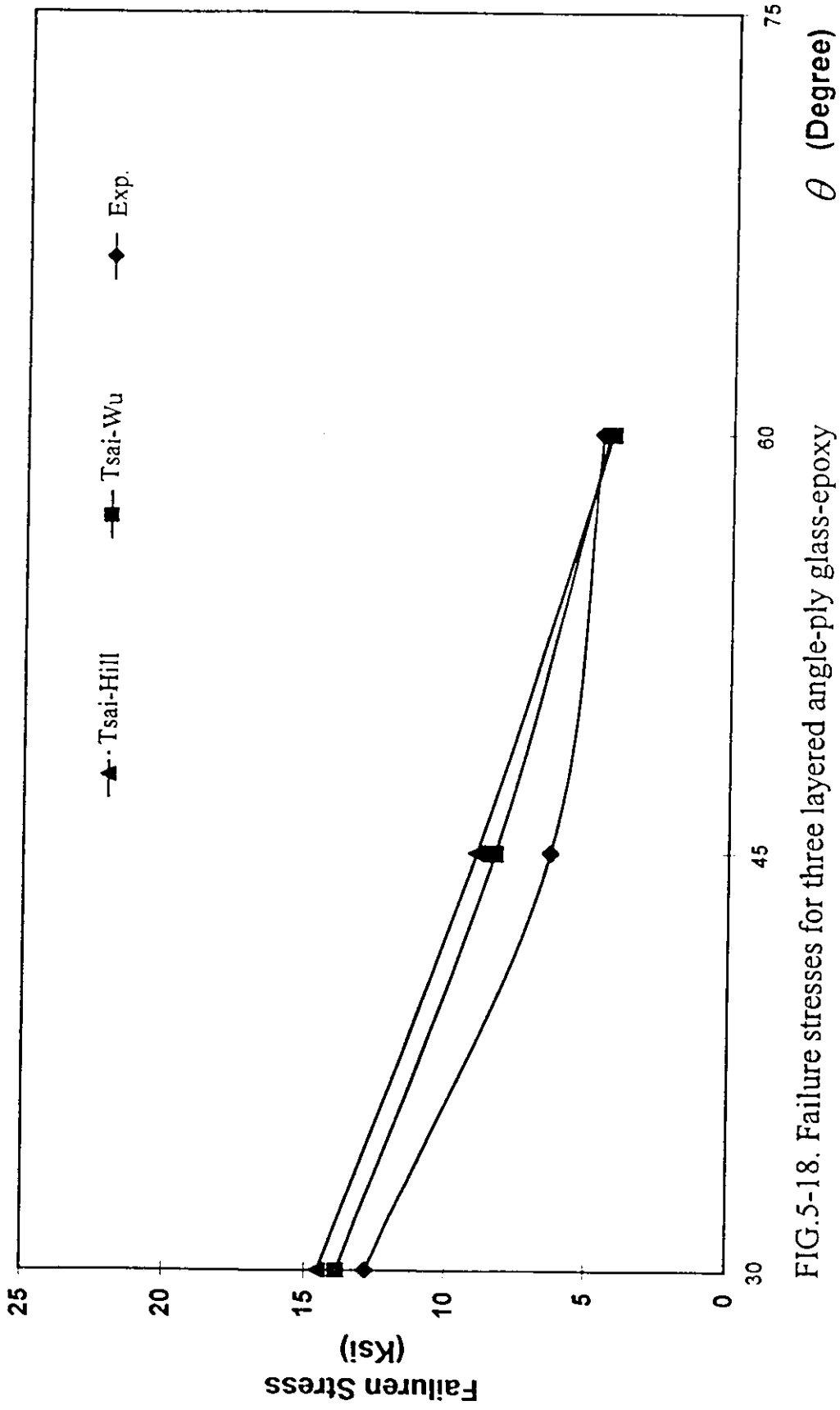
FIG.5-18. Failure stresses for three layered angle-ply glass-epoxy
3M XP251S laminate under tension loads .
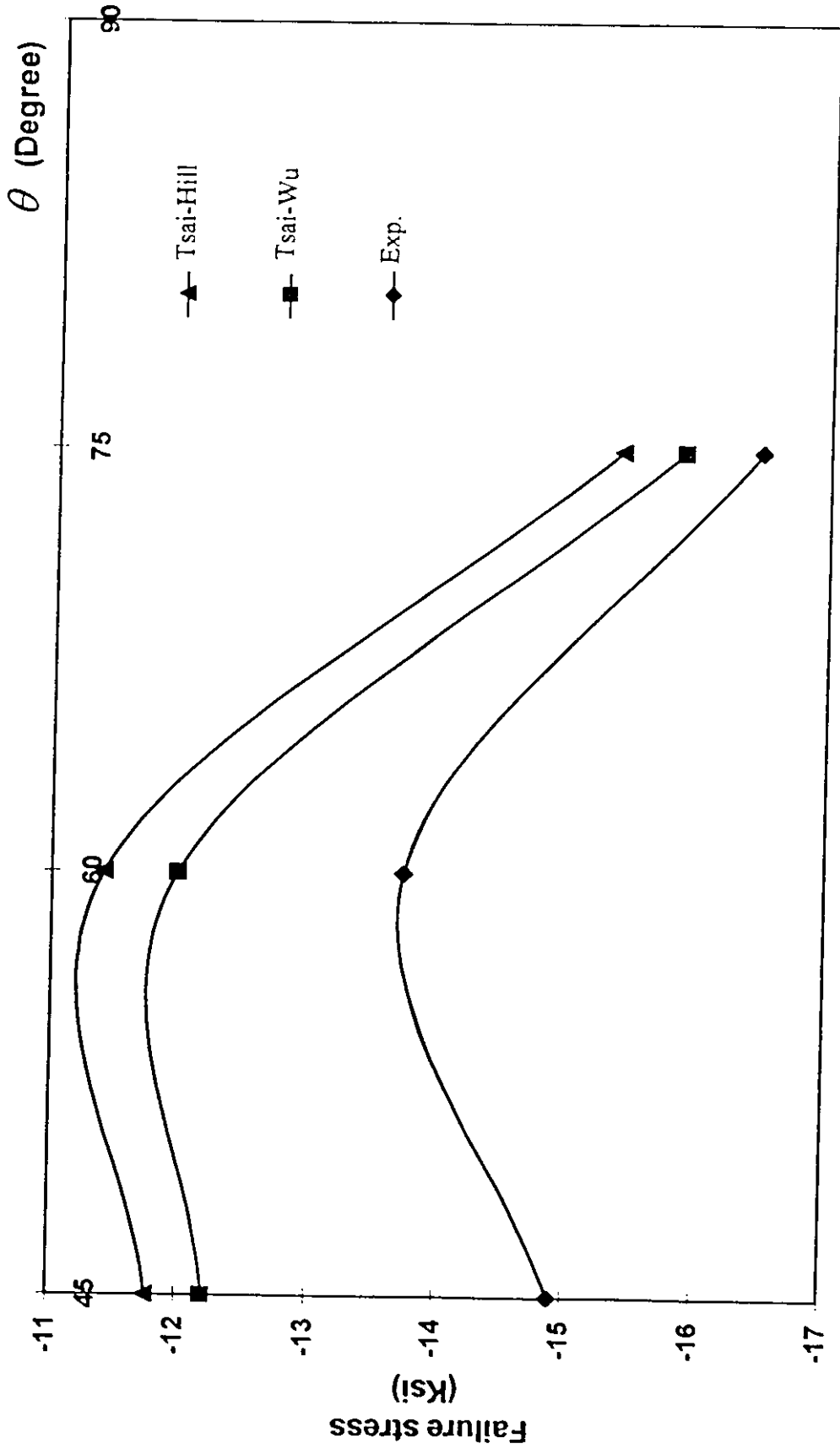
FIG.5-19. Failure stresses for three layered angle-ply glass-epoxy
3M XP251S laminate under compressive loads .

5.5 Bending Stresses In Plates And Beams Made Of Composite Materials

Bending stresses in a plate simply supported at all four edges and made of E glass-epoxy composite material are analyzed at five points in the plate to find where maximum stresses occur. Also, bending stresses in a beam made of the same composite material are analyzed for two different boundary condition, and for the two cases first-ply failure is determined.

Complete results and discussion for bending of such plates and beams are given in the following subsections.

5.5.1 Bending Of A Simply Supported Plate.

A simply supported plate is studied for the two following cases;

- The plate is made of three layers of E glass- epoxy composite material, where all the three layers are unidirectional, $\theta = 0°$.
- The plate is made of a cross-play laminate with three layers of a 0° / 90°/0° stacking sequence.

The plate in the above two cases has the following dimensions:
- Length (a) = 12 in.
- Width (b) = 12 in.

- Thickness (t) = 0.06 in .

- Lamina thickness (t_k) = 0.02 in.

For this plate and by using Navier solution, it is found that the stresses in each lamina of the plate for the case of P (x,y) = ¯Po are given as in equation (4.17) . These stresses are normalized as

$$\bar{\sigma}_{ij} = \sigma_{ij} / Po .$$

(5.1)

Normalized stresses are shown at different points in the plate where five points are considered with the following positions ;

- point 1 : x = 6 in. , y = 6 in .
- point 2 : x = 3 in . , y= 3 in.
- point 3 : x = 3 in ., y = 9 in.
- point 4 : x = 3 in ., y = 9 in.
- point 5 : x = 9 in ., y = 3 in.

5.5.1.1 A Plate Made Of Three Unidirectional Laminae

As shown in Fig. 5-20 through Fig. 5-25 , the normalized stresses are given for different values of z, where z is the position of material from the mid-plane of the laminate.

Normalized stresses, $\bar{\sigma}_x$ and $\bar{\sigma}_y$, have negative values in the upper part of the plate and positive values for the lower part, i.e. the

upper part of plate is in compression while the lower part is in tension and always $\overline{\sigma}_x \rangle \overline{\sigma}_y$.

Maximum stresses occur at $Z = \mp t/2$, yet first-ply failure occur at $Z= t/2$ at the upper surface of the plate which is under compression . The reason is that the stresngh of the lamina is compression is lower than its strength in tension, Table 5-1.

Normalized stresses, $\overline{\sigma}_x$ and $\overline{\sigma}_y$, are the same at points 2,3,4 and 5, compression in the upper part and tension in the lower part.

For stresses $(\overline{\tau}_{xy})$, zero values are at the mid-point position, and for points 2 and 4, positive values of stresses are in the upper part of the plate while the lower part is under the same stresses but with a negative sign. For points 3 and 5, $\overline{\tau}_{xy}$ has the same values of stresses as in points 2 and 4 but with a negative sign in the upper part and positive sign in the lower part of the plate.

5.5.1.2 A Plate Made Of A Cross-Ply Laminate

Fig.5-26 through Fig.5-29 show that normalized stresses $(\overline{\sigma}_x)$ and $(\overline{\sigma}_y)$ are not linear in tension or compression with (z) values. This happened at the interface points between layers with angles of rotation equal $0°$ and $90°$. Also, the upper part of the plate is under compression and the lower part is under tension.

Normalized stresses, $\overline{\sigma_x}$, have same values for points 2,3,4 and 5 as shown in Fig. 5-28 and same thing is true for $\overline{\sigma_y}$ as shown in Fig.5-29.

Normalized shear stresses, ($\overline{\tau_{xy}}$), have zero values at the mid-point of the plate, while ($\overline{\tau_{xy}}$) has positive values for ($z > 0$) and negative values for ($z < 0$) for points 2 and 4 and same values for points 3 and 5 but with opposite signs as shown in Fig.5-30 and Fig.5-31.
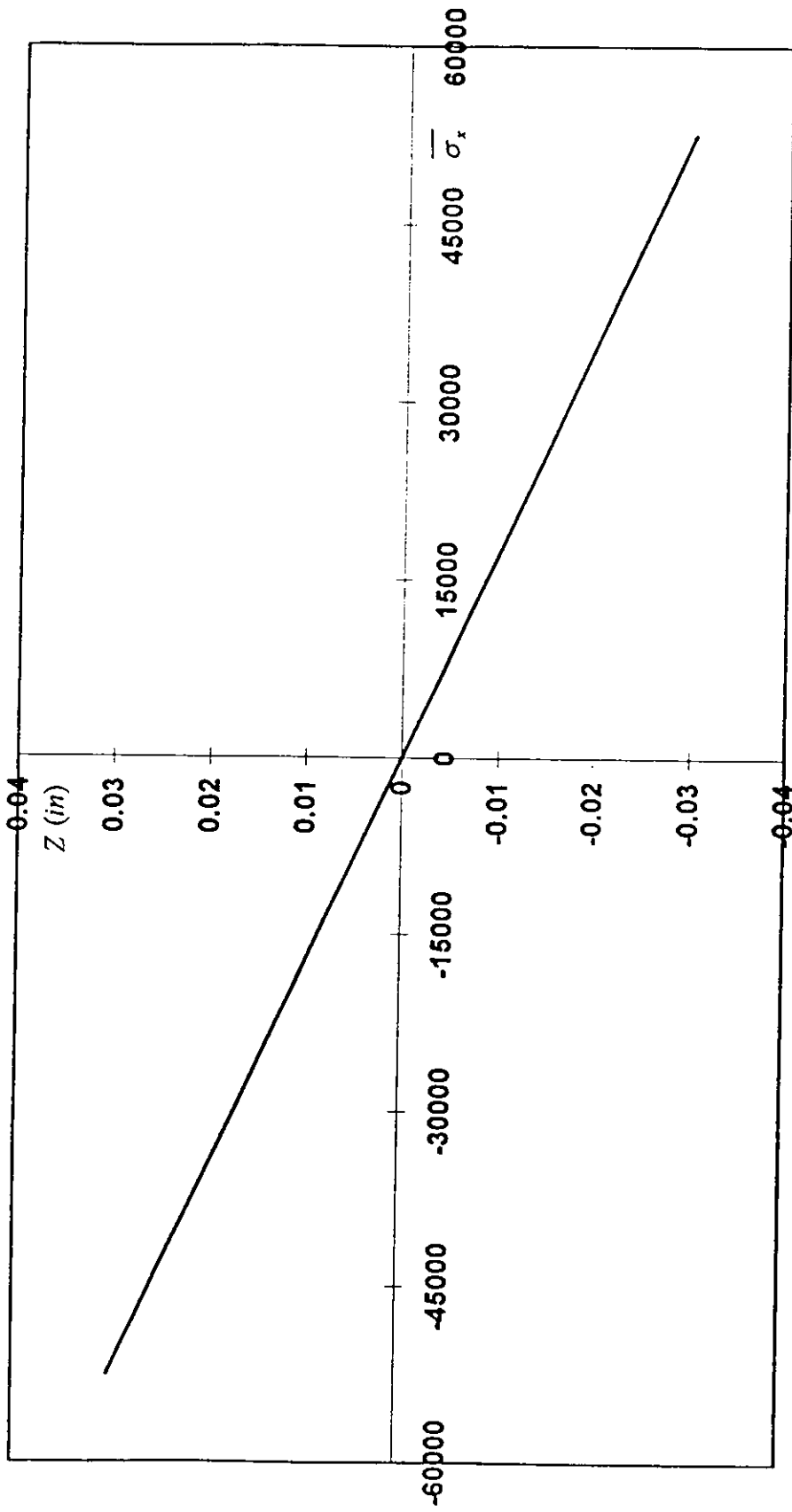
FIG.5-20. Normalized stresses, $(\overline{\sigma_x})$, at point 1 of the plate made

of three unidirectional laminae .
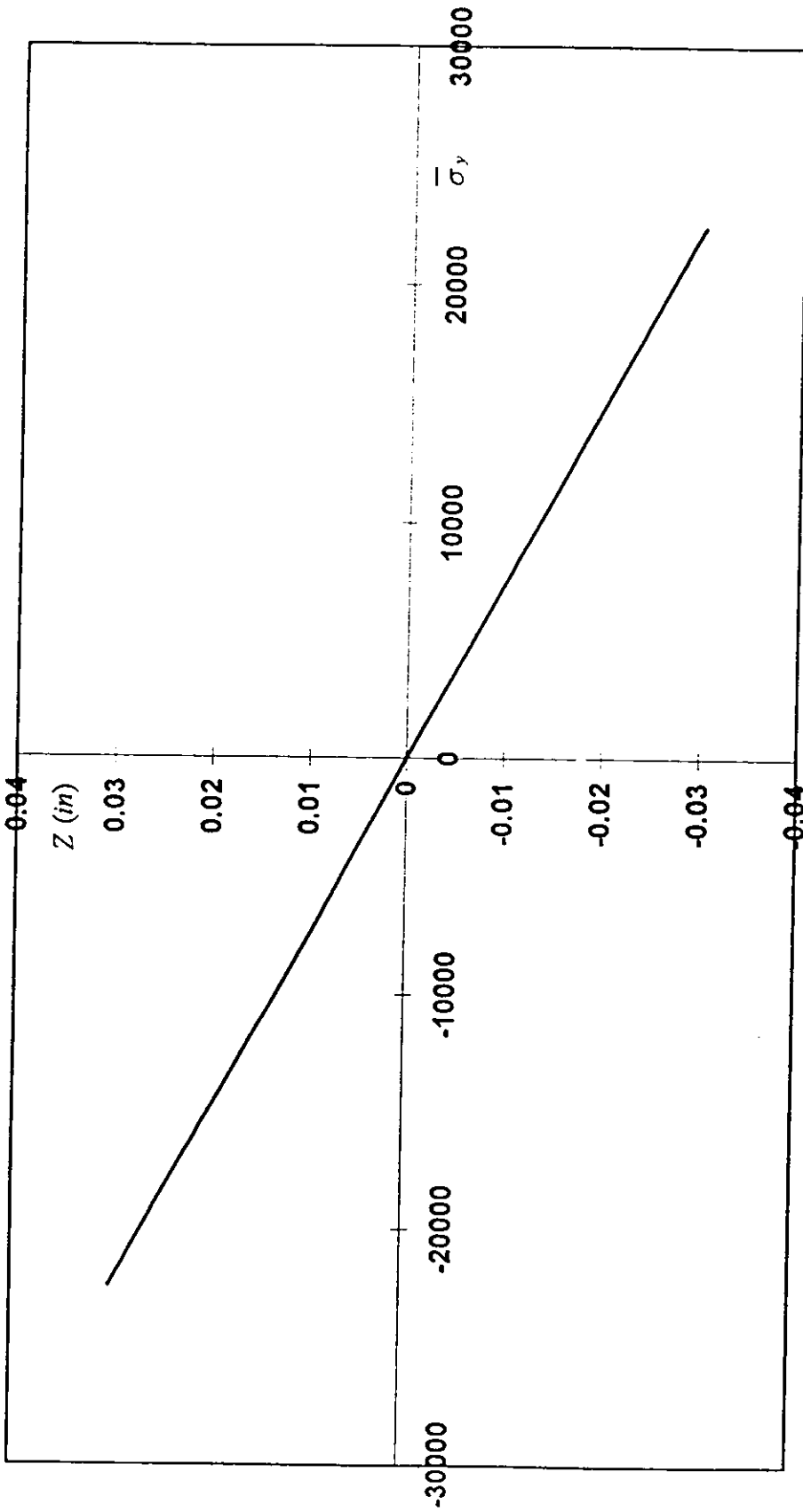
FIG.5-21. Normalized stresses, $(\bar{\sigma}_y)$, at point 1 of the plate made of three unidirectional laminae.
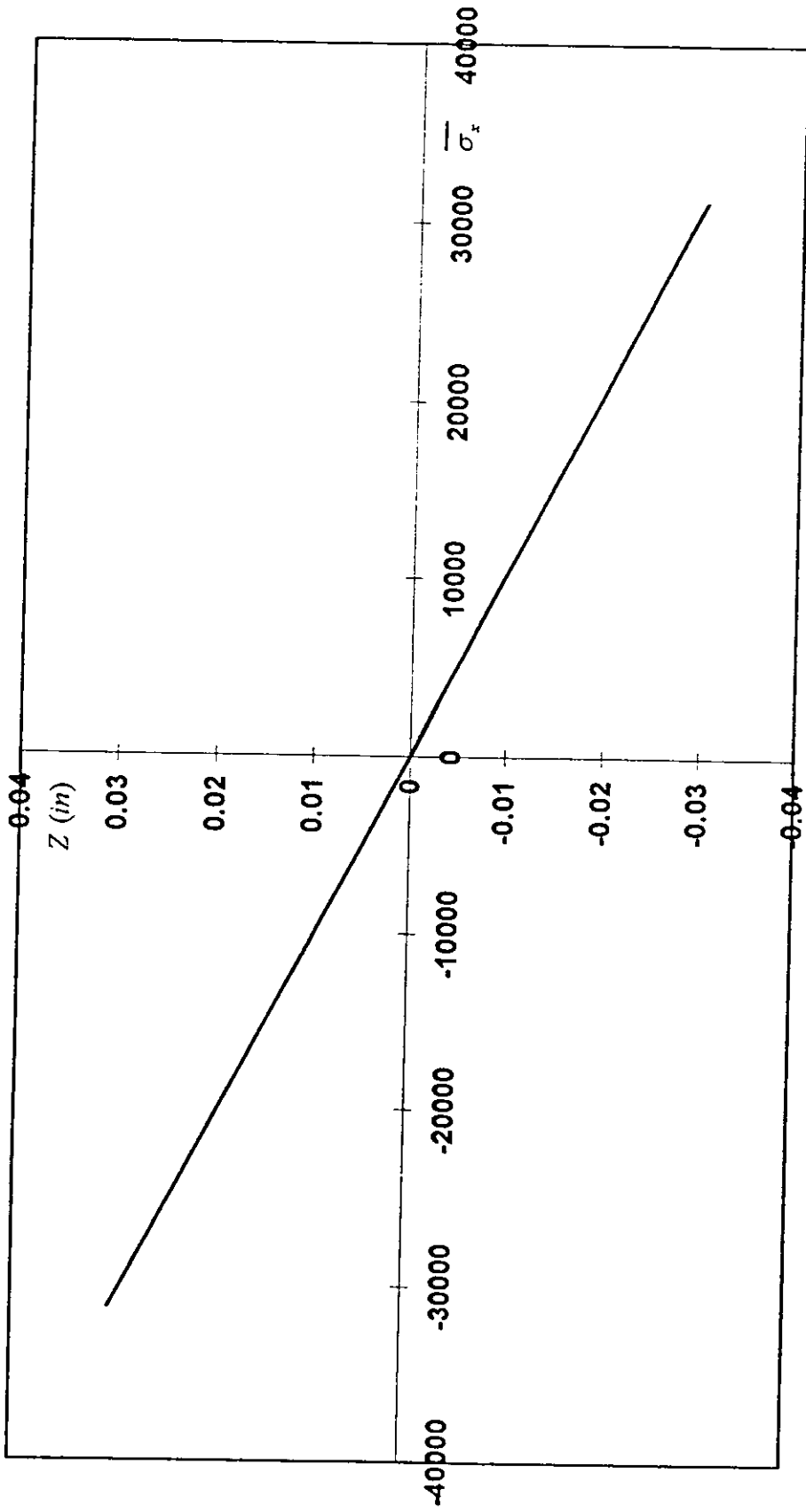
FIG.5-22. Normalized stresses , $(\overline{\sigma_x})$, at points 2,3,4, and 5 of the
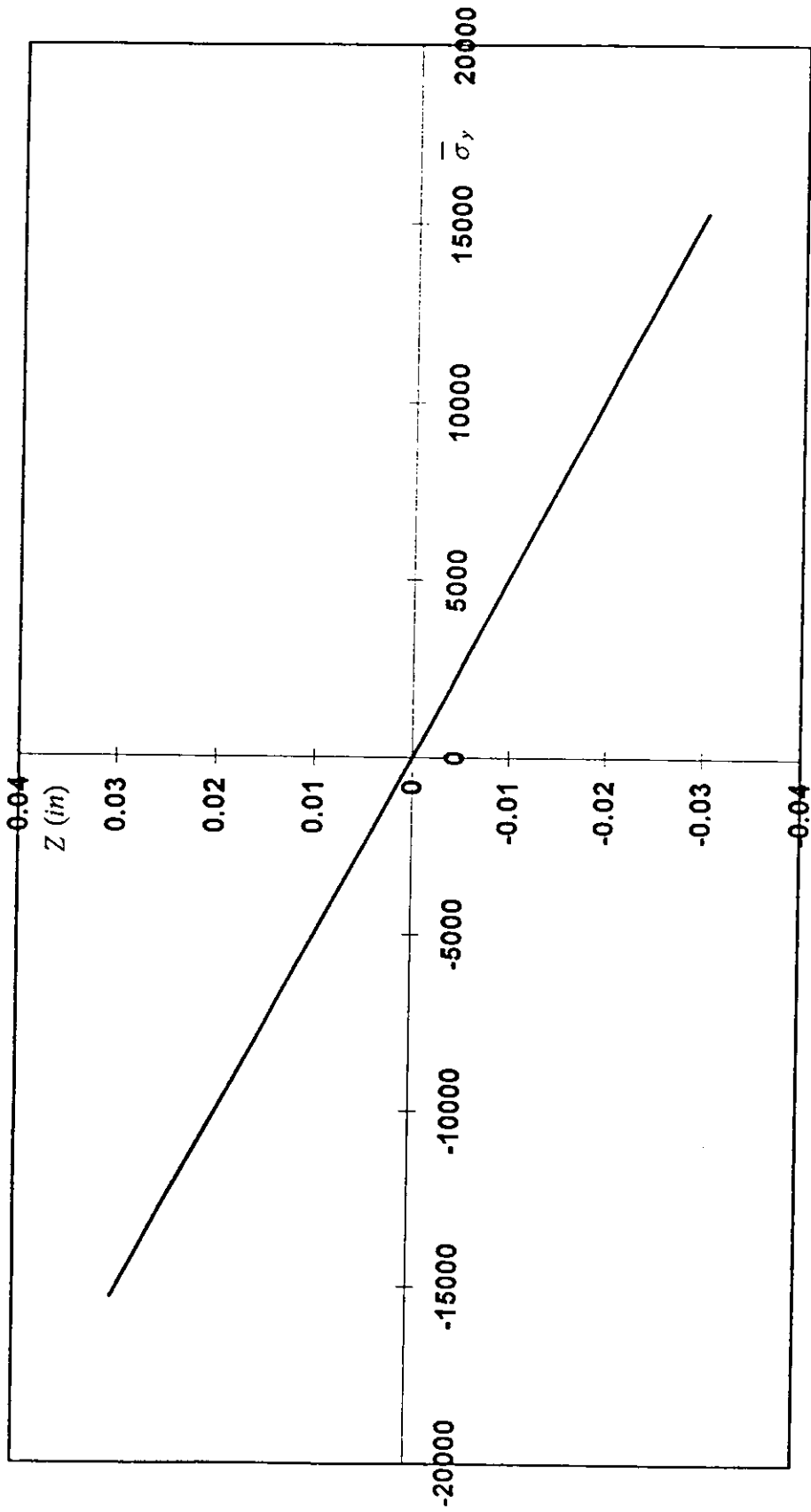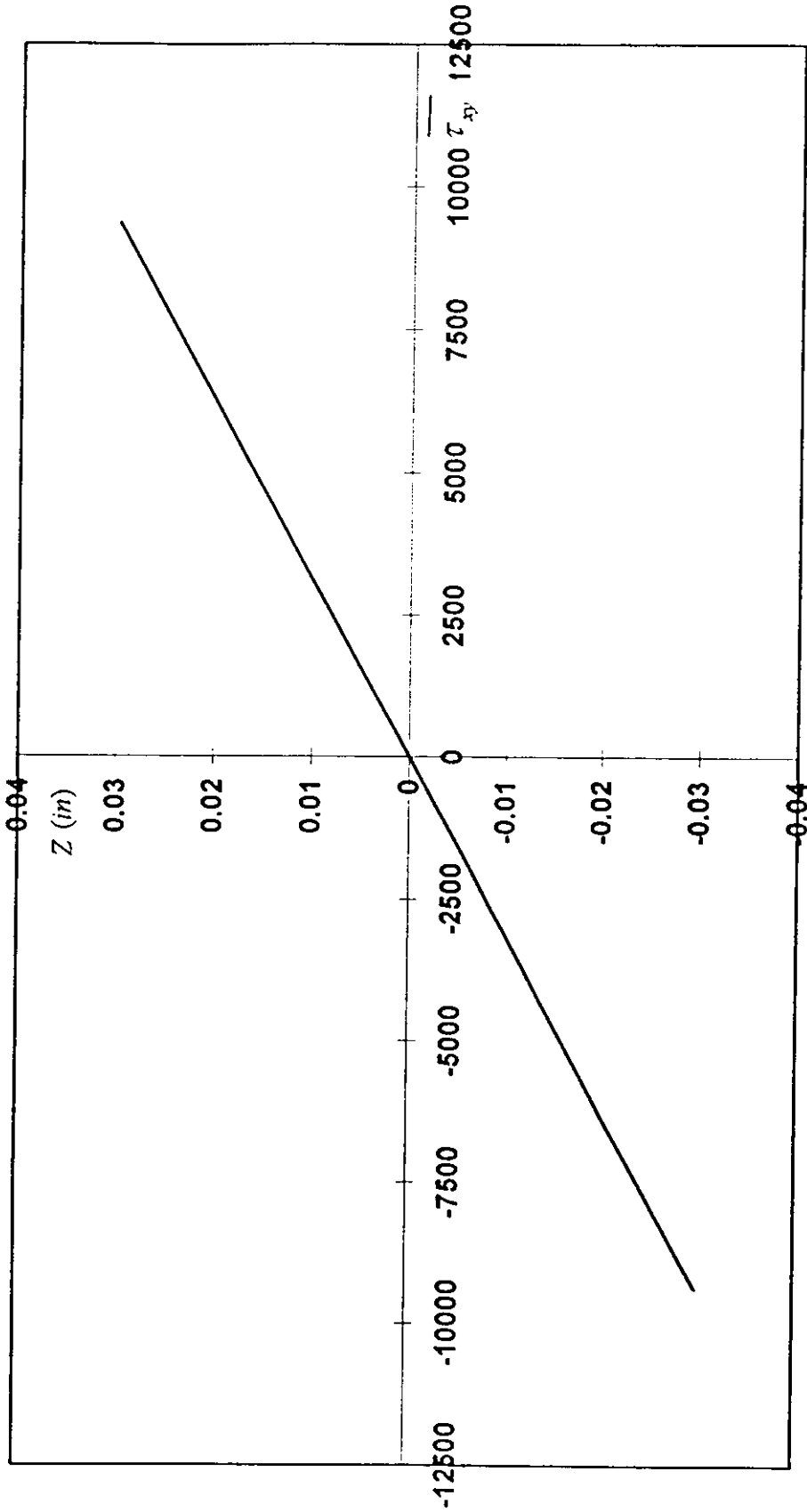
plate made of three unidirectional laminate .

FIG.5-23. Normalized stresses, $(\overline{\sigma}_y)$, at point 2,3,4, and 5 of the plate made of three unidirectional laminate .

FIG.5-24. Normalized stresses , $(\overline{\tau_{xy}})$, at points 2 and 4 of the

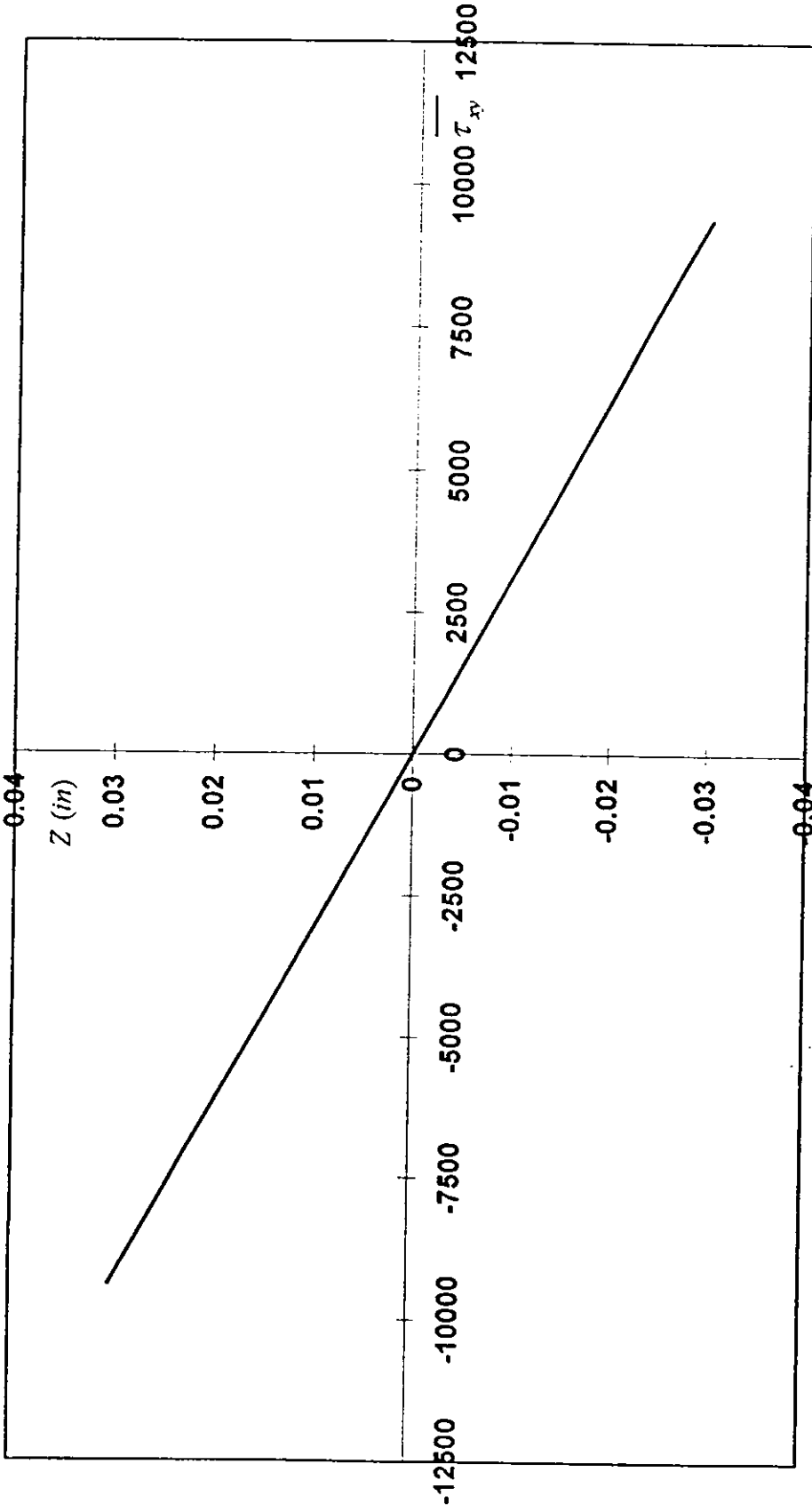plate made of three unidirectional laminae .

FIG.5-25. Normalized stresses ($\overline{\tau_{xy}}$) , at points 3 and 5 of the

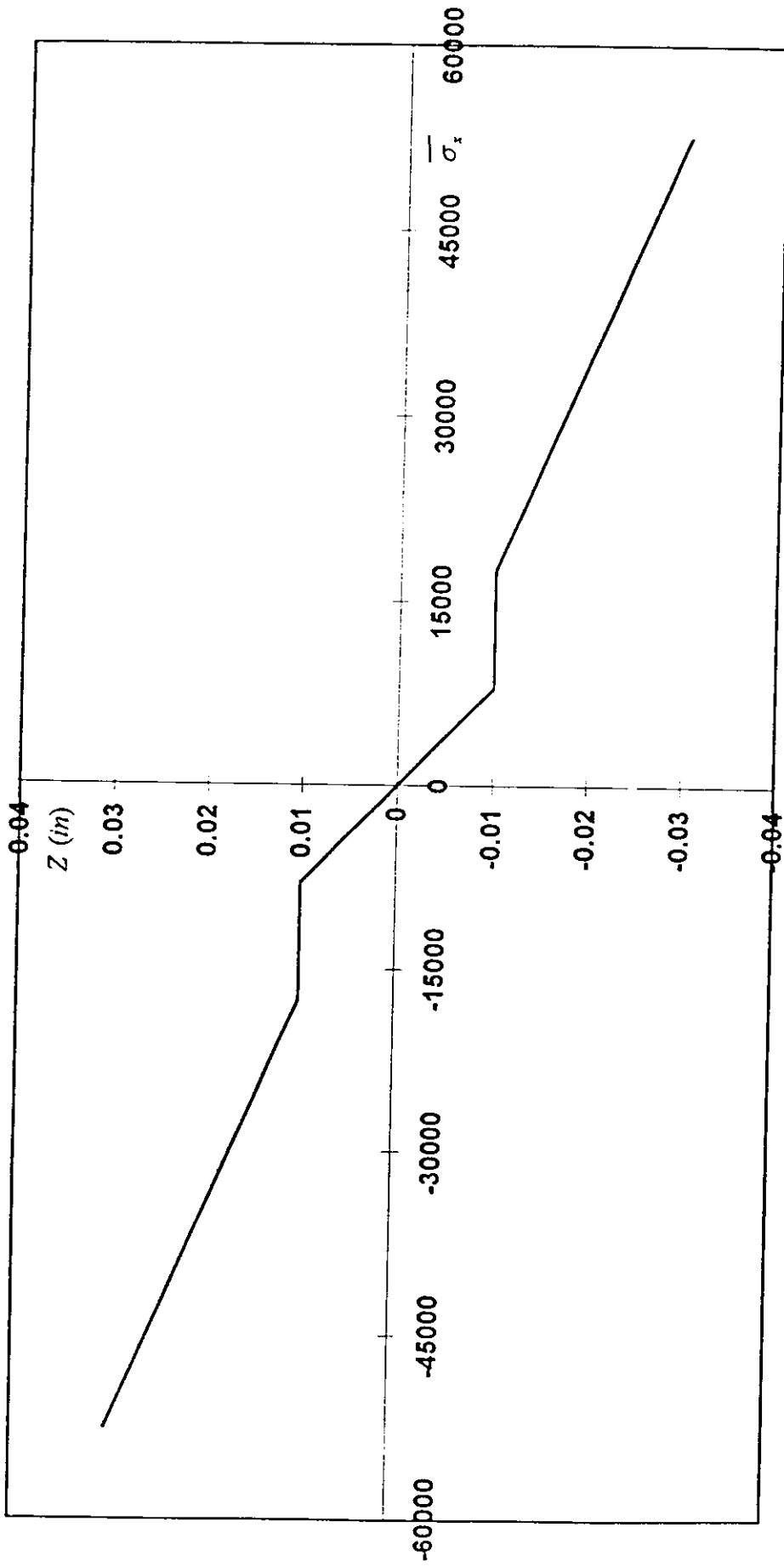plate made of three unidirectional laminae .

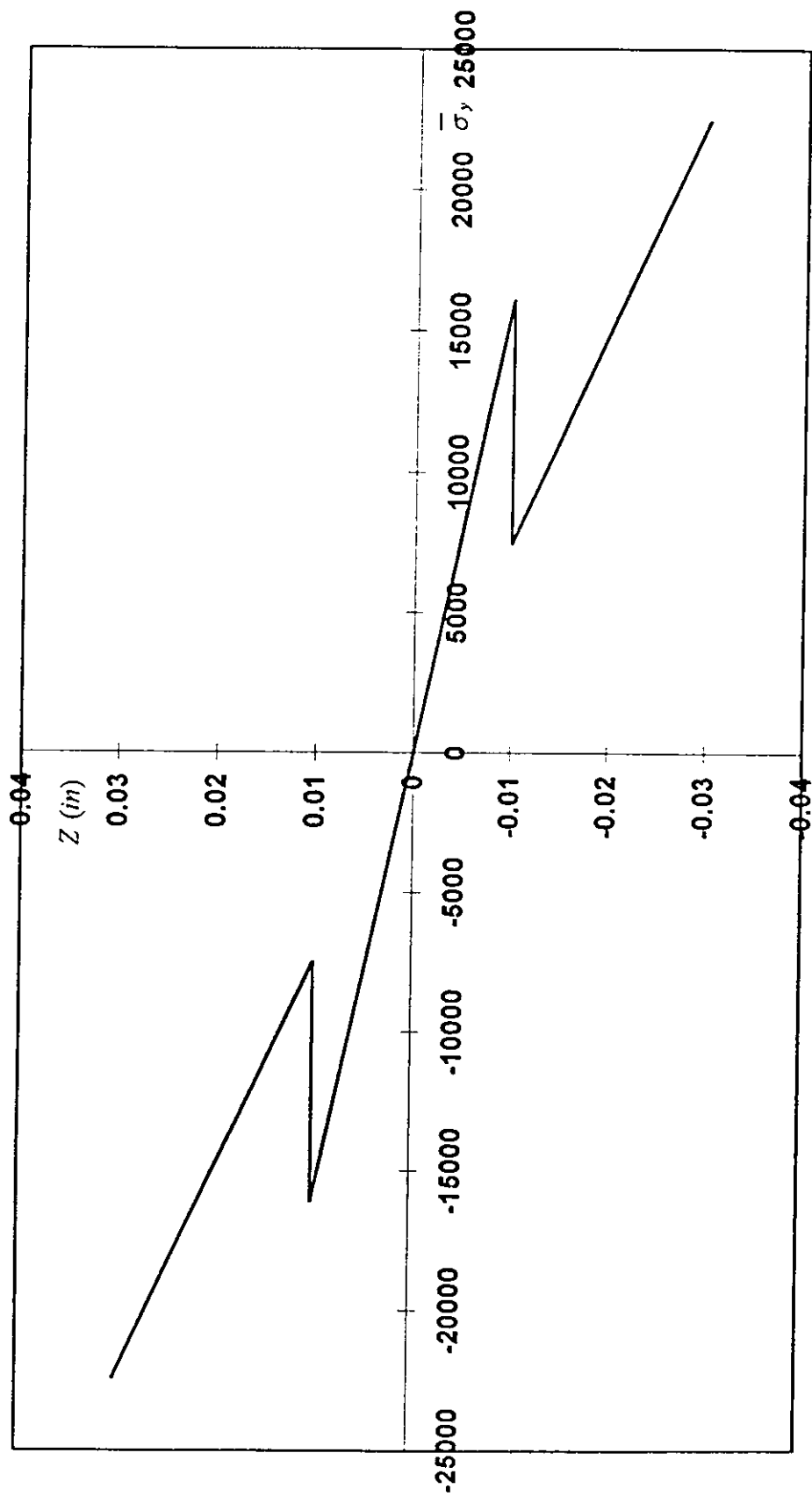FIG.5-26. Normalized stresses, $(\bar{\sigma}_x)$, at point 1 of the plate made of a cross-ply laminae.

FIG.5-27. Normalized stresses, $(\overline{\sigma_y})$, at point 1 of the plate made
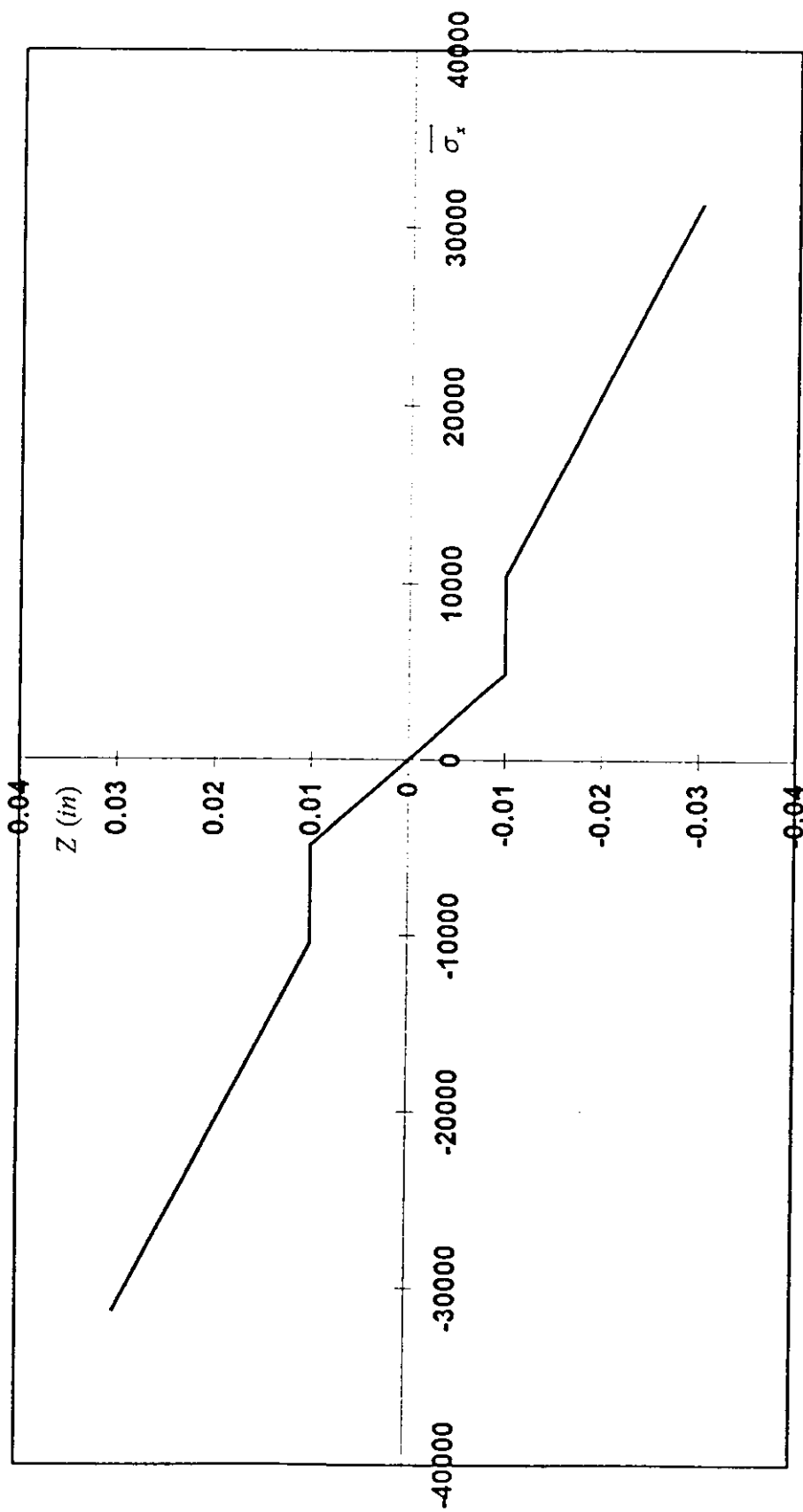
of a cross-ply laminate.

FIG.5-28. Normalized stresses , ($\overline{\sigma}_x$) , at points 2,3,4 and 5 of

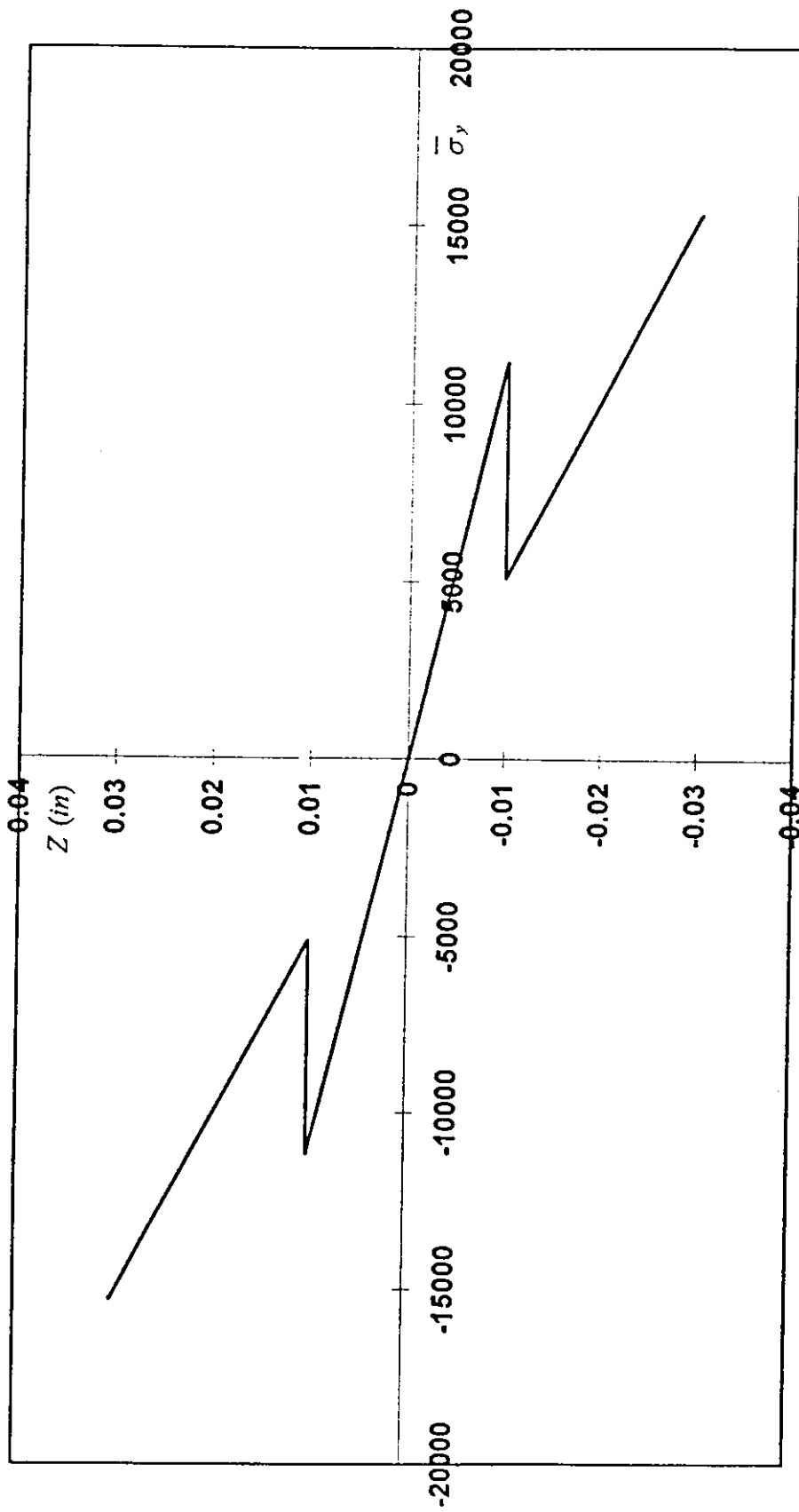the plate made of a cross-ply laminate .

FIG.5-29.   Normalized stresses, $(\overline{\sigma_y})$, at points 2,3,4 and 5 of the

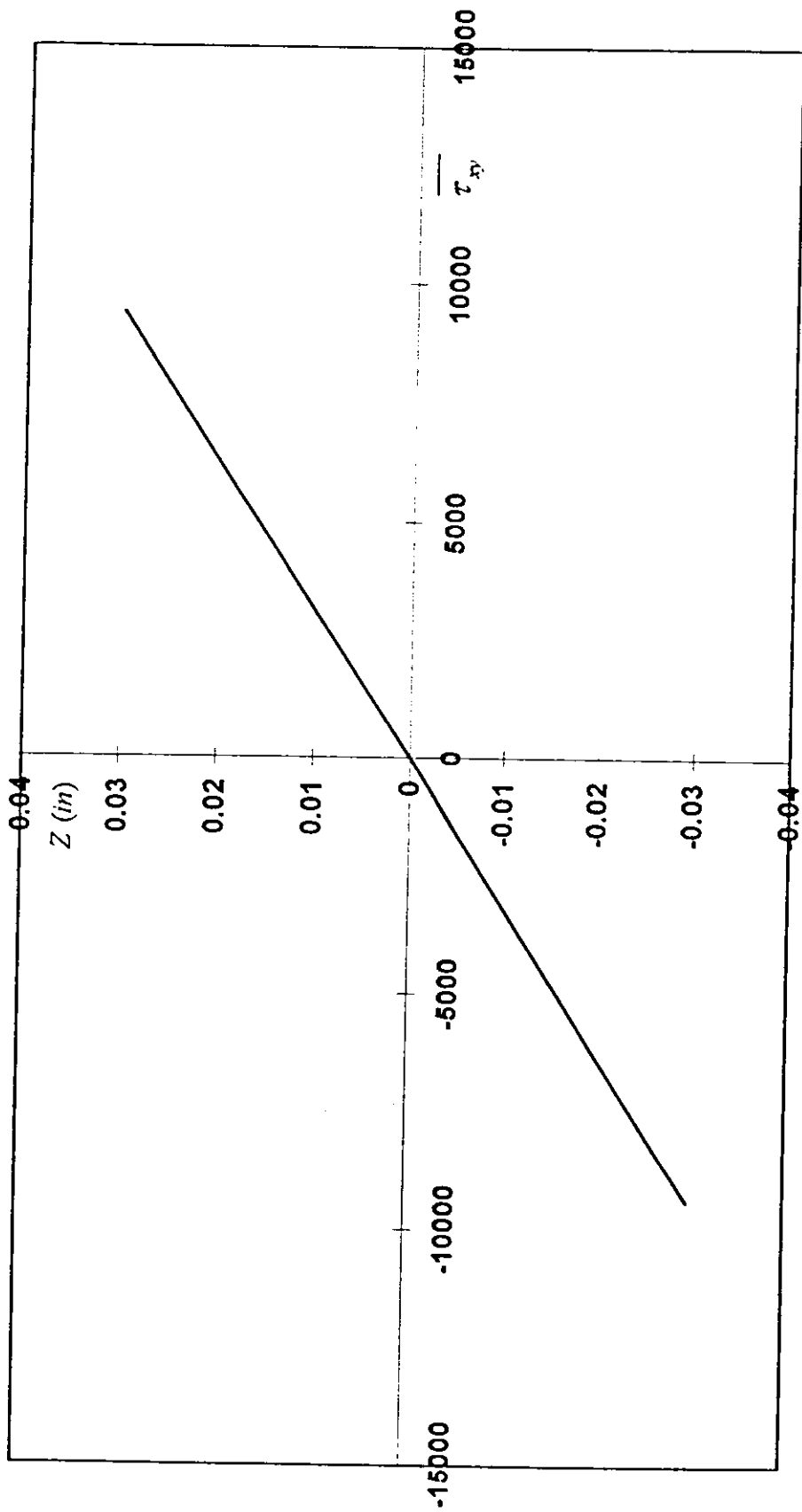plate made of a cross-ply laminate .

FIG.5-30. Normalized stresses , ($\overline{\tau_{xy}}$) , at points 2 and 4 of the

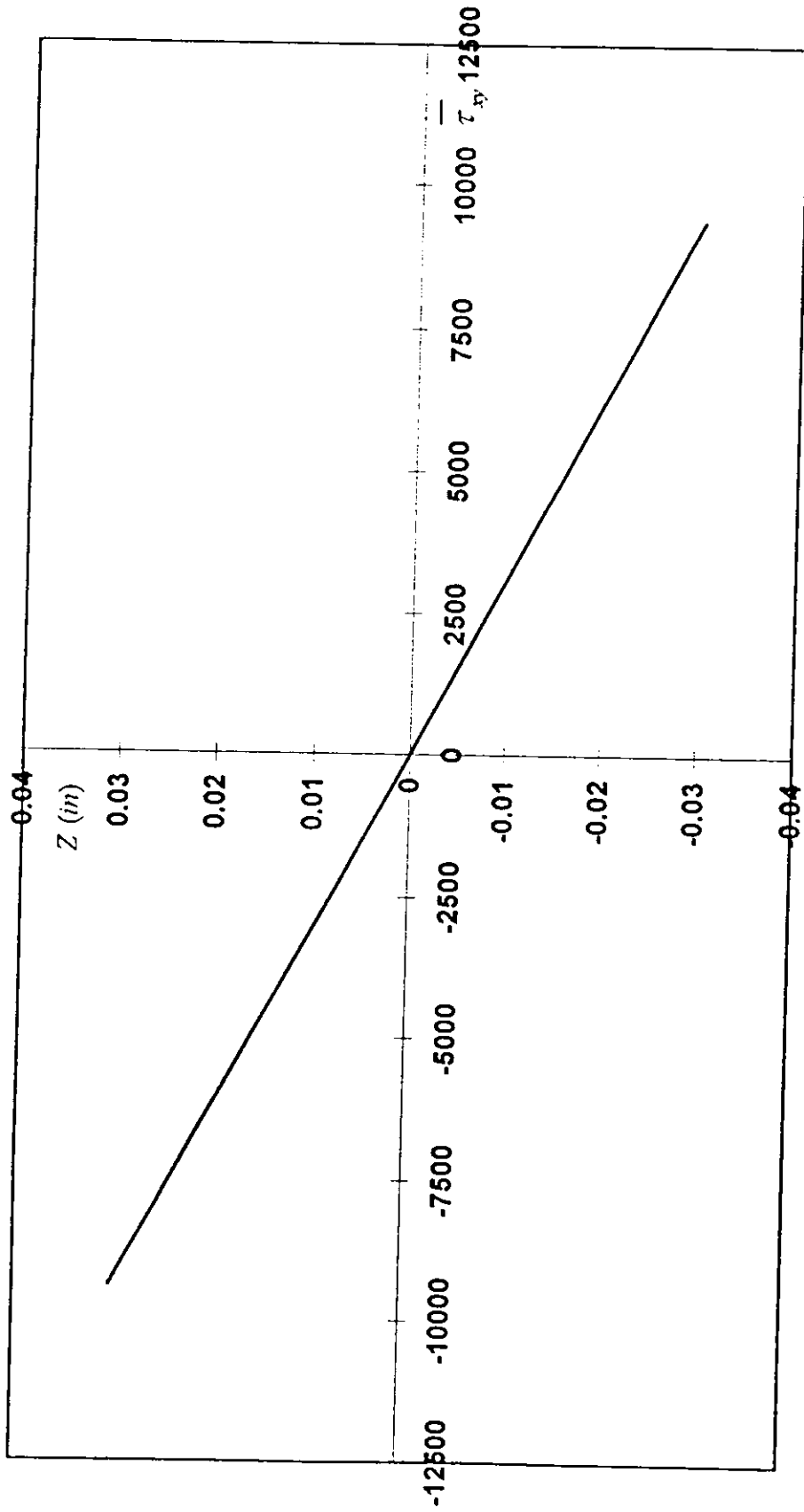plate made of a cross-ply laminate .

FIG.5-31. Normalized stresses , $(\overline{\tau_{xy}})$, at points 3 and 5 of the plate made of a cross-ply laminate .

5.5.2 Bending Of Clamped-Clamped And Clamped–Free Beams

Bending stresses in beams made of E glass-epoxy composite material and subjected to a uniform lateral load with two different boundary condition are determined and represented in figures. Also, failure loads at first-ply failure are recorded.

Dimensions of the considered beams are as following :
- Length (l) = 10 in.
- Width (b) = 0.5 in.
- Thickness (t) = 0.3in.
- Lamina thickness (t_k) = 0.1 in.

5.5.2.1 Clamped-Clamped Beam.

Two cases of clamped-clamped beam are considered:

- The beam is made of three unidirectional layers with angle $(\theta = 0^\circ)$.
- The beam is made of cross-ply laminate with $(0^\circ/90^\circ/0^\circ)$ stacking sequence.

stresses for the two cases are determined and presented in Fig.5-32 and Fig.5-33, receptively. Failure loads predicted but using the maximum stress theory of the beam made of a unidirectional

laminate are given in Table 5 -7 , where first-ply failure will occur at load q_o = -107.11 Ib/in at Z= 0.15 in. in layer 1 which is under compression .

For the beam made of a cross-ply laminate , failure loads are given in Table 5-8, where first-ply failure occur at load q_o = ⁻43.9 Ib/in at Z=0.05 in the upper part of layer 2 which is under compression .

As shown in Fig.5-32, and Fig.5-33, the upper part of the beam is under compression stresses and the lower part is under tension stresses .

Deflections in the beam made of a unidirectional laminate is shown in Fig. 5-34 and the deflections of the beam made of cross-ply laminate is shown Fig.5-35 Maximum deflection of the two cases can be determined by using curves of deflection at the position of x = L/2.

TABLE 5-7 Failure loads at different /z/ values in a clamped-clamped beam made of a unidirectional laminate.

Layer Angle	/Z/ (in)	Failure Loads q_o (Ib/in)	Failure Location
90°	0.01 0.03 0.05	1606.51 535.51 321.40	Upper part of layer 2
0°	0.09 0.15	178.51 107.11	Layer 1

TABLE 5-8 Failure loads at different /z/ values in a clamped-clamped beam made of a cross-ply laminate.

Layer Angle	/Z/ (in)	Failure Loads q_o (Ib/in)	Failure Location
90°	0.01	215.5	Upper part of layer 2.
	0.02	107.7	
	0.04	53.87	
	0.05	43.9	
0°	0.05	314.28	Layer 1
	0.07	224.48	
	0.09	174.60	
	0.11	142.85	
	0.13	120.88	
	0.15	104.88	

5.5.2.2 Clamped-Free Beam

The same beam discussed previously is considered under a different boundary condition where in this beam the upper part is under tension and the lower part is under compression as shown in Fig.5-36 and Fig.5-37 for two cases of laminated composite; the unidirectional laminate and the cross-ply laminate, respectively .

For the beam made of the unidirectional laminate, failure loads are given in Table 5-9, where first-ply failure occur at load $q_o = -17.86$ Ib/in in layer 3 at $Z = 0.15$ in which is under compression .

For the beam of the cross-ply laminate , failure loads are given in Table 5-10 and first-ply failure occur at load $q_o = ^-7.18$ Ib/in in layer 2 at $Z = ^-0.05$ in which is also under compression .

Deflections in the beam made of the unidirectional laminate is shown in Fig.5-38 and the deflections of the same beam but made of cross-ply laminate is shown in Fig.5-39. Maximum deflection can be calculated either by using equations that defined the maximum deflection or from deflection curves presented in figures .

TABLE 5-9 Failure loads at different /z/ values in a clamped-free beam made of a unidirectional laminate.

Layer Angle	/Z/ (in)	Failure Loads q_o (Ib/in)	Failure Location
90°	0.01 0.05	267.76 53.56	Upper part of layer 2.
0°	0.09 0.15	29.76 17.886	Layer 3

TABLE 5-10 Failure loads at different /z/ values in a clamped-free beam made of a cross-ply laminate.

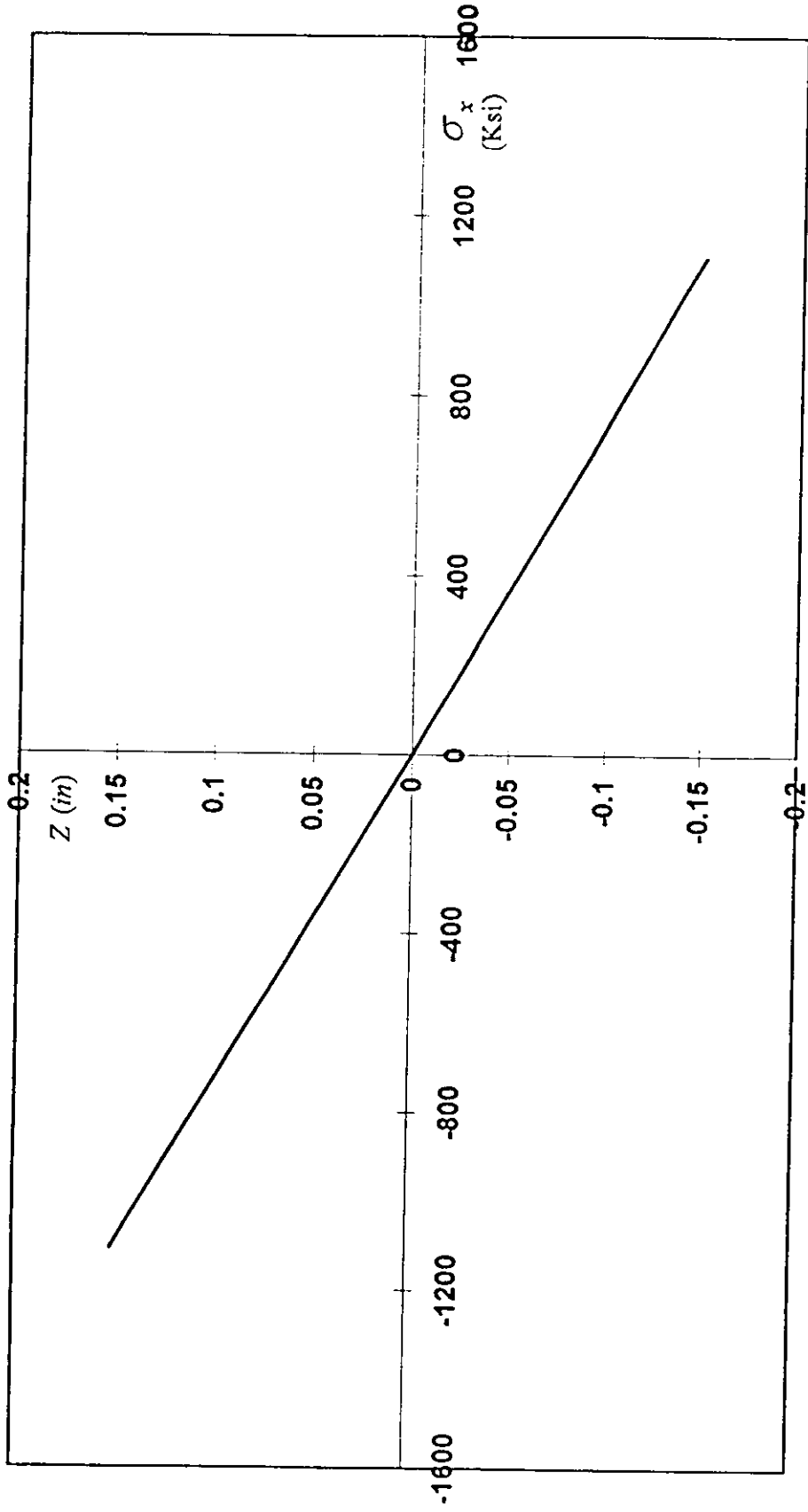| Layer Angle	/Z/ (in)	Failure Loads q_o (Ib/in)	Failure Location
90	0.01 0.02 0.04 0.05	35.96 17.95 8.98 7.18	Lower part of layer 2.
$0°$	0.05 0.07 0.09 0.11 0.13 0.15	52.42 37.44 29.11 23.81 20.15 17.46	Layer 3

FIG.5-32. Bending stresses in a clamped – clamped beam made
of a unidirectional laminate ($q_o = 1$ lb/in) .

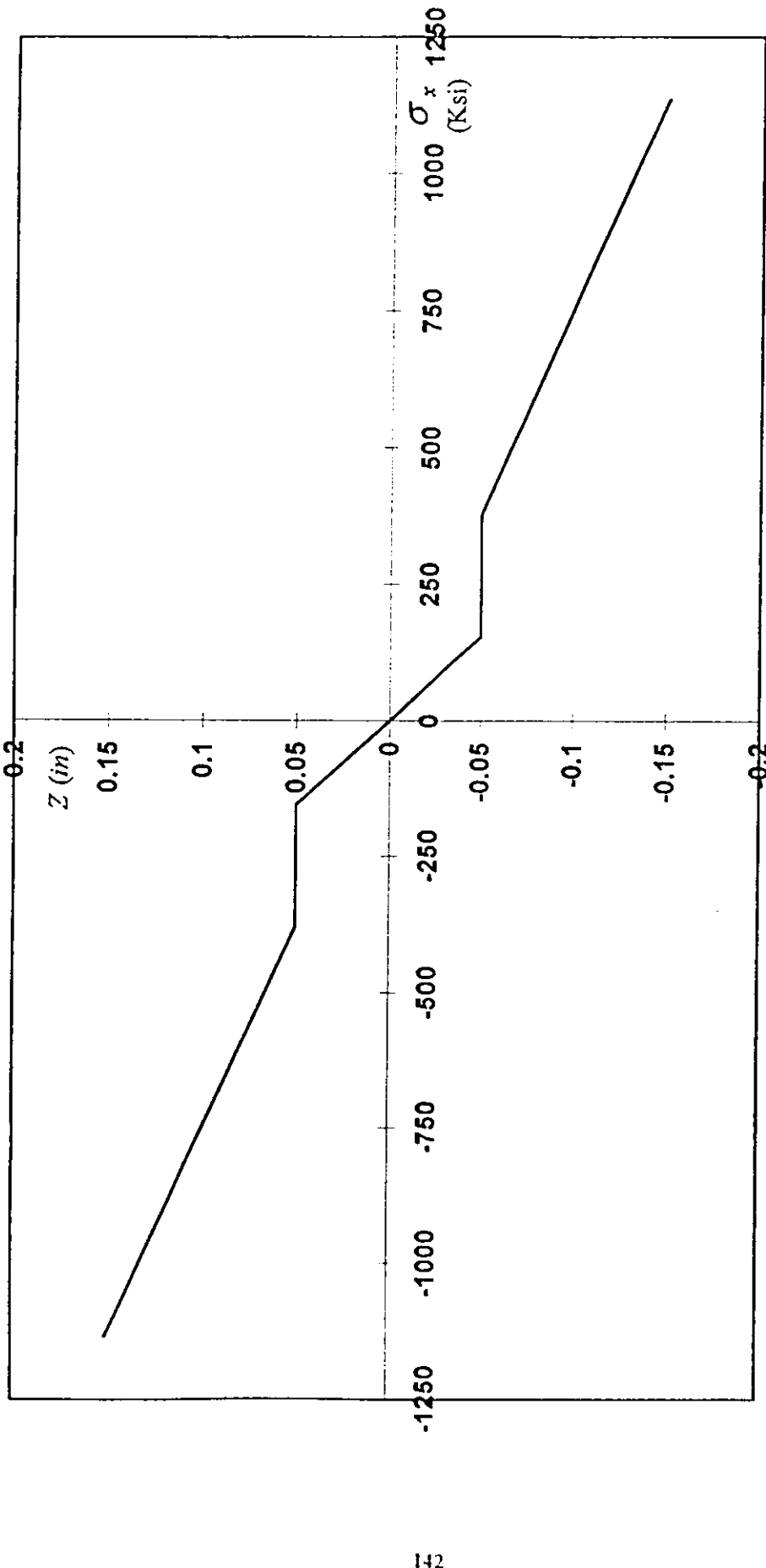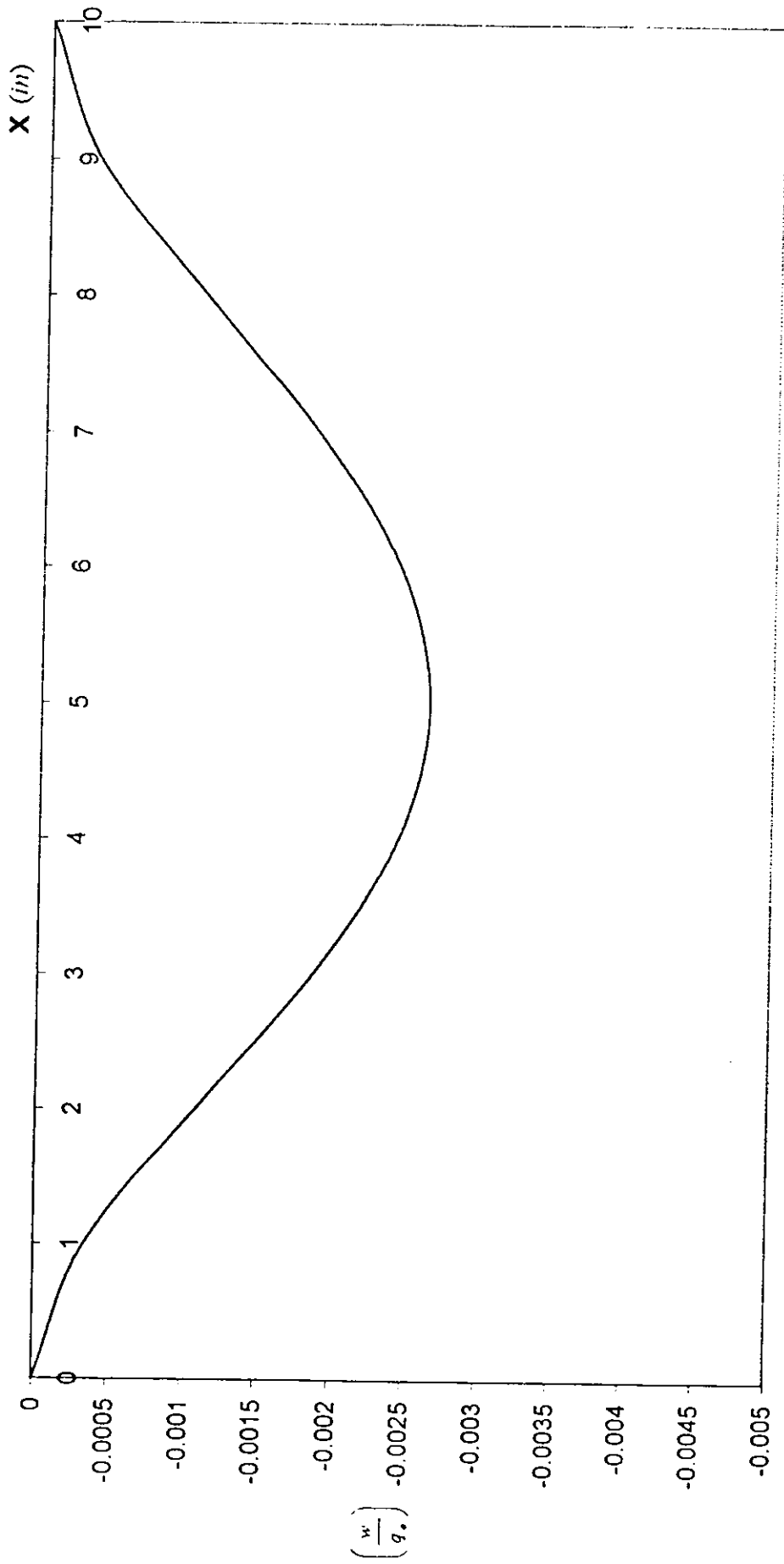FIG.5-33. Bending stresses in a clamped-clamped beam made of cross-ply laminate ($q_0= 1$ 1b/in) .

FIG.5-34. Deflections in the clamped-clamped beam made of a

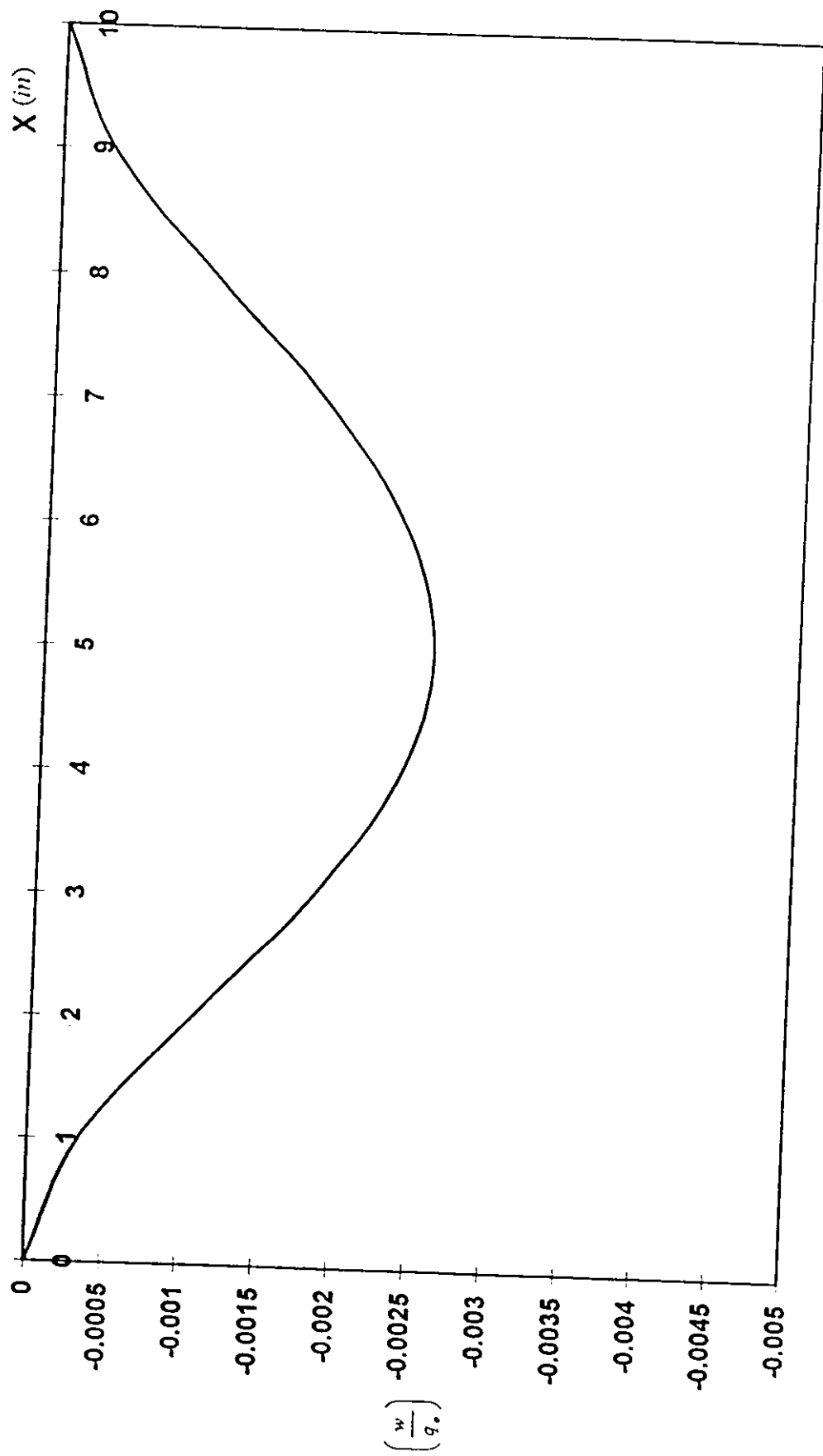unidirectional laminate ($D_{11} = 20250.0$ 1b-in)

FIG.5-35. Deflections in the clamped-clamped beam made of a cross-ply laminate ($D_{11} = 19806.7$ lb-in)
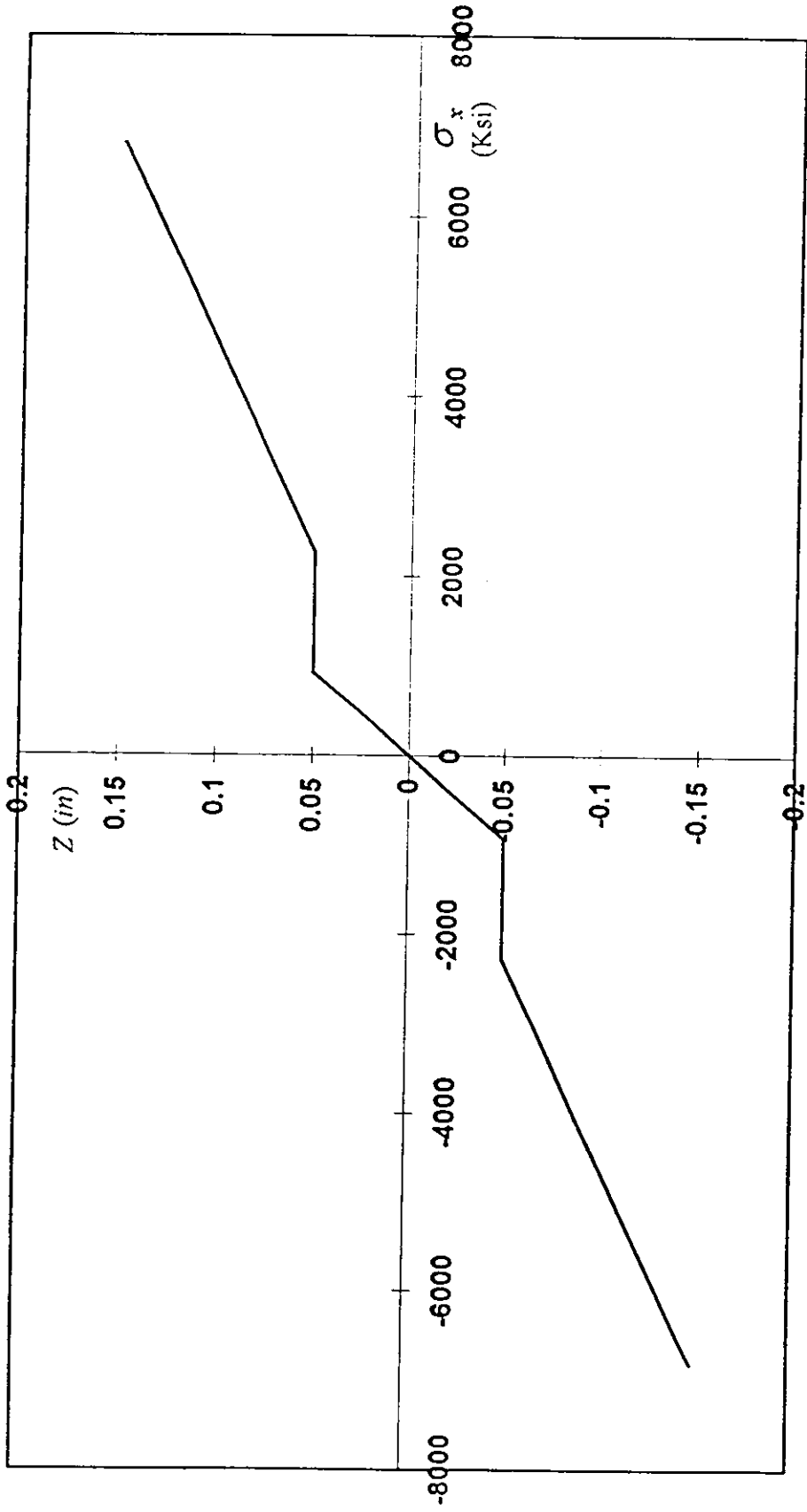
FIG.5-37. Bending stresses in a clamped-free beam made of a

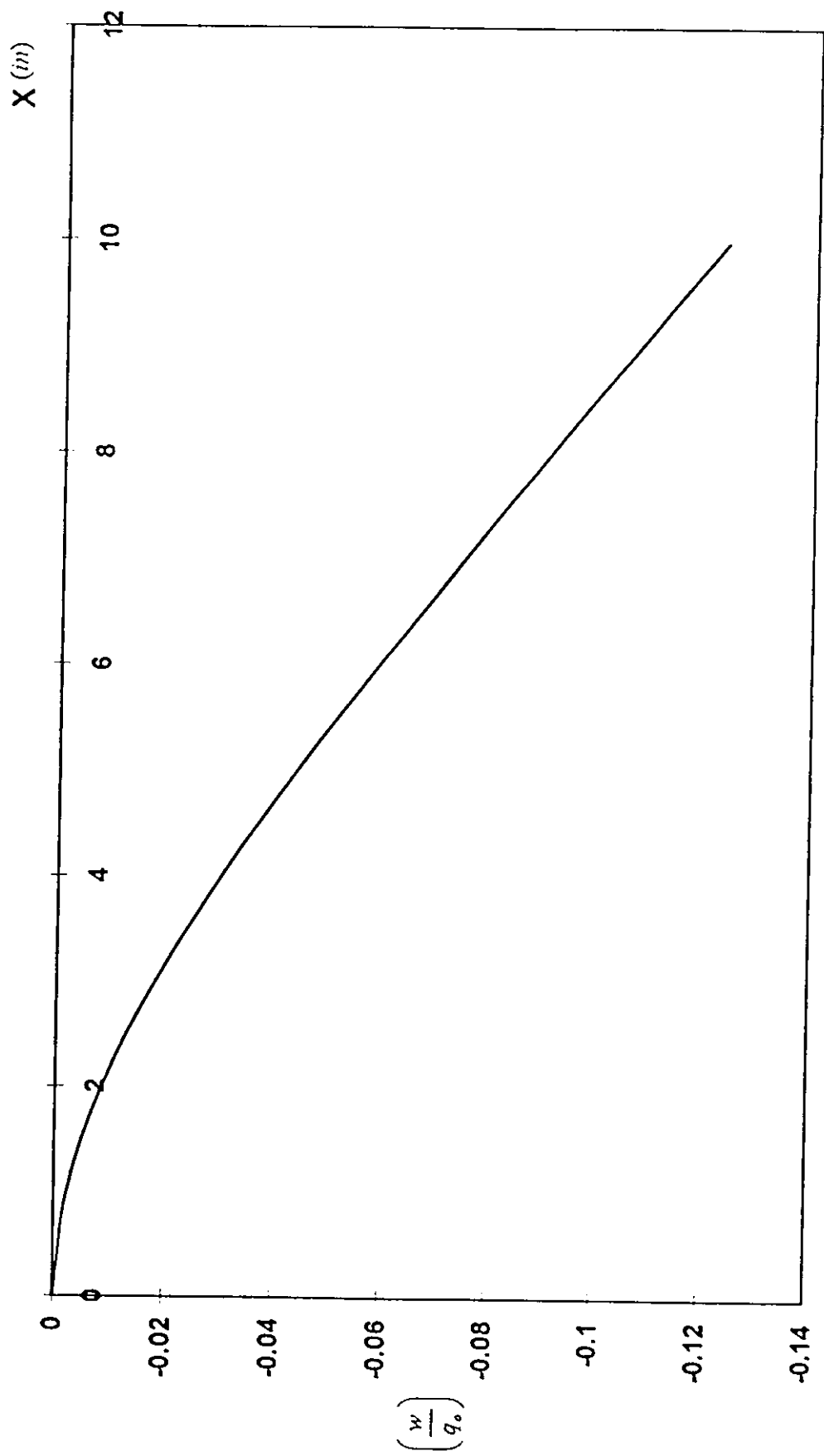cross-ply laminate (q_o= 1 lb/in) .

FIG.5-38. Deflections in the clamped-free beam made of a

unidirectional laminate ($D_{11} = 20250.0$ 1b-in)

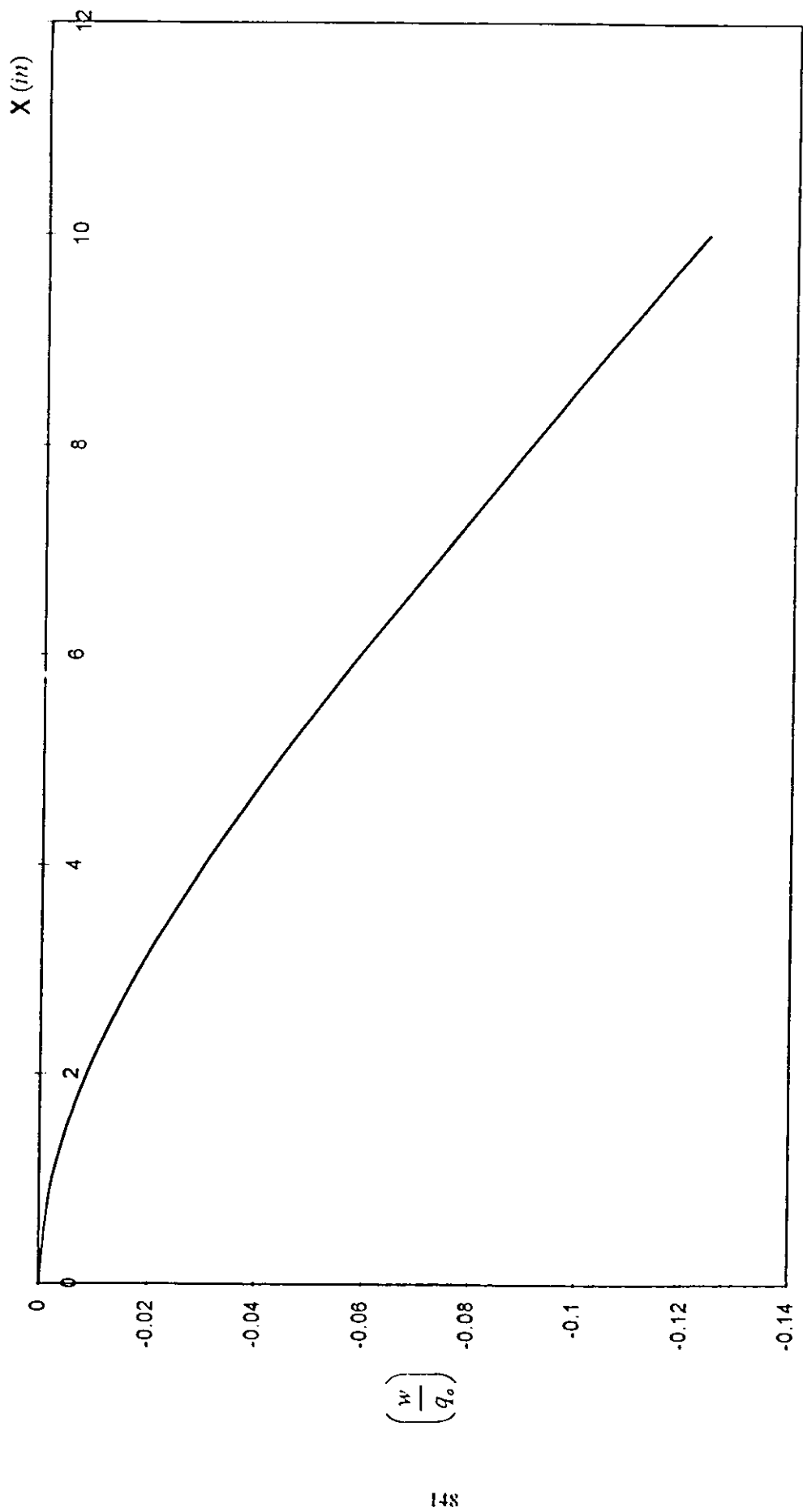FIG.3-39. Deflections in the clamped-free beam made of a cross-
ply laminate (D_{11} = 19806.7 lb-in)

CHAPTER SIX

CONCLUSIONS AND RECOMMENDATIONS

6.1 Conclusions

1- Different failure theories can be applied to structures made of composite materials, and in general their results are in good agreement with the experimental results.

2- Many composite materials have nonlinear behavior in stress-strain curves so the failure theory that did not take into consideration this nonlinearity will not predict the strength correctly.

3- The failure theory that includes more parameters in the prediction equation is the theory that can be more accurate in predication of failure stresses, Thus Tsai-Wu theory can predict failure stresses better than Tsai-Hill theory.

4- In Tsai-Hill and Tsai-Wu failure theories, considerable interaction exists between the failure strengths X,Y and S, but none exists in the maximum stress theory.

5- Angle of rotation is the main factor that can affect the lamina stiffnesses.

6- For cross-ply laminates, cross-ply ratio and stiffness ratio are very important in the prediction of failure stresses, for their effect on extensional stiffnesses, [A].

7- In general, many structures made of a fibrous composite material fail under compression stresses rather than tension stresses.

8- For bending of plates and beams made of fibrous composites, failure loads in structures made of a unidirectional laminate is higher than those of the structures made of a cross-ply laminate.

6.2 Recommendations

1- Micromechanical behavior of fibrous composite material needs further research, especially on the determination of lamina properties.

2- More experiments on fibrous composites under different stress combination are needed.

3- It is important to study the effect of temperature on fibrous composites.

4- It is recommended to study different failure theories, especially those that take into consideration the nonlinearity in composite materials.

5- It is recommended to use finite element approach to predict failure stresses in structures made of fibrous composites.

6- More research on bending in fibrous composite structures is needed under different loads and boundary conditions.

7- Buckling failure in composite structures needs to be studied at different loading and boundary conditions.

REFERENCES

Aboudi, J., 1988. Micromechanical Analysis of the Strength of Unidirectional Fiber Composites, Composite Science and Technology, Vol. 33, pp. 79-96.

Abu-Ayada, H., 1998. Design of Engineering Structures Using Fiber Reinforced Composites, Under graduate project, University of Jordan, Jordan.

Abu-Farsakh, G.A., and Abdel-Jawad, Y.A., 1994. A New Failure Criterion for Nonlinear Composite Materials, Journal of Composites Technology and Research, Vol. 16, pp. 138 – 145 .

Al-Huniti, N.S., 1996. Micromechanical Modeling of Woven and Textile Composites, Ph.D. Thesis, University of Cincinnati, U.S.A.

Azzi, V.D., and Tsai, S.W., 1965. Anisotropic Strength of Components, Experimental Mechanics, Vol.15 , No. 9, pp. 283-288

Cole, B.W., and Pipes, R,B., 1973. Filamentary composite Laminates Subject to Biaxial Stress Fields , IIT Research Institute, Chicago, IL and Drexel University, Philadelphia, PA , Air Force Flight Dynamics Laboratory Technical Report AFFDL-TR-73-115.

Feng, W.W., 1991. A Failure Criterion for Composite Materials, Journal of Composite Material , Vol.25, pp .88-100 .

Harris, B., Dorey, S.E., and Cooke, R.G., 1988. Strength and Toughness of Fibre Composites, Composites Science and Technology , Vol.31,pp. 121-141 .

Herrmann, K.P., and Ferber, F., 1992 . Numerical Modeling of Elementary failure Mechanisms and Associated caustics in Two-Phase Composite Structures, Computers and Structures, Vol.44, No.12, pp. 41-53 .

Hill, R., 1948. A Theory of Yielding and Plastic Flow of Anistropic Metals, Proceeding of the Royal Society, London, Series A, Vol.193 , pp . 281 –297 .

Hoffman, O., 1967. The Brittle Strength of Orthotropic Materials, Journal of Composite Materials, Vol.1, pp. 200-206.

Jaing , Z., and Tennyson , R.C , 1989 . Clousure of Cubic Tensor Polynomial Failure Surface , Journal of composite Materials, Vol. 23, pp. 208-231 .

Jones, R.M., 1975 . Mechanics of composite Materials , McGraw - Hill , New York .

Kapania , R.K., and Raciti S., 1989 . Recent Advances in Analysis of laminated Beams and Plates , Part I : Shear Effect and Buckling , AIAA Journal , Vol.27 , No.7 , pp. 923 – 934 .

Mal, A.K., and Chatterjee, A.K., 1977. The Elastic Moduli of a Fiber Reinforced composite , Journal of Applied Mechanics , March, pp. 61-67 .

Marin, J., 1957 . Theories of Strength for Combined Stresses and Non Isotropic Materials , Journal of Aerospace Science , Vol. 24, pp. 265-268 .

Marin, J., 1966. Mechanical Behavior of Engineering Materials, Prentice – Hall of India (Private) LTD , New Delhi .

Pindera, M.J, and Aboudi, J., 1988. Micromechanical Analysis of Yieding of Metal Matrix Compsites , Int. J. Plasticity , Vol.5.

Popov, E.P., 1968 . Introduction to Mechanics of Solids , Prentice Hall , Inc . Engle Wood Cliffs., New Jersey .

Rankine, W. J. M., 1858 . Applied Mechanics , London .

Sandhu, R. S., 1976 . Nonlinear Behavior of Unidirectional and Angle-ply Laminates, Journal of Aircraft , Vol.13,pp. 104-111 .

Spencer, A., 1986 . The Transverse Moduli of Fibre- Composite Material , Composites Science and Technology , Vol.27, pp . 93 – 109 .

Tsai , S.W., 1968 . Strength Theories of Filamentary Structures, Fundamental Aspects of Fiber Reinforced Plastic composites , R. T. Schwartz and H.S. Schwartz Eds., Wiley Interscience , New York, pp. 3-11 .

Tsai , S.W., Donald , F.A., and Douglas, S.D., 1966 . Analysis of Composite Structures, NASA CR-620 ,.

Tsai, S.W., and Hahn , H. T., 1980 . Introduction to Composite Materials , Technomic Publishing Company, Westport, CT.

Tsai , S.W., and Wu , E.M., 1970 . A General Theory of Strength for Anisotropic Materials , Journal of composite Material, Vol. 5, No. 1, pp. 58 – 80.

Vinson, J.R., and Chou, T.W., 1975 . Composite Materials and Their Use in Structures , Applied Science Publishers , London .

Vinson, J.R., and Sierakowski, R.L., 1986. The Behavior of Structures Composed of Composite Materials, Martinus Nijhoff Publishers , Boston .

Waddoups, M.E ., 1967. Advanced Composite Material Mechanics for the Design and Stress Analyst , General Dynamics , Ft.Worth,TX , Report FZM-4763 .

Whitney, J.M., 1987. Structural Analysis of Laminated Anisotropic `Plates , Technomic Publishing Co.

Appendix A

TYPICAL MECHANICAL PROPERTIES OF SOME COMPOSITES

Typical mechanical properties of some composites are adapted from Jones (1975), and Vinson and Sierakowski (1986), and given in Table A-1.

TABLE A-1. Typical mechanical properties of some composite materials.

| Material Proprty	S Glas / XP-251	Eglass /EP	T300/ 5208	AS/ 3501	T300 / 934	T300/ SP- 286	Boron / EP	Kevlar 49/EP
	Psi	Psi	Psi	Psi	Psi	Psi	Psi	Psi
E_1	8.29×10^6	8.8×10^6	22.2×10^6	20.02×10^6	23.69×10^6	21.9×10^6	30.3×10^6	11.02×10^6
E_2	2.92×10^6	3.6×10^6	1.58×10^6	1.3×10^6	1.7×10^6	1.53×10^6	2.8×10^6	0.798×10^6
υ_{12}	0.262	0.23	0.30	0.30	0.30	0.31	0.21	0.34
G_{12}	0.86×10^6	1.74×10^6	0.81×10^6	1.03×10^6	0.94×10^6	0.96×10^6	0.93×10^6	0.334×10^6
X_t	289×10^3	187×10^3	100×10^3	209.9×10^3	107×10^3	203×10^3	185.6×10^3	203.05×10^3
X_c	170×10^3	119×10^3	110×10^3	209×10^3	105×10^3	164×10^3	362×10^3	34.08×10^3
Y_t	11×10^3	6.67×10^3	4×10^3	7.5×10^3	*	7.8×10^3	8.8×10^3	1.74×10^3
Y_c	29×10^3	25.3×10^3	13.9×10^3	29.9×10^3	*	30.6×10^3	44.7×10^3	7.69×10^3
S	9×10^6	6.5×10^6	9×10^6	13.5×10^3	14.8×10^3	10.5×10^3	15.2×10^3	4.93×10^3
V_F	0.67	0.72	0.70	0.67	0.60	0.60	0.67	0.60

Note : 1 psi = 6.894 KPa.
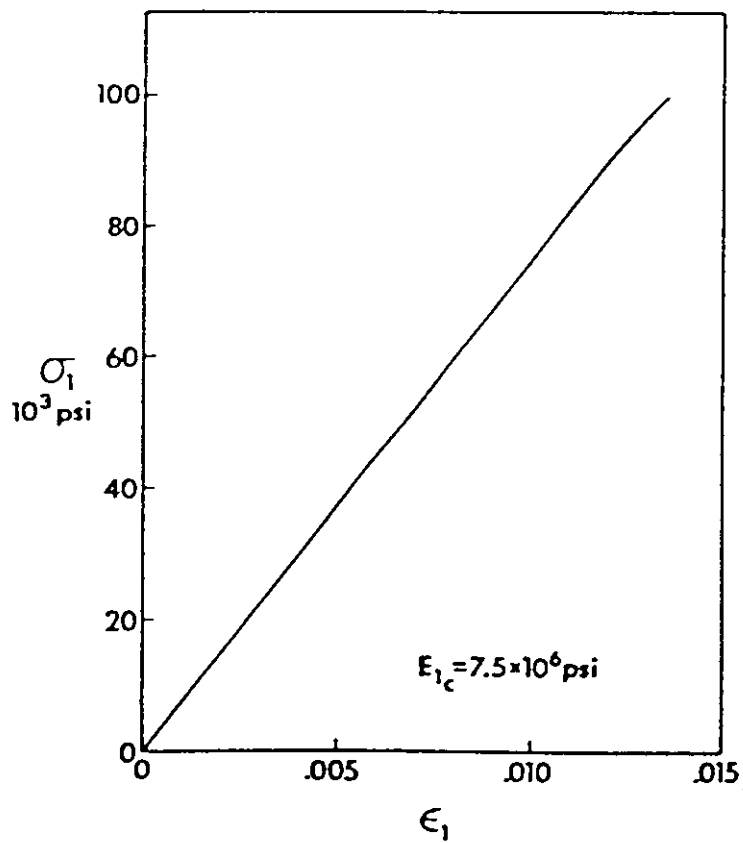
FIG. B-2. Compressive $\sigma_1 - \varepsilon_1$ curve for 3M XP251S glass-epoxy.
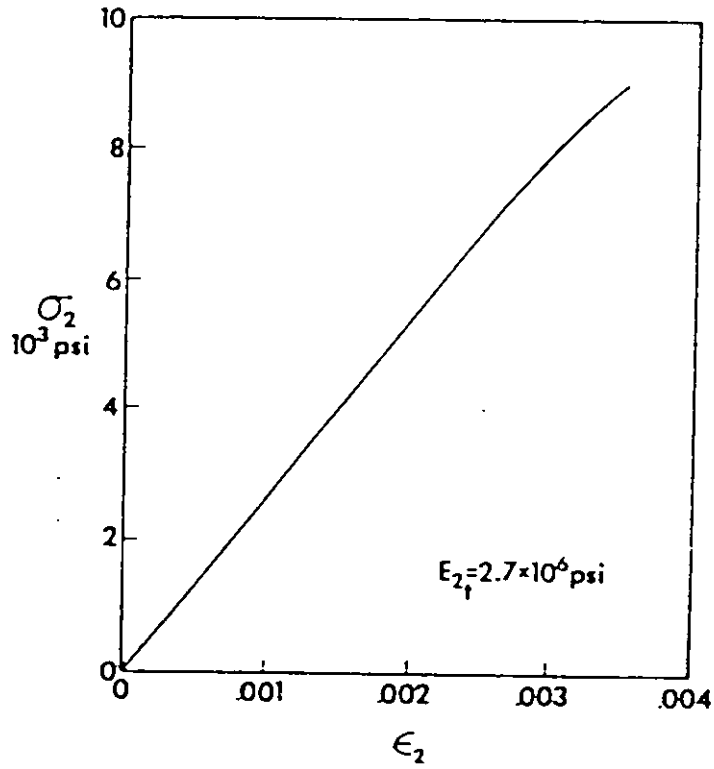
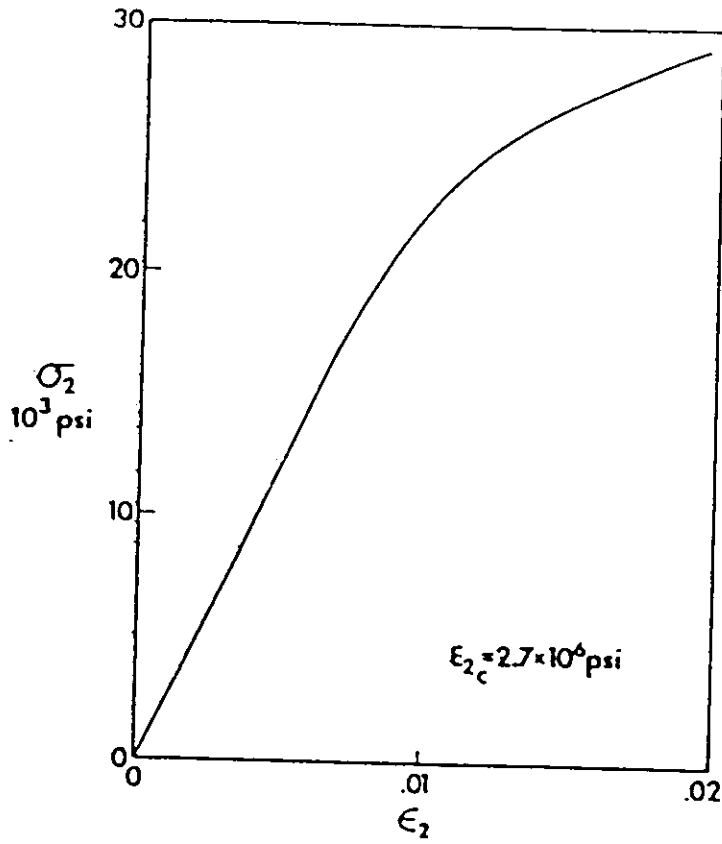FIG. B-3. Tensile $\sigma_2 - \varepsilon_2$ curve for 3M XP251S glass-epoxy.

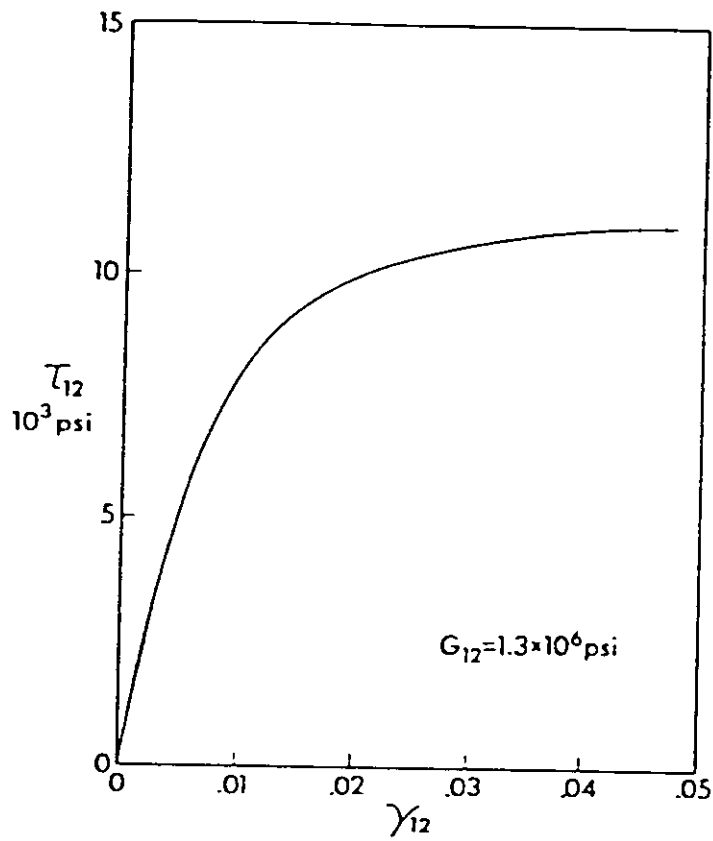FIG. B-4. Compressive $\sigma_2 - \varepsilon_2$ curve for 3M XP251S glass-epoxy.

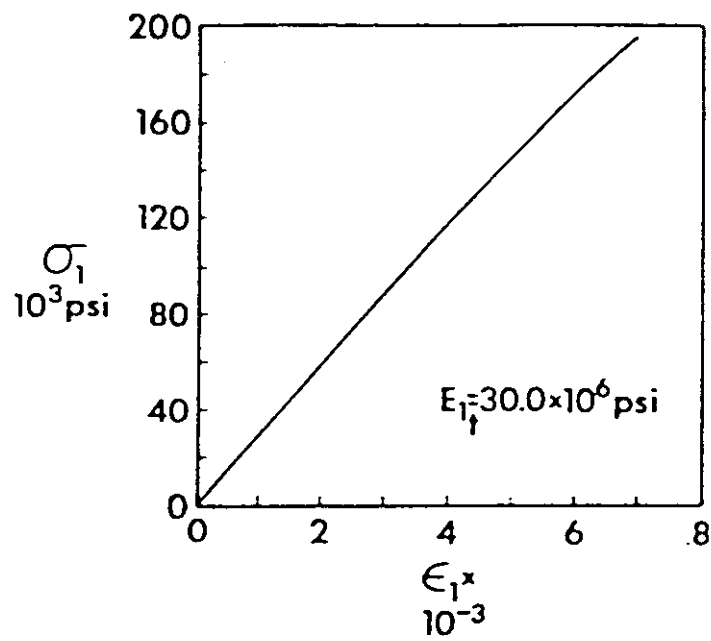FIG. B-5. Shear stress- strain curve for 3M XP251S glass-epoxy.

FIG. B-6. Tensile $\sigma_1 - \varepsilon_1$ curve for boron- epoxy Narmco 5505.
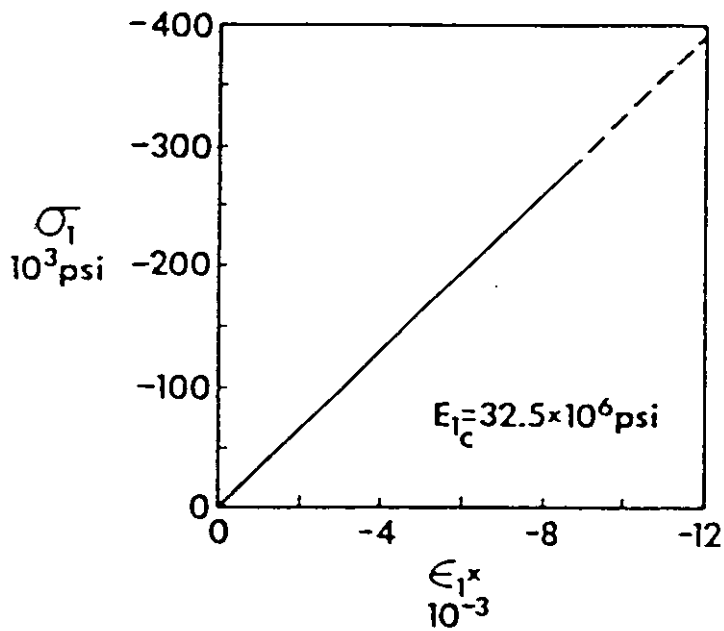
FIG. B-7. Compressive $\sigma_1 - \varepsilon_1$ curve for boron- epoxy Narmco 5505.

σ_2
10^3psi

14

12

10

8

6

4

2

0

$E_{2_t}=3.2\times10^6$psi

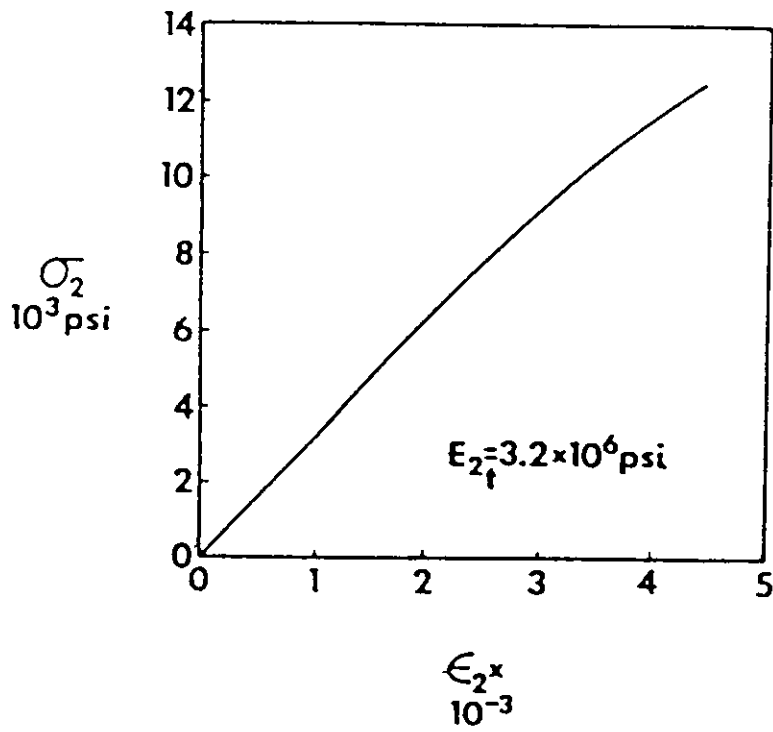0   1   2   3   4   5

$\epsilon_2 \times$
10^{-3}

FIG. B-8. Tensile $\sigma_2 - \epsilon_2$ curve for boron- epoxy Narmco 5505.

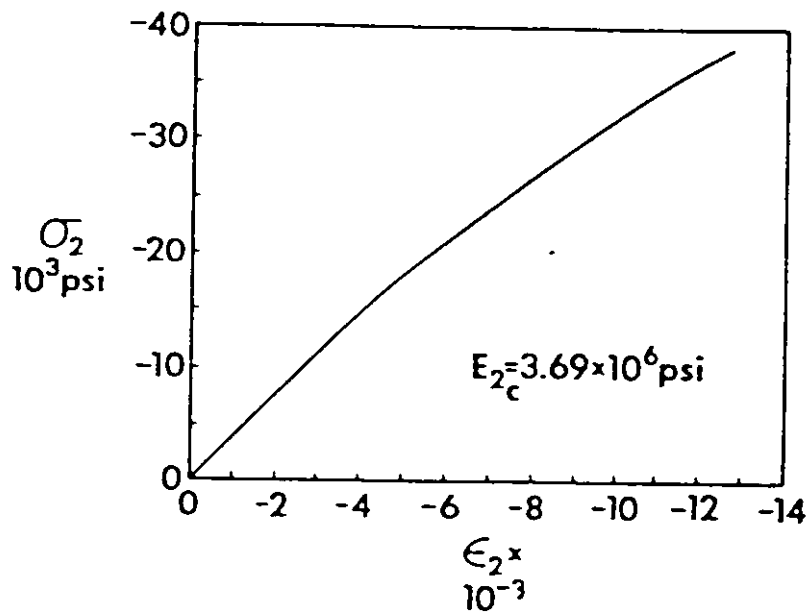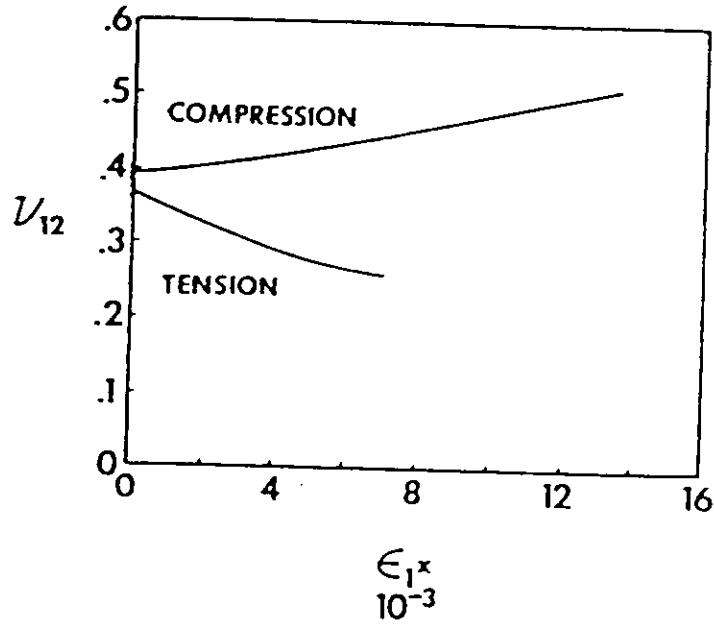FIG. B-9. Compressive $\sigma_2 - \varepsilon_2$ curve for boron-epoxy Narmco 5505.

Chart axes and labels:
- Y-axis: σ_2 10^3psi, values: -40, -30, -20, -10, 0
- X-axis: $\varepsilon_2 \times 10^{-3}$, values: 0, -2, -4, -6, -8, -10, -12, -14
- $E_{2_c} = 3.69 \times 10^6$psi

FIG. B-11.Poisson's ratio curve for boron-epoxy Narmco 5505.

ملخص
دراسة نظرية الانهيار في إنشاءات
مصنوعة من المواد المركبة والمعززة بالليف
إعداد
إياد محمود علي مصلح
المشرف
الدكتور سعد محمد الحبالي

في هذه الدراسة تم البحث في نمذجة المواد المركبة والمعـــززة بـــالليف باسـتخدام طريقة (Strain Energy) وتم كذلك البحث في نظرية الانهيار في إنشاءات مصنوعة مـن المواد المركبة والمعززة بالليف عن طريق استخدام نظريات مختلفة هي نظريـة (Tsai – Wu) و نظرية (Tsai – Hill) و نظرية الإجهاد الأكبر .

وكتطبيق تم دراسة الاجهادات المؤدية للانهيار في إنشاءات مصنوعة مـــن مـواد (Boron-epoxy) و (Glass-epoxy) و (Eglass-epoxy) . تمـت هـذه الدراسـة لحالات خاصة من المواد المركبة والمشكلة من عدة طبقات متماثلة وذات ترتيبات مختلفـة لأنواع مثل (Cross-ply laminates) و (Angle-ply laminates) .

وكذلك تمت دراسة تأثير القوى على صفائح وقضبان مصنوعة من المـــواد المركبـة والمعززة بالليف ومعرضة لظروف مختلفة من حيث القوى والتثبيت ومرتبة في طبقات مـن المواد المركبة في حالتي الاتجاه الواحد والاتجاه المتعامد .

نتائج هذه الدراسة تمت مقارنتها مع النتائج المتوفرة في الأبحاث الســـابقة، بحيث أوضحت المقارنة ان نتائج الدراسة قريبة من النتائج المخبرية للمـــواد والطبقـات المركبة المستخدمة في هذه الدراسة .